U. S. Department of Transportation
Federal Railroad Administration

Crashworthiness of Passenger Trains

Office of Research and Development
Washington, D.C. 20590

Safety of High-Speed Ground Transportation Systems

DOT/FRA/ORD
DOT-VNTSC-FRA-96-5

Final Report
September 1996

REPORT DOCUMENTATION PAGE

Form Approved
OMB No. 0704-0188

1. AGENCY USE ONLY (Leave blank)	2. REPORT DATE September 1996	3. REPORT TYPE AND DATES COVERED Final Report March 1996 - September 1996

4. TITLE AND SUBTITLE
Crashworthiness of Passenger Trains
Safety of High-Speed Ground Transportation Systems

5. FUNDING NUMBERS
RR693/R6018

6. AUTHOR(S)
David Tyrell, Kristine Severson, Brian Marquis

7. PERFORMING ORGANIZATION NAME(S) AND ADDRESS(ES)
U.S. Department of Transportation
Office of Systems Engineering
Research and Special Programs Administration
John A. Volpe National Transportation Systems Center
Cambridge, MA 02142

8. PERFORMING ORGANIZATION REPORT NUMBER
DOT-VNTSC-FRA-96-5

9. SPONSORING/MONITORING AGENCY NAME(S) AND ADDRESS(ES)
U.S. Department of Transportation
Federal Railroad Administration
Office of Research and Development
Washington, DC 20590

10. SPONSORING/MONITORING AGENCY REPORT NUMBER

11. SUPPLEMENTARY NOTES

12a. DISTRIBUTION/AVAILABILITY STATEMENT

This document is available to the public through the National Technical Information Service, Springfield, VA 22161

12b. DISTRIBUTION CODE

13. ABSTRACT (Maximum 200 words)

Studies were conducted evaluating the effectiveness of alternative strategies for providing crashworthiness of the vehicle structures and on the effectiveness of alternative strategies for protecting occupants in train collisions, including friendly interior arrangements and occupant restraints.

Conventional practice results in cars of essentially uniform longitudinal strength. The crash energy management approach requires varying strength through the train, with high strength in the occupied areas and lower strength in the unoccupied areas. For train-to-train collisions at closing speeds above 112 km/h (70 mph), the crash energy management approach is more effective than the conventional approach in preserving occupant volume. For closing speeds below 112 km/h (70 mph), both strategies are equally effective in preserving occupant volume. The crash energy management design results in gentler secondary impacts for train-to-train collisions than the conventional design of cars behind the first coach car, at all speeds analyzed.

Head Injury Criteria (HIC), chest deceleration, and axial neck load were used to evaluate interior performance; the probability of fatality resulting from secondary impacts was evaluated for each of the interior configurations and restraint systems modeled based on these criteria. The results indicate that compartmentalization can be as effective as a lap belt in minimizing probability of fatality for the 50th percentile male simulated when the seats are arranged in forward-facing rows. Compartmentalization is an occupant protection strategy that requires seats or restraining barriers to be positioned in a manner that provides a compact, cushioned protection zone surrounding each occupant.

14. SUBJECT TERMS
structural crashworthiness, crash energy management, interior crashworthiness, occupant restraint, passenger train

15. NUMBER OF PAGES
112

16. PRICE CODE

17. SECURITY CLASSIFICATION OF REPORT	18. SECURITY CLASSIFICATION OF THIS PAGE	19. SECURITY CLASSIFICATION OF ABSTRACT	20. LIMITATION OF ABSTRACT
Unclassified	Unclassified	Unclassified	

PREFACE

The Volpe Center has been providing support to the Federal Railroad Administration (FRA) in developing the technical basis for crashworthiness specifications for rail passenger equipment. As part of this support, the Volpe Center has conducted studies to evaluate the effectiveness of different strategies for providing crashworthiness of the vehicle structures and interiors. The results of these studies have been used in discussions with Amtrak on safety considerations for the purchase of Northeast Corridor high-speed trainsets.

The work described here was performed as part of the High Speed Ground Transportation Safety Program sponsored by the FRA's Office of Research and Development of the U.S. Department of Transportation. The authors would like to thank Thomas Schultz of the Office of Research and Development, and Thomas Peacock and Rolf Mowatt-Larssen of the Office of Safety, for their assistance in developing the force/crush characteristic of the conventional design and the constraints for the force/crush characteristics for the crash-energy management design. The authors would also like to thank Dr. W. Thomas Hollowell, Chief of the National Highway Traffic Safety Administration's (NHTSA) Safety Systems Engineering and Analysis Division for the use of the MADYMO simulation program, and John Guglielmi and Larry Simeone of the Volpe Center's Crashworthiness Division for their assistance in exercising MADYMO. Finally, the authors would like to thank Dr. Herbert Weinstock, Chief of the Volpe Center's Structures and Dynamics Division, for the many helpful discussions on the modeling of dynamic systems.

METRIC/ENGLISH CONVERSION FACTORS

ENGLISH TO METRIC	METRIC TO ENGLISH
LENGTH (APPROXIMATE)	**LENGTH (APPROXIMATE)**
1 inch (in) = 2.5 centimeters (cm)	1 millimeter (mm) = 0.04 inch (in)
1 foot (ft) = 30 centimeters (cm)	1 centimeter (cm) = 0.4 inch (in)
1 yard (yd) = 0.9 meter (m)	1 meter (m) = 3.3 feet (ft)
1 mile (mi) = 1.6 kilometers (km)	1 meter (m) = 1.1 yards (yd)
	1 kilometer (km) = 0.6 mile (mi)
AREA (APPROXIMATE)	**AREA (APPROXIMATE)**
1 square inch (sq in, in^2) = 6.5 square centimeters (cm^2)	1 square centimeter (cm^2) = 0.16 square inch (sq in, in^2)
1 square foot (sq ft, ft^2) = 0.09 square meter (m^2)	1 square meter (m^2) = 1.2 square yards (sq yd, yd^2)
1 square yard (sq yd, yd^2) = 0.8 square meter (m^2)	1 square kilometer (km^2) = 0.4 square mile (sq mi, mi^2)
1 square mile (sq mi, mi^2) = 2.6 square kilometers (km^2)	10,000 square meters (m^2) = 1 hectare (ha) = 2.5 acres
1 acre = 0.4 hectare (ha) = 4,000 square meters (m^2)	
MASS - WEIGHT (APPROXIMATE)	**MASS - WEIGHT (APPROXIMATE)**
1 ounce (oz) = 28 grams (gm)	1 gram (gm) = 0.036 ounce (oz)
1 pound (lb) = .45 kilogram (kg)	1 kilogram (kg) = 2.2 pounds (lb)
1 short ton = 2,000 pounds (lb) = 0.9 tonne (t)	1 tonne (t) = 1,000 kilograms (kg) = 1.1 short tons
VOLUME (APPROXIMATE)	**VOLUME (APPROXIMATE)**
1 teaspoon (tsp) = 5 milliliters (ml)	1 milliliter (ml) = 0.03 fluid ounce (fl oz)
1 tablespoon (tbsp) = 15 milliliters (ml)	1 liter (l) = 2.1 pints (pt)
1 fluid ounce (fl oz) = 30 milliliters (ml)	1 liter (l) = 1.06 quarts (qt)
1 cup (c) = 0.24 liter (l)	1 liter (l) = 0.26 gallon (gal)
1 pint (pt) = 0.47 liter (l)	1 cubic meter (m^3) = 36 cubic feet (cu ft, ft^3)
1 quart (qt) = 0.96 liter (l)	1 cubic meter (m^3) = 1.3 cubic yards (cu yd, yd^3)
1 gallon (gal) = 3.8 liters (l)	
1 cubic foot (cu ft, ft^3) = 0.03 cubic meter (m^3)	
1 cubic yard (cu yd, yd^3) = 0.76 cubic meter (m^3)	
TEMPERATURE (EXACT)	**TEMPERATURE (EXACT)**
°C=5/9(°F - 32)	°F=9/5(°C) + 32

QUICK INCH-CENTIMETER LENGTH CONVERSION

INCHES	0	1	2	3	4	5

CENTIMETERS	0	1	2	3	4	5	6	7	8	9	10	11	12	13

QUICK FAHRENHEIT-CELSIUS TEMPERATURE CONVERSION

°F	-40°	-22°	-4°	14°	32°	50°	68°	86°	104°	122°	140°	158°	176°	194°	212°
°C	-40°	-30°	-20°	-10°	0°	10°	20°	30°	40°	50°	60°	70°	80°	90°	100°

For more exact and or other conversion factors, see NIST Miscellaneous Publication 286, Units of Weights and Measures. Price $2.50. SD Catalog No. C13 10286.

Updated 8/1/96

TABLE OF CONTENTS

Section **Page**

1. INTRODUCTION 1
   - 1.1 Background 1
   - 1.2 Structural Crashworthiness 1
   - 1.3 Interior Crashworthiness 2
2. OCCUPANT SURVIVABILITY FOR SELECTED STRUCTURAL CRASHWORTHINESS DESIGN OPTIONS 3
   - 2.1 Introduction 3
   - 2.2 Analysis Approach 4
     - 2.2.1 Scenarios 9
     - 2.2.2 Force/Crush Characteristics 9
       - 2.2.2.1 Conventional Design Train 10
       - 2.2.2.2 Crash-Energy Management Design Train 11
       - 2.2.2.3 Commuter Train 13
   - 2.3. Analysis Results 13
     - 2.3.1 Power Car, Six Coach, Power Car Collision with Similar Train . . . 14
     - 2.3.2 Power Car, Five Coach, Cab Car Collision with Similar Train 19
       - 2.3.2.1 Power Car to Power Car Collision 19
       - 2.3.2.2 Power Car to Cab Car Collision 24
       - 2.3.2.3 Cab Car to Cab Car Collision 28
     - 2.3.3 Power Car, Five Coach, Cab Car Collision with Commuter Train . 31
       - 2.3.3.1 Power Car to Commuter MU 31
       - 2.3.3.2 Cab Car to Commuter MU 38
   - 2.4 Analysis Conclusions 43
3. ANALYSIS OF INTERIOR OCCUPANT PROTECTION STRATEGIES 45
   - 3.1 Introduction 45
   - 3.2 Analysis Approach 45
     - 3.2.1 Secondary Impact Model 45
     - 3.2.2 Interior Arrangements 47

TABLE OF CONTENTS (continued)

Section **Page**

3.2.3 Occupant Protection Strategies 47
3.2.4 Vehicle Deceleration Time Histories (Crash Pulses) 50
3.2.5 Injury Criteria 51

3.3 Analysis Results 57

3.3.1 Seats in Rows Interior 57
3.3.2 Seats Facing 70
3.3.3 Seats and Table 75

3.4 Analysis Conclusions 79

3.4.1 Compartmentalization 79
3.4.2 Occupant Restraint 79
3.4.3 Crash Pulse 80

4. CONCLUSIONS 81

APPENDIX A. CRASH-ENERGY MANAGEMENT DESIGN 83

REFERENCES 97

LIST OF FIGURES

Figure		Page
2-1	Structural Crashworthiness Analysis Model	5
2-2	Interior Model	6
2-3	Seatback Force/Deflection Characteristic	7
2-4	Head Injury Criteria as a Function of Secondary Impact Velocity for Assumed Interior Conditions	8
2-5	Probability of Fatality as a Function of Head Injury Criteria	8
2-6	Conventional Design Car-to-Car Crush Characteristics	10
2-7	Car-to-Car Crush Characteristics, Power Car, Six Coach, Power Car Consist	11
2-8	Car-to-Car Crush Characteristics, Power Car, Five Coach, Cab Car Consist	12
2-9	Car-to-Car Crush Characteristics, Power Car, Five Coach, Cab Car Consist	12
2-10	Commuter MU Train Car-to-Car Crush Characteristic	13
2-11	Acceleration Time Histories, Each Car in the Consist, 100 mph Closing Speed	15
2-12	Velocity Time Histories, Each Car in the Consist, 100 mph Closing Speed	16
2-13	Relative Displacement Time Histories, Each Car in the Consist, 100 mph Closing Speed	17
2-14	Occupant Volume Loss for a Range of Closing Speeds, Power Car to Power Car Collision, Initially Moving Consist, Conventional Design	18
2-15	Occupant Volume Loss for a Range of Closing Speeds, Power Car to Power Car Collision, Initially Moving Consist, Crash-Energy Management Design	18
2-16	Occupant Relative Displacement Versus Occupant Relative Velocity, Cab Car to Power Car Collision, Initially Moving Consist	20
2-17	Occupant Secondary Impact Velocities, Initially Moving Consist	21
2-18	Occupant Volume Loss for a Range of Closing Speeds, Power Car to Power Car Collision, Initially Moving Consist, Conventional Design	23
2-19	Occupant Volume Loss for a Range of Closing Speeds, Power Car to Power Car Collision, Initially Moving Consist, Constrained Crash-Energy Design	23

LIST OF FIGURES (continued)

Figure **Page**

2-20 Occupant Secondary Impact Velocities, Initially Moving Consist 25

2-21 Occupant Volume Loss for a Range of Closing Speeds, Cab Car to Power Car Collision, Initially Moving Consist, Conventional Design 26

2-22 Occupant Volume Loss for a Range of Closing Speeds, Cab Car to Power Car Collision, Initially Moving Consist, Crash-Energy Management Design 26

2-23 Occupant Secondary Impact Velocities, Initially Moving Consist 27

2-24 Occupant Volume Loss for a Range of Closing Speeds, Cab Car to Cab Car Collision, Initially Moving Consist, Conventional Design 29

2-25 Occupant Volume Loss for a Range of Closing Speeds, Cab Car to Power Car Collision, Initially Moving Consist, Crash-Energy Management Design 29

2-26 Occupant Secondary Impact Velocities, Initially Moving Consist 30

2-27 Occupant Volume Loss for a Range of Closing Speeds, Power Car to Commuter MU, Power Car Propelled Passenger Train, Conventional Design 32

2-28 Occupant Volume Loss for a Range of Closing Speeds, Power Car to Commuter MU, Power Car Propelled Passenger Train, Crash-Energy Management Design 32

2-29 Occupant Volume Loss for a Range of Closing Speeds, Power Car to Commuter MU, Commuter Train, Conventional Design 33

2-30 Occupant Volume Loss for a Range of Closing Speeds, Power Car to Commuter MU, Commuter Train, Crash-Energy Management Design 33

2-31 Bar Chart of Occupant Secondary Impact Velocity, Power Car to Commuter MU, Power Car Propelled Passenger Train 35

2-32 Bar Chart of Occupant Secondary Impact Velocity, Power Car to Commuter MU, Commuter Train 36

2-33 Occupant Volume Loss for a Range of Closing Speeds, Cab Car to Commuter MU, Power Car Propelled Passenger Train, Conventional Design 39

2-34 Occupant Volume Loss for a Range of Closing Speeds, Cab Car to Commuter MU, Power Car Propelled Passenger Train, Crash-Energy Management Design 39

LIST OF FIGURES (continued)

Figure **Page**

2-35 Occupant Volume Loss for a Range of Closing Speeds, Cab Car to Commuter MU, Commuter Train, Conventional Design 40

2-36 Occupant Volume Loss for a Range of Closing Speeds, Cab Car to Commuter MU, Commuter Train, Crash-Energy Management Design 40

2-37 Bar Chart of Occupant Secondary Impact Velocity, Cab Car to Commuter MU, Power Car Propelled Passenger Train 41

2-38 Bar Chart of Occupant Secondary Impact Velocity, Cab Car to Commuter MU, Commuter Train 42

3-1 MADYMO Human Body Model 46

3-2 Interior Configurations 48

3-3 Interior Dimensions 49

3-4 Force /Deflection Characteristic of Seat Back 50

3-5 Basic Trainset Configuration 51

3-6 Deceleration of Each Car in the Consist, Head-to-Head Collision With 140 mph Closing Speed 52

3-7 Influence of Speed on First Coach Crash Pulse, 140 mph Head-to-Head Collision 53

3-8 Crash Pulses Used in Secondary Collision Analyses 54

3-9 Crash Pulse, First Coach, 140 mph Head-to-Head Collision, Crash-Energy Management Design, MADYMO Input and Train Model Results 55

3-10 Probability of Fatality Versus Head Injury Criteria 56

3-11 Injury Criteria for Tensile Neck Loads 58

3-12 Injury Criteria for Compressive Neck Loads 58

3-13 Occupant Motion, Unrestrained, Seats in Rows Interior 59

3-14 Comparison of MADYMO and Simplified Model Analysis Predictions, Occupant Relative Velocity Versus Occupant Relative Displacement, First Coach Car, 140 mph Head-to-Head Collision 60

LIST OF FIGURES (continued)

Figure **Page**

3-15 Comparison of MADYMO and Simplified Model Analysis Predictions, Occupant Relative Velocity Versus Occupant Relative Displacement, Cab Car, 140 mph Head-to-Head Collision 61

3-16 Human Body Kinematic Response to Initially Abrupt and Initially Gentle Crash Pulse, Seats in Rows Interior 62

3-17 Unrestrained Passenger and Vehicle Decelerations, 140 mph Head-to-Head Collision 63

3-18 Unrestrained Passenger and Vehicle Velocities, 140 mph Head-to-Head Collision 64

3-19 Secondary Impact Velocities for Occupants by Passenger Car 65

3-20 Occupant Motion, Restrained With Seat Belt and With Seat Belt and Shoulder Harness, Seats in Rows Interior 66

3-21 Restrained Passenger and Vehicle Decelerations 67

3-22 Restrained Passenger and Vehicle Velocities 68

3-23 Shear Force and Moment Acting on Seat Attachment 69

3-24 Forces on Forward Seat Back Due to Unrestrained Occupant (by Car) 71

3-25 Sum of Moments about Seat Floor Fixture Due to Unrestrained Occupant (by Car) 72

3-26 Forces on Seat Due to Restrained Occupant in First Coach Car 73

3-27 Moments on Seat Due to Restrained Occupant in First Coach Car 74

3-28 Motions for Occupants in Facing Seats Interior 77

3-29 Motions for Occupants in Seats and Table Interior 78

A-1 Crash-Energy Management Design Crush-Zone Locations 83

A-2 Crash-Energy Management Design Force/Crush Characteristic Development 84

A-3 Lumped Mass Model of Train Cars into Wall 84

A-4 Ideal Deceleration Characteristic 85

A-5 Schematic of Ideal Crush Zones Required to Impart Ideal Deceleration 86

LIST OF FIGURES (continued)

Figure **Page**

A-6 Desired Deceleration Characteristic for 70 mph Brick Wall Collision, Power Car Leading 87

A-7 Free Body Diagram of a Single Lumped Mass 88

A-8 Force Versus Time for All Cars 89

A-9 Velocity Versus Time for All Cars 89

A-10 Displacement Versus Time for All Cars 90

A-11 Power Car to Brick Wall Crush Zones Force/Deflection Characteristic Required to Ensure Occupant Survival in 140 mph Train-to-Train Collision 91

A-12 Coach Car to Coach Car Crush Zones Force Deflection Characteristic Required to Ensure Occupant Survival in 140 mph Train-to-Train Collision 91

A-13 Power Car to First Coach and Fifth Coach to Cab Car Crush Zone Force Deflection Characteristics Required to Ensure Occupant Survival in 140 mph Train-to-Train Collision 92

A-14 Power Car, Five Coach, Cab Car Consist Deceleration Characteristic, 45 mph Brick Wall Collision, Power Car Leading 93

A-15 Power Car, Five Coach, Cab Car Consist Deceleration Characteristic, 30 mph Brick Wall Collision, Cab Car Leading 93

A-16 Car-to-Car Crush Characteristics, Power Car, Five Coach, Cab Car Consist 94

A-17 Car-to-Car Crush Characteristics, Power Car, Five Coach, Cab Car Consist 94

A-18 Power Car, Six Coach, Cab Car Consist Deceleration Characteristic, 45 mph Brick Wall Collision, Cab Car Leading 95

A-19 Car-to-Car Crush Characteristics, Power Car, Six Coach, Power Car Consist 96

LIST OF TABLES

Table		Page
2-1	Weight of Each Car Type	4
2-2	Number of Occupants in Each Car Type	5
2-3	Scenarios Analyzed	9
2-4	Weight of Each Car Type	10
2-5	HIC, Cab Car to Power Car Collision, Initially Moving Consist, Conventional and Crash-Energy Management Designs	22
2-6	Fatalities, Conventional and Crash-Energy Management Designs	22
2-7	Fatalities, Conventional and Crash-Energy Management Designs, Power Car to Power Car Collision	24
2-8	Fatalities, Conventional and Crash-Energy Management Designs, Power Car to Cab Car Collision	28
2-9	Fatalities, Conventional and Crash-Energy Management Designs, Cab Car to Cab Car Collision	31
2-10	Total Fatalities, Power Car to Commuter MU Collision	37
2-11	Power Car Propelled Passenger Train Fatalities, Power Car to Commuter MU Collision	37
2-12	Commuter Train Fatalities, Power Car to Commuter MU Collision	37
2-13	Total Fatalities, Cab Car to Commuter MU Collision	43
2-14	Power Car Propelled Passenger Train Fatalities, Cab Car to Commuter MU Collision	43
2-15	Commuter Train Fatalities, Cab Car to Commuter MU Collision	44
3-1	AIS Code, HIC, and Chest Deceleration	55
3-2	Injury Criteria for Secondary Collisions of Unrestrained Occupants, Seats in Rows Interior	66
3-3	Peak Forces and Moments for Unrestrained Occupants Seated in Each Passenger Car During 140 mph Collision	75
3-4	Peak Forces and Moments for Occupants Seated in the First Coach Car During 140 mph Collision	75

LIST OF TABLES (continued)

Table **Page**

3-5 Injury Criteria and Fatality Rates for Secondary Collisions, Seated Rows 76

3-6 Injury Criteria and Fatality Rates for Secondary Collisions, Facing Seats 76

3-7 Injury Criteria and Fatality Rate for Secondary Collisions, Seats and Table 78

1. INTRODUCTION

1.1 BACKGROUND

This report evaluates different strategies for design of rail vehicle structures to provide crashworthiness of rail-passenger vehicles and different strategies for occupant protection. The results are presented in two sections: an analysis of occupant suvivability in train collisions for selected structural crashworthiness design options is presented in Section 2 and an analysis of the interior occupant protection strategies is presented in Section 3.

Trains may collide with a wide range of objects at various speeds under a number of different circumstances. Objects range from small, such as an animal on the tracks, to highway vehicles to maintenance-of-way equipment to another train. Most of these collisions can occur only in the normal running direction of the train, however, impact into the side of the train can occur at grade crossings. In addition, derailment can lead to the train rolling over, inducing high loads into the side of the cars and roof. Longitudinal collisions can occur at any speed up to the operating speed of the train. Highway vehicle collisions into the side of the train can occur for lower speeds.

In addition to the primary collision between the train and the impacted object, there is also a secondary collision between the occupants and the interior, including an occupant colliding with loose objects inside the train, such as baggage. Causes of any fatality associated with the primary collision include crushing of the occupant compartment, in which the occupants themselves are crushed, local penetration into the occupant compartment, where an object intrudes into the occupant compartment and directly strikes an occupant, and occupant ejection from the occupant compartment, where an occupant is thrown from the train and subsequently strikes some element of the wayside. Causes of any fatality associated with the secondary collisions include excessive deceleration of the head or chest of the occupant and excessive forces imparted to the body, such as axial neck loads.

In designing for crashworthiness, the first objective is to preserve a minimum occupant volume for the occupants to ride out the collision without being crushed, thrown from the train, or directly struck from something outside the train. The second objective is to limit the forces and decelerations imparted to the occupants to acceptable levels of human tolerance. Preserving occupant volume is accomplished with strength of the structure, i.e., if the occupant compartment is sufficiently strong, then there will be sufficient space for the occupants to ride out the collision and not be crushed. Limiting the decelerations and forces is accomplished through a combination of structural crashworthiness measures, allowing portions of the vehicle to crush in a pre-determined manner. This controlled crush, in turn, limits the decelerations of the vehicle and other interior crashworthiness measures, including the use of occupant restraints, such as seatbelts and shoulder harnesses, and the application of strategies such as compartmentalization [1].

1.2 STRUCTURAL CRASHWORTHINESS

The two structural design strategies evaluated are the conventional approach and the crash-energy management approach. Conventional practice is oriented toward making the individual cars as strong as they can be reasonably made, within weight and other design constraints, i.e., this approach attempts to control the behavior of individual cars during the collision. The crash-energy management approach is train oriented, allowing structural crushing to be distributed throughout the train to the unoccupied areas in order to preserve the occupant volumes and to limit the decelerations of the cars, i.e., this approach attempts to control the behavior of the entire train during the collision. This analysis compares the structural crashworthiness of passenger vehicles designed to conventional U.S. practice for crashworthiness and passenger vehicles designed to allow the ends of the cars to crush. This strategy of crash-energy management has received much attention in recent years in Japan [2], France [3], and England [4, 5, and 6].

1.3 INTERIOR CRASHWORTHINESS

The influences of the vehicle deceleration, the effectiveness of compartmentalization, lap belts, and lap belts and shoulder harnesses have been evaluated for three different interior configurations. Vehicle deceleration influences how hard the occupant strikes the interior, while compartmentalization is a strategy for limiting the forces and accelerations experienced by an unrestrained occupant. Passenger restraints (lap and shoulder belts) act to constrain the motion of the occupant during a collision. The interior configurations analyzed are seated rows, with consecutive rows of forward-facing seats, facing seats, with alternating rows of forward and rearward facing seats, and facing seats with a table. The interior configuration influences which interior surface the occupant strikes, and which part of the occupant strikes the interior.

2. OCCUPANT SURVIVABILITY FOR SELECTED STRUCTURAL CRASHWORTHINESS DESIGN OPTIONS

2.1. INTRODUCTION

Collision performance is defined as the ability to preserve occupant volume and the ability to limit secondary impact velocities to survivable levels during a collision. If these two objectives are met, then fatality due to the collision is avoided.

Conventional practice is oriented toward making the individual cars as strong as they can be reasonably made, within weight and other design constraints. This approach attempts to control the behavior of individual cars during the collision. A method for developing the crush-zone force/displacement characteristics and occupant volume strength required to limit secondary impact velocities and to preserve occupant volumes is described in Appendix A. This crash-energy management approach is train oriented, allowing structural crushing to be distributed throughout the train to the unoccupied areas in order to preserve the occupant volumes and to limit the decelerations of the cars. This approach attempts to control the behavior of the entire train during the collision.

This section presents a comparison of the structural crashworthiness of passenger vehicles designed to conventional practice for crashworthiness and passenger vehicles designed to allow the ends of the cars to crush. The performance of the two strategies has been evaluated in a number of different collision scenarios by exercising analytic models of two trains colliding and of occupant interior collisions. The train model consists of lumped masses connected with non-linear force/deformation characteristics, while the occupant model consists of a single lumped mass, representative of the occupant's head, which collides with the interior and is assumed to have some resiliency. The occupant model used to evaluate the interior occupant protection strategies is substantially more detailed than the occupant model used to evaluate the structural crashworthiness strategies. The simple model is sufficient for determining the influence of the vehicle structure on occupant fatality due to secondary impact, while the detailed model is necessary to evaluate changes in the nature of the secondary impact (such as those changes which occur when a lap belt is added to restrain the occupant). The train model is used to calculate the loss of occupant volume and the speed at which the occupant strikes the interior, while the occupant model is used to determine the deceleration of the head during the collision. Loss of occupant volume is used to predict crushing of seat space, and the head deceleration is used to calculate injury criteria, which are further related to probability of fatality. These analytic models were developed as part of this study and are described in detail in Section 2.

2.2 ANALYSIS APPROACH

To evaluate the performance of a train in a particular collision, the collision mechanics of the train must be estimated or determined; the likelihood of car-to-car override and lateral buckling of the train needs to be known; and the forces acting between cars and the crushing behavior of the cars must be developed. Once the behavior of the cars and the train have been determined, the interior performance can be evaluated. (A detailed review of transportation crashworthiness practice and research, and its applicability to passenger rail transportation, is presented in reference [17].)

The comparison between the two structural crashworthiness strategies is accomplished by developing the non-linear spring force/crush characteristics for the cars and applying a lumped-mass model to determine the occupant volume lost and the secondary impact velocities for a range of collision scenarios. The model consists of lumped masses connected by non-linear springs. It is assumed that the train stays in line and that individual cars can crush solid. Secondary impact velocities are calculated assuming that the occupants are seated in consecutive rows of forward-facing seats, with 2 $^1/_2$ feet from the occupant's forehead to the seatback ahead of him or her, and that the occupant remains at the initial train speed until he or she impacts an interior surface. Figure 2-1 shows a schematic of a lumped-mass train model, representative of the models used in the analysis.

In order to allow substantial crushing of the cars, the distributed mass of the carbody is approximated by a lumped mass at the rear of the car. For the same car type, both the conventional and the crash-energy management design are assumed to have equal weight. Table 2-1 lists the weights associated with each car type considered in the analysis. In order to conserve energy, each mass may rebound. The moving train is assumed to be in emergency braking at a rate of 0.2 gs. Each car in the standing consist can develop the braking force associated with a wheel/rail coefficient of friction of 0.2.

Table 2-1. Weight of Each Car Type

Car Type	Weight, Kips
Power Car	180
Cab Car	120
1st Class, Coach, and Food-Service Cars	120
MU Commuter Car	140

Loss of Occupant Volume

Fatality due to loss of occupant volume is estimated by calculating the reduction in occupant volume length and by assuming that fatalities are proportional to this length normalized to the initial occupant volume length. Table 2-2 lists the number of occupants and initial occupant volume lengths for each of the car types considered.

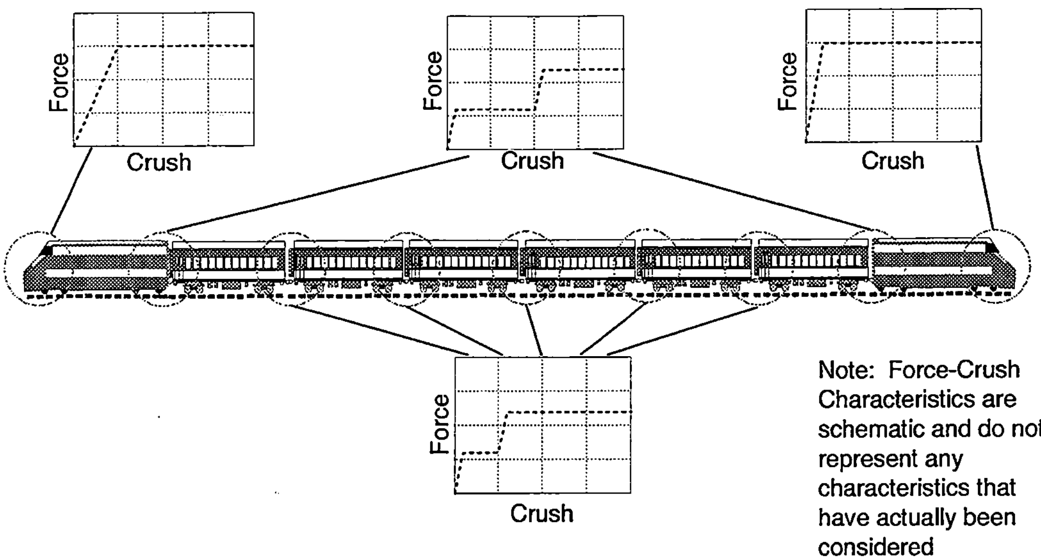

Figure 2-1. Structural Crashworthiness Analysis Model

Table 2-2. Number of Occupants in Each Car Type

Car Type	Number of Occupants	Initial Occupant Volume Length (Feet)	
		Conventional Design	Crash-Energy Management Design
Power Car	2	7.00	7.00
1st Class Car	44	77.00	72.00
Coach Car	74	77.00	72.00
Food-Service Car	74	77.00	72.00
Cab Car	48	77.00	58.50
MU Commuter Car	125	82.00	N/A

Secondary Impact

When sufficient volume is preserved for the occupant to ride out the collision, the occupant can still be injured by excessive deceleration or forces. These forces and decelerations principally come about, for an unrestrained occupant, when the occupant strikes the interior. (Occupant impacts with the interior or collisions between occupants and loose objects thrown about during the collision are usually termed secondary collisions; the primary collision considered here is the collision between the two trains.) How hard the occupant strikes the interior depends upon the deceleration of the train itself during the collision and the degree of “friendliness” of the interior. In order to provide a basis for comparison between the decelerations generated by the conventional design and by the constrained crash-energy management design, a simplified model of an occupant is used to calculate the decelerations of the occupants head. These decelerations are then compared with accepted injury criteria.

A sketch of the occupant model is shown in Figure 2-2. The occupant model is based on the assumption that the occupant goes into free flight at the start of the collision and subsequently, after traveling some distance, strikes the interior. The occupant is assumed to strike the seatback ahead of him or her, which has some amount of padding and flexibility. Given the seatback force/deflection characteristic and the nominal mass of the head, the deceleration of the head can be calculated from the velocity with which the head impacts the seatback. The head deceleration can then be evaluated based upon generally accepted injury criteria. The distance from the occupant’s nose to the seatback ahead of him or her is assumed to be 2 1/2 feet, i.e., the seat pitch is assumed to be 42 inches, and the occupant’s head is assumed to be 8-inches deep, and the padding on the seat is assumed to be 4-inches thick.

The seatback force/deflection characteristics used in the analysis are shown in Figure 2-3. The characteristic for the power car propelled passenger train seats used in the analysis is the softest characteristic described in the NHTSA Standard 49CFR571.222 - School Bus Seating and Crash Protection [18], while the characteristic used for the commuter train seats is the stiffest characteristic described in the Standard.

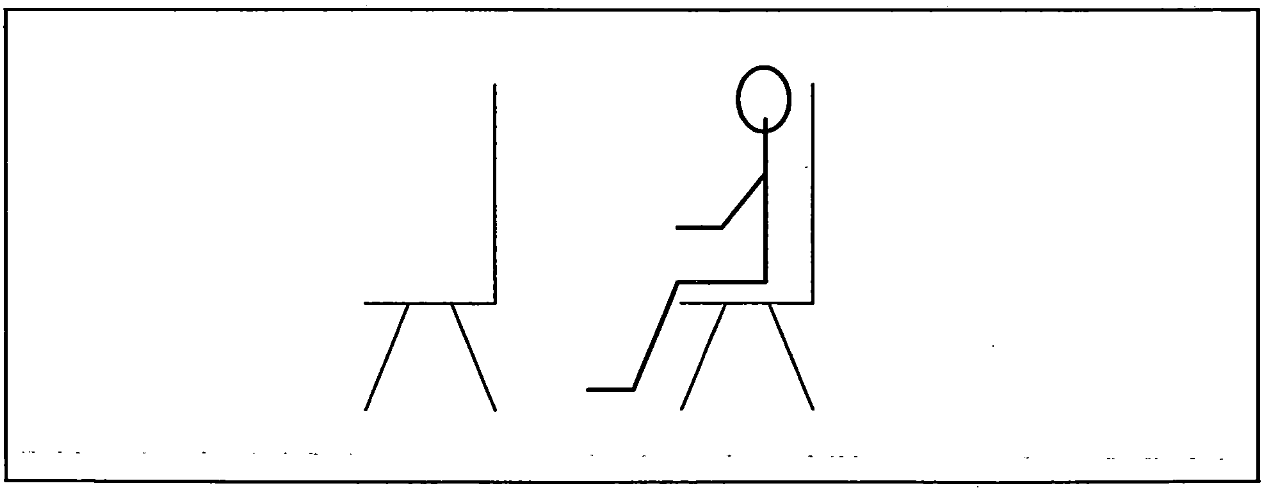

Figure 2-2. Interior Model

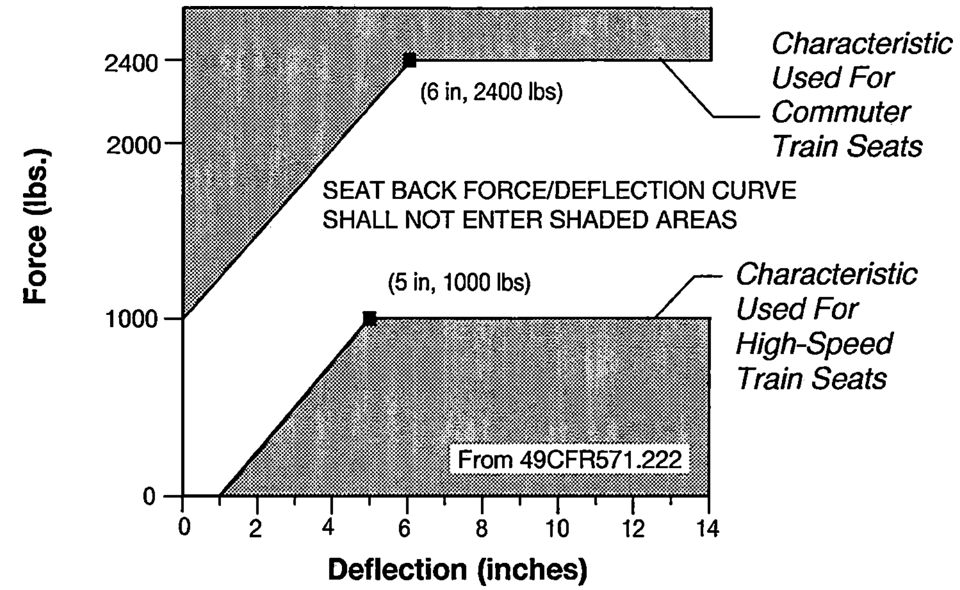

Figure 2-3. Seatback Force/Deflection Characteristic

The deceleration time history of the head can be used to calculate the HIC [19], an injury criteria widely applied in the automotive and aircraft industries to evaluate test and analysis data.

Figure 2-4 shows a plot of HIC as a function of secondary impact velocity for the seatback force/deflection characteristics shown in Figure 2-3. The force/deflections shown in Figure 2-4 do not fully describe the seatback behavior; the seatback may behave in either of two different extremes, or in some combination of those two extremes. In an elastic secondary collision, the occupant is fully pushed back into his initial position. In a plastic secondary collision, however, the seatback does not push back at all.

The HIC is a function of the acceleration of the head during impact [20] and is used to predict the probability of fatality resulting from head injury. As required in Standard 49CFR571.208 by the NHTSA, the HIC value shall not exceed 1000 for a vehicle impacting a fixed collision barrier at speeds up to 30 mph. This corresponds to a predicted fatality rate of approximately 18 percent. This probability of fatality is predicted for the 50th percentile male. Figure 2-5 from reference [21] shows a plot of the probability of fatality as a function of HIC.

The occupant's velocity relative to the car is calculated from a lumped-mass train collision model. This velocity is then used to determine the range of injury criteria, shown in Figure 2-4. The injury criteria are then used to determine the probability of fatality for the 50th percentile male, shown in Figure 2-5. Fatality due to secondary collision is then calculated by taking the percentage of occupants with sufficient occupant volume to survive the collision — the analysis only allows the occupants to be killed by loss of occupant volume or by the secondary collision, not by both. Fatality figures for the train are produced by repeating this procedure for each car in the train.

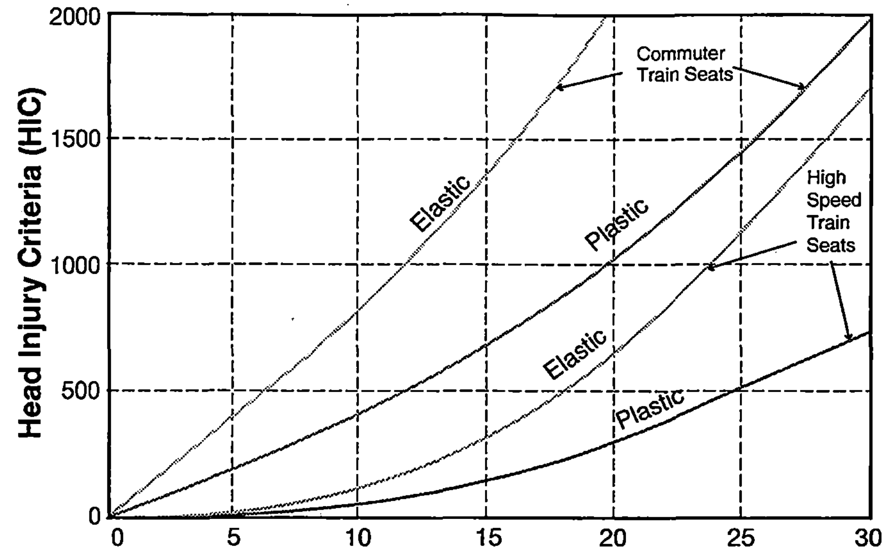

Figure 2-4. Head Injury Criteria as a Function of Secondary Impact Velocity for Assumed Interior Conditions

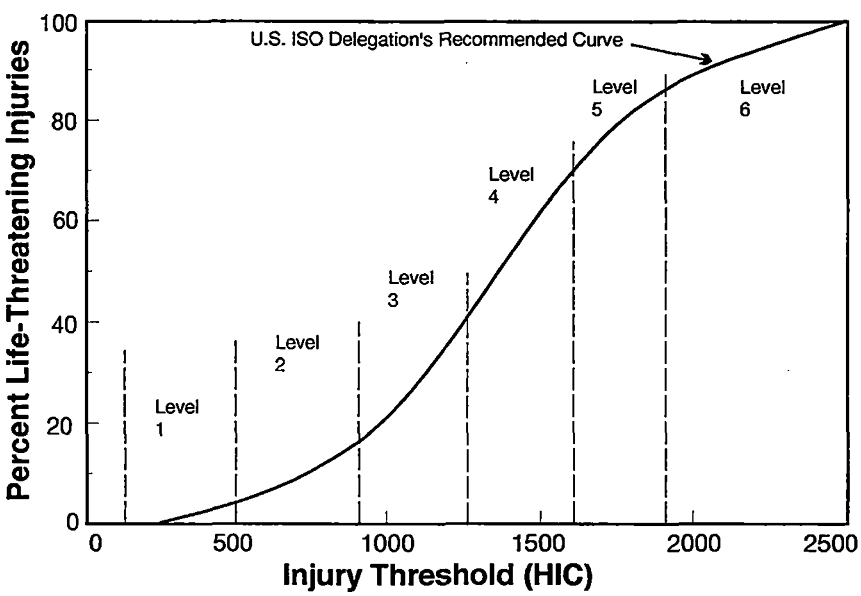

Figure 2-5. Probability of Fatality as a Function of Head Injury Criteria [21]

2.2.1 Scenarios

The two different structural design strategies were evaluated for several train-to-train collision scenarios. Two different power car propelled passenger train consists were evaluated: a power car, six coach, power car consist and a power car, five coach, cab car consist. Collision scenarios evaluated include power car propelled passenger train to power car propelled train collisions and power car propelled train to Multiple-Unit (MU) train collisions. This combination of train consists allowed the evaluation of the influence of power car leading versus cab car leading in a collision, as well as the influence of structural similarity (power car propelled train colliding with similar power car propelled train versus power car propelled train colliding with commuter MU train) in a collision. The scenarios analyzed are briefly described in Table 2-3. These descriptions include the train make-ups analyzed and the cars which initially meet in the collision. In each of the scenarios, one train is initially stationary, while the other train collides with it at some initial speed. Each of the scenarios was evaluated for closing speeds of 35, 70, 110, and 140 mph.

Table 2-3. Scenarios Analyzed

Moving Consist Makeup (Train 1)	Standing Consist Makeup (Train 2)	Colliding Cars
Power car, six coach, power	Power car, six coach, power	Power car, six coach, power
Power car, five coach, cab car	Power car, five coach, cab car	Power car to power car Power car to cab car Cab car to cab car
Power car, five coach, cab car	Ten car commuter MU	Power car to commuter MU Cab car to commuter MU

2.2.2 Force/Crush Characteristics

The comparison between the two structural crashworthiness strategies is accomplished by developing the non-linear force/crush characteristics for the cars and applying a lumped-mass model to determine the occupant volume lost and the secondary impact velocities for a range of collision scenarios. For a particular train-to-train collision scenario, the principal train characteristics that influence the results of the collision are the non-linear force/crush characteristic and the masses of the cars. The masses of the cars are the same for both the crash-energy management design and the conventional design power car propelled trains and were assumed to be fixed for this analysis. The weights of the various cars, including the commuter MU cars, are listed in Table 2-4. The principal characteristic that varied in the analysis was the force/crush characteristic between the cars.

Table 2-4. Weight of Each Car Type

Car Type	Weight, Kips
Power Car	180
Cab Car	120
1st Class, Coach, and Food-Service Cars	120
MU Commuter Car	140

2.2.2.1 Conventional Design Train

Figure 2-6 shows the car-to-car force/crush characteristic used for the conventional car in the analysis. This characteristic is based upon the force/crush characteristic developed by Calspan for the Silverliner car [7], modified to allow for a shear-back coupler design and a more gradual crushing of the end structure. It should be noted that the maximum strength developed is the force required to cause gross yielding of the structure, which is considerably higher than the force required to cause permanent deformation.

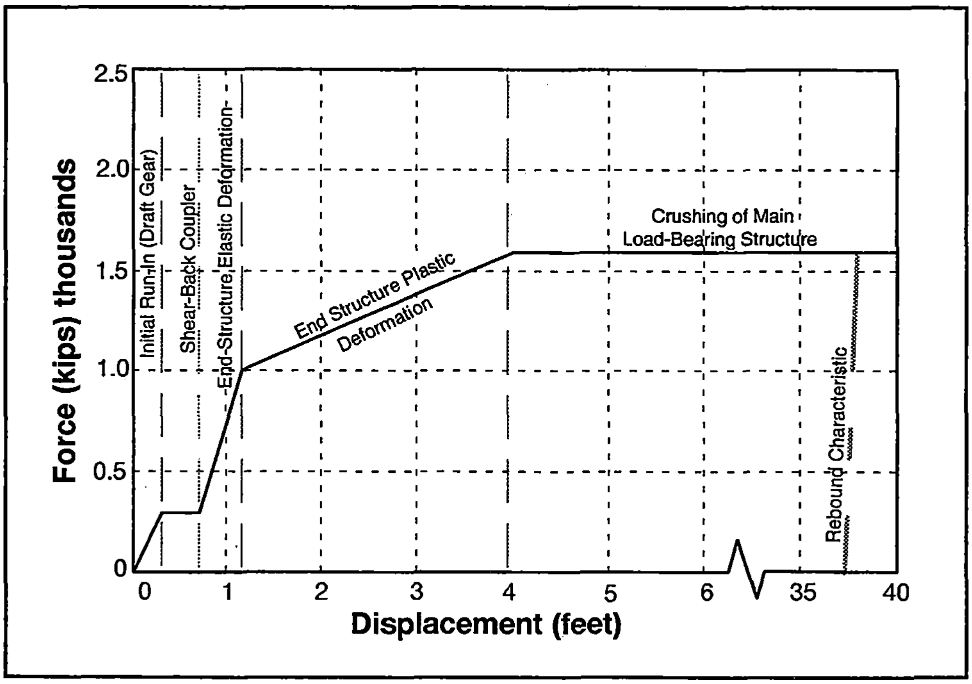

Figure 2-6. Conventional Design Car-to-Car Crush Characteristics

2.2.2.2 Crash-Energy Management Design Train

The force/crush characteristics between the cars of the crash-energy management design train were determined by developing and applying a design strategy for preserving the occupant volumes in the cars and limiting the secondary impact velocities in the cars. These force/crush characteristics were developed with constraints on the distances crushed and the longitudinal carbody forces developed. For the coach cars, the longitudinal forces were constrained to be between 1.6 million pounds, presuming that greater strength would incur excessive vehicle weight, and 400 thousand pounds, presuming that less strength would impair the vehicle's ability to support service loads. For the relatively short length of the operator's cab, the maximum force is constrained to 2 million pounds. Constraints placed on crush distances included 4 feet of available crush distance ahead of the operator's cab, 25.5 feet of available crush distance at the rear of the power car, 11 feet behind the operator's cab in the cab car, and 4.5 feet of available crush distance at each end of all the coach cars. This design strategy and the development of the corresponding force/crush characteristics are described in detail in Appendix A. The force/crush characteristics for the power car, six coach, power car consist are shown in Figure 2-7. The force/crush characteristics for the power car, five coach, cab car consist are shown in Figures 2-8 and 2-9. The cab car has a crush zone between the operator's cab and the occupant compartment, and the maximum total crush of the operator's cabs when two cab cars collide head on is 18 feet. The force/crush characteristic for two colliding cab cars (i.e., two colliding operator's cabs) is denoted as 'Cab Car - Cab Car' in Figure 2-9 while the force/crush characteristic for the crush zone between the operator's cab and the occupant compartment is denoted as 'Half Cab Car - Half Cab Car'.

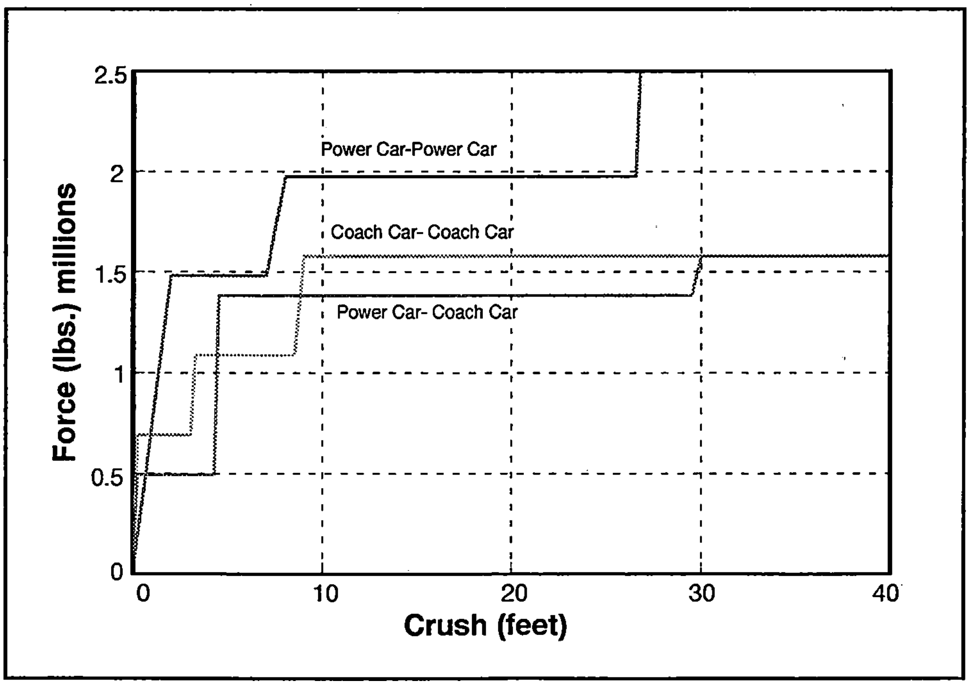

Figure 2-7. Car-to-Car Crush Characteristics, Power Car, Six Coach, Power Car Consist

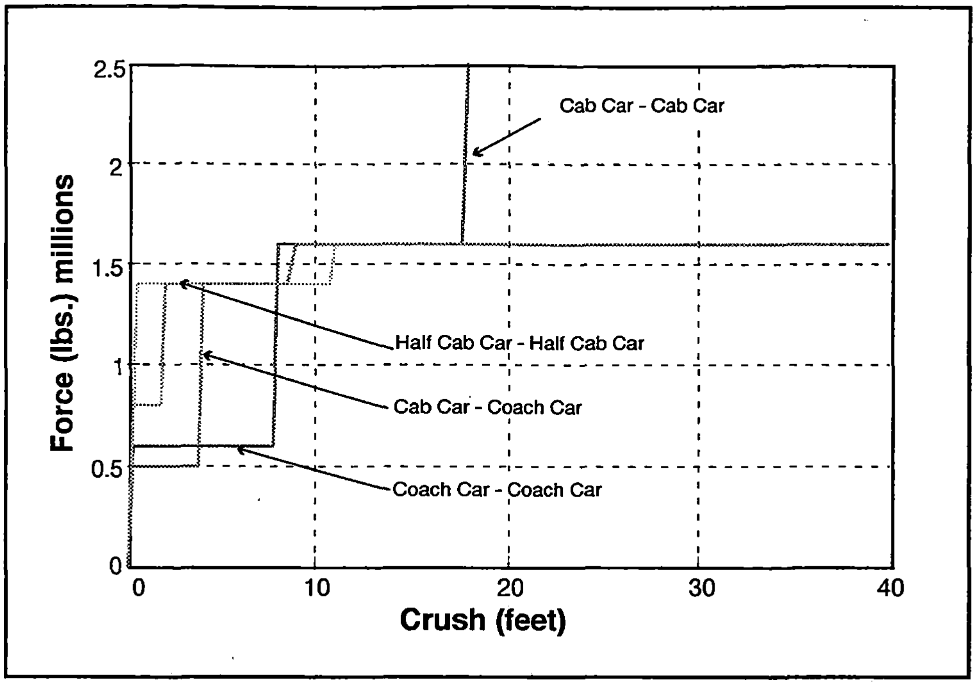

Figure 2-8. Car-to-Car Crush Characteristics, Power Car, Five Coach, Cab Car Consist

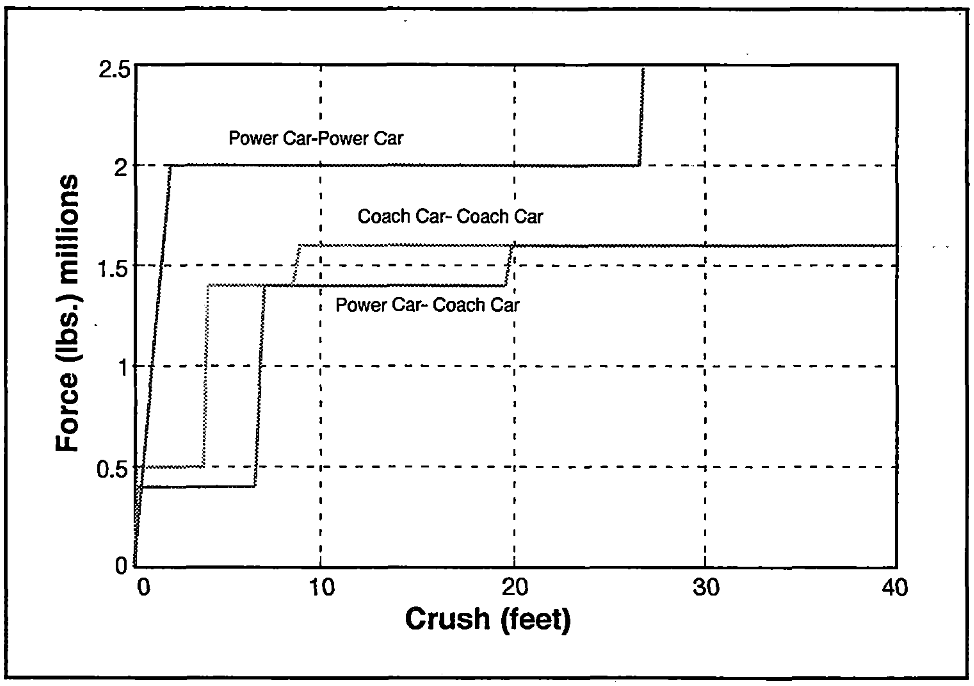

Figure 2-9. Car-to-Car Crush Characteristics, Power Car, Five Coach, Cab Car Consist

2.2.2.3 Commuter Train

The commuter consist is made up of ten identical cars, and the commuter car to commuter car force/crush characteristic is shown in Figure 2-10. (The commuter car to power car propelled train power car and the commuter car to power car propelled train cab car force/crush characteristics are developed from the commuter car to commuter car, power car to power car, and cab car to cab characteristics.) The interior of the commuter train is assumed to be less friendly than the interior of the power car propelled train, with the seatbacks of the commuter car stiffer than the seatbacks of the power car propelled train, as discussed in Section 2.

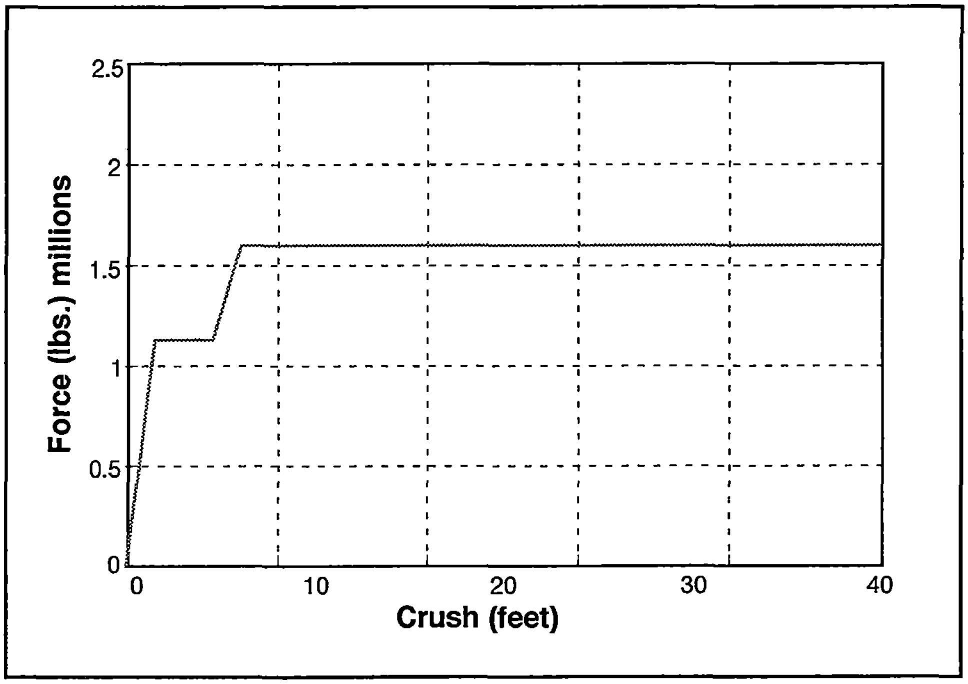

Figure 2-10. Commuter MU Train Car-to-Car Crush Characteristic

2.3 ANALYSIS RESULTS

The collision scenarios analyzed are all of a moving power car propelled train colliding with a standing train. These scenarios were analyzed for both design strategies, the conventional and the constrained crash-energy management. Three different power car propelled train make-ups were analyzed: a power car, six coach, power car consist, and two power car, five coach, cab car consists. The power car, five coach, cab car consist was analyzed for three different power car propelled train to (identical) power car propelled train collision conditions: power car to power car; power car to cab car; and cab car to cab car. This consist also was analyzed for two different power car propelled train to commuter train collision conditions: power car to commuter MU and cab car to commuter MU. The basis for comparison is the loss of occupant volume, expressed as a percentage of reduction in occupant volume length, and the deceleration imparted to the occupants during the secondary impact between the occupant and the seatback or barrier ahead of him or her.

2.3.1 Power Car, Six Coach, Power Car Collision With Similar Train

The scenario considered is a moving train colliding with a standing train. Both designs were analyzed for their performance in this scenario for a range of closing speeds. The basis for comparison is the loss of occupant volume and the deceleration imparted to the occupants during the secondary impact between the occupant and the seat back ahead of him.

Figure 2-11 shows the time histories for the accelerations of each of the cars in the initially moving train for a collision of a train moving at 100 mph into a standing train for both the conventional design and the constrained crash-energy management design. This figure shows that each design goes through the collision in substantially different ways. For the conventional design there is substantial overlap in the deceleration time histories of the cars, while for the crash-energy management design there is a large degree of separation between the deceleration time histories of each of the cars. The deceleration time history plot shows a large deceleration at approximately 1 second for the lead power cars. This large deceleration is a consequence of the cars being crushed solid.

Figure 2-12 shows the velocity time histories for each of the cars in both the initially standing and initially moving trains. This figure also shows that each design goes through the collision in substantially different ways. For the conventional design the train essentially acts as a single unit during the collision, while for the crash-energy management design each car largely undergoes its own collision.

Figure 2-13 shows the relative displacements between the centers of gravity of each of the cars in the two trains. Essentially, for the conventional design, the crush progresses from the front of the train toward the rear of the train during the collision, moving through both occupied and unoccupied portions of the train. For the constrained crash-energy management design, a substantial amount of crush is moved to the unoccupied areas between the cars which are away from the point of impact.

Loss of occupant volume is calculated from the relative displacement of the cars. For the two cars which meet in the collision, the crushing of the fronts of the cars is symmetric. Between cars in a train, the force/crush characteristic can be used to determine which car crushes, until the maximum force is achieved. Once the maximum force is reached, the crushing proceeds from front to back (away from the center of the collision). The amount of occupant volume lost is the distance of the car crushed less the distance associated with the structure at each end of the car, as discussed in Section 2.

Occupant Volume - Figure 2-14 illustrates the occupant volume lost in each of the cars for the conventional design train for four closing speeds ranging from 35 mph to 140 mph. Most of the occupant volume lost is in the first coach car. The figure shows that the crushing of the train starts at the front and proceeds toward the rear of the train. Figure 2-15 illustrates the occupant volume lost in each of the cars for the constrained crash-energy management design train for four closing speeds ranging from 35 mph to 140 mph. The figure shows that this design approach is successful in distributing the crush throughout the train. The figures show that for closing speeds up to about 70 mph, the conventional design preserves all the passenger volume, while the constrained crash-energy management design preserves most of the passenger volumes up to 110

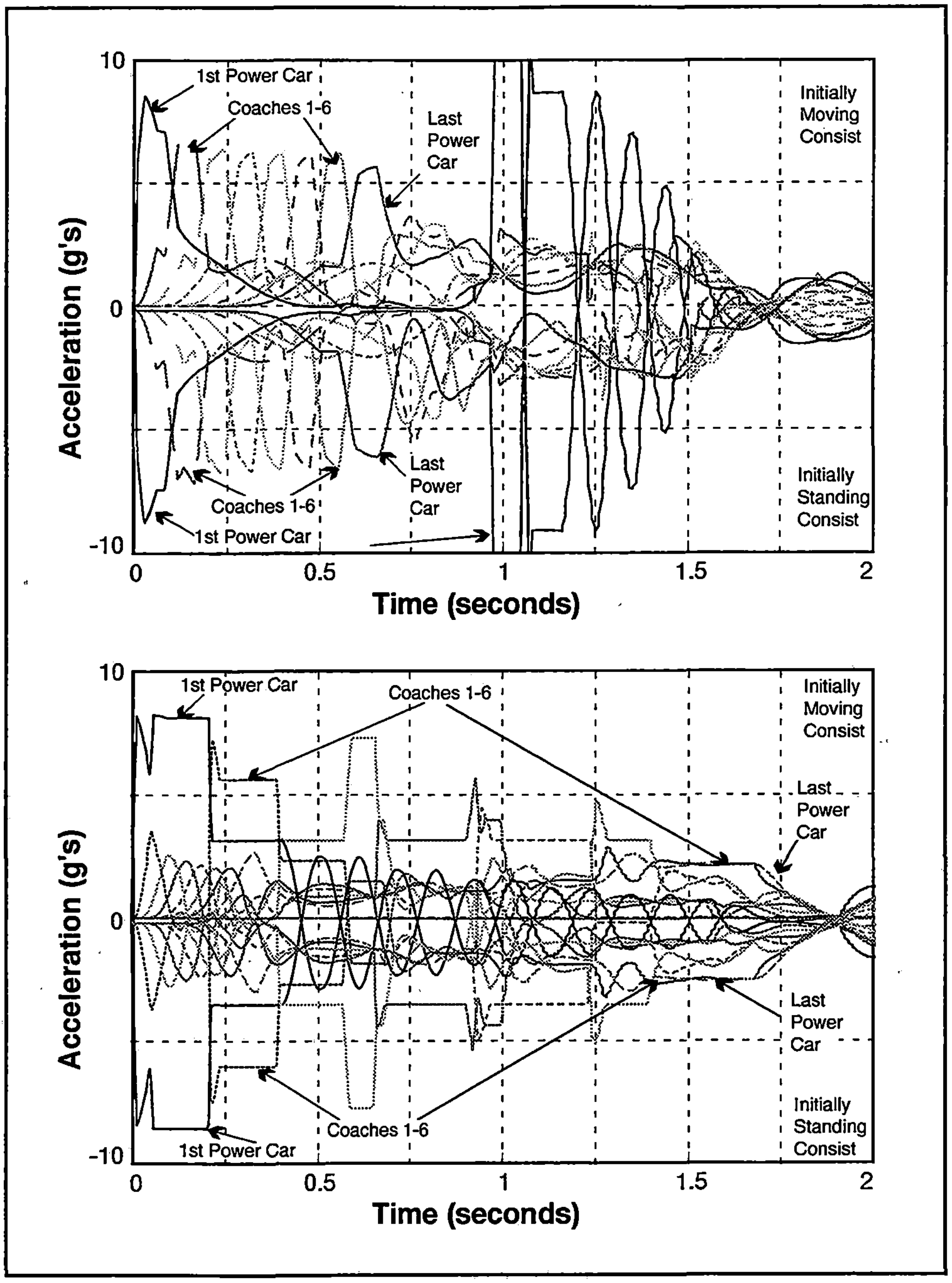

Note: Conventional Design (top), Crash-Energy Management Design (bottom)

Figure 2-11. Acceleration Time Histories, Each Car in the Consist, 100 mph Closing Speed

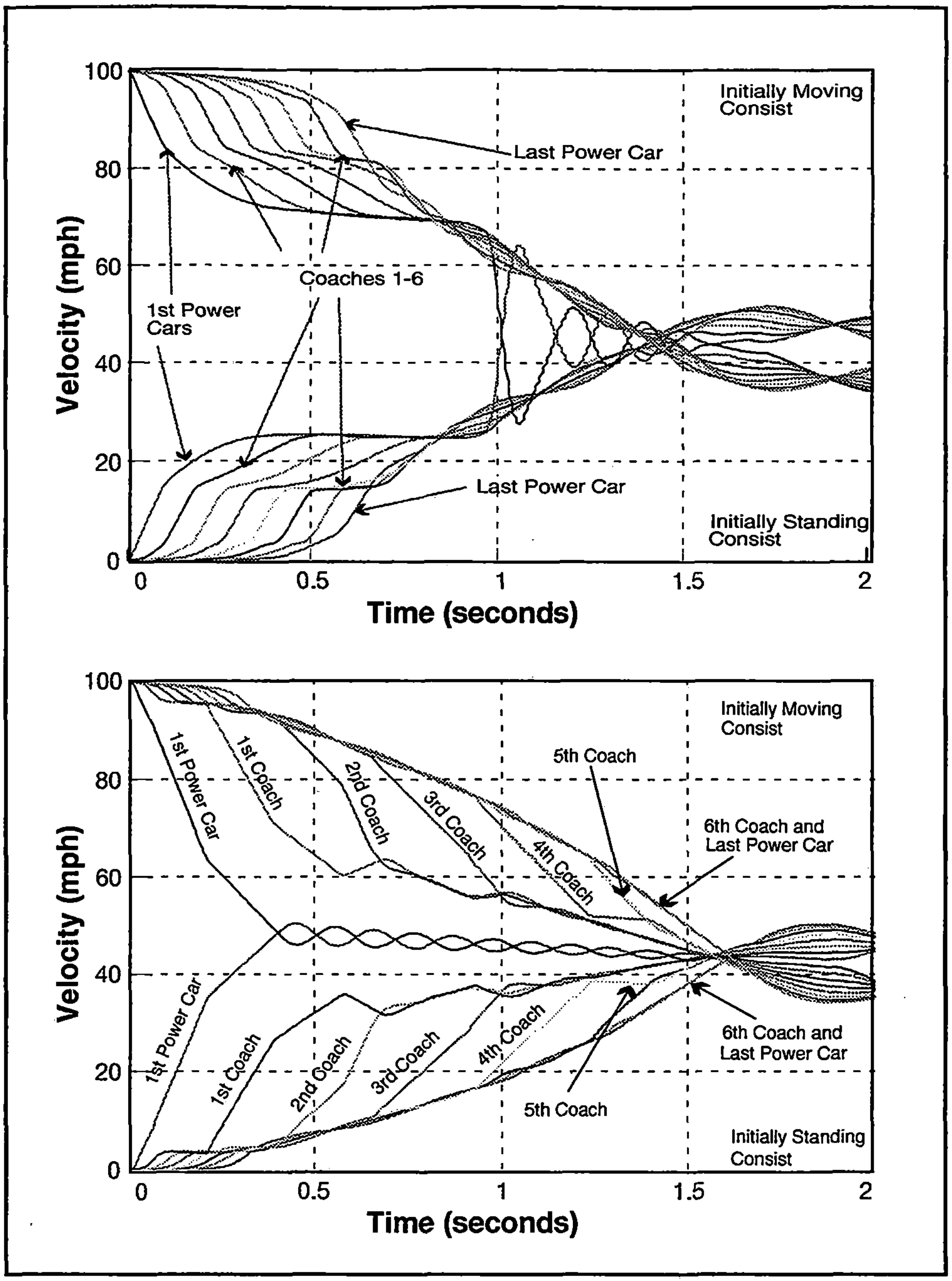

Note: Conventional Design (top), Crash-Energy Management Design (bottom)

Figure 2-12. Velocity Time Histories, Each Car in the Consist, 100 mph Closing Speed

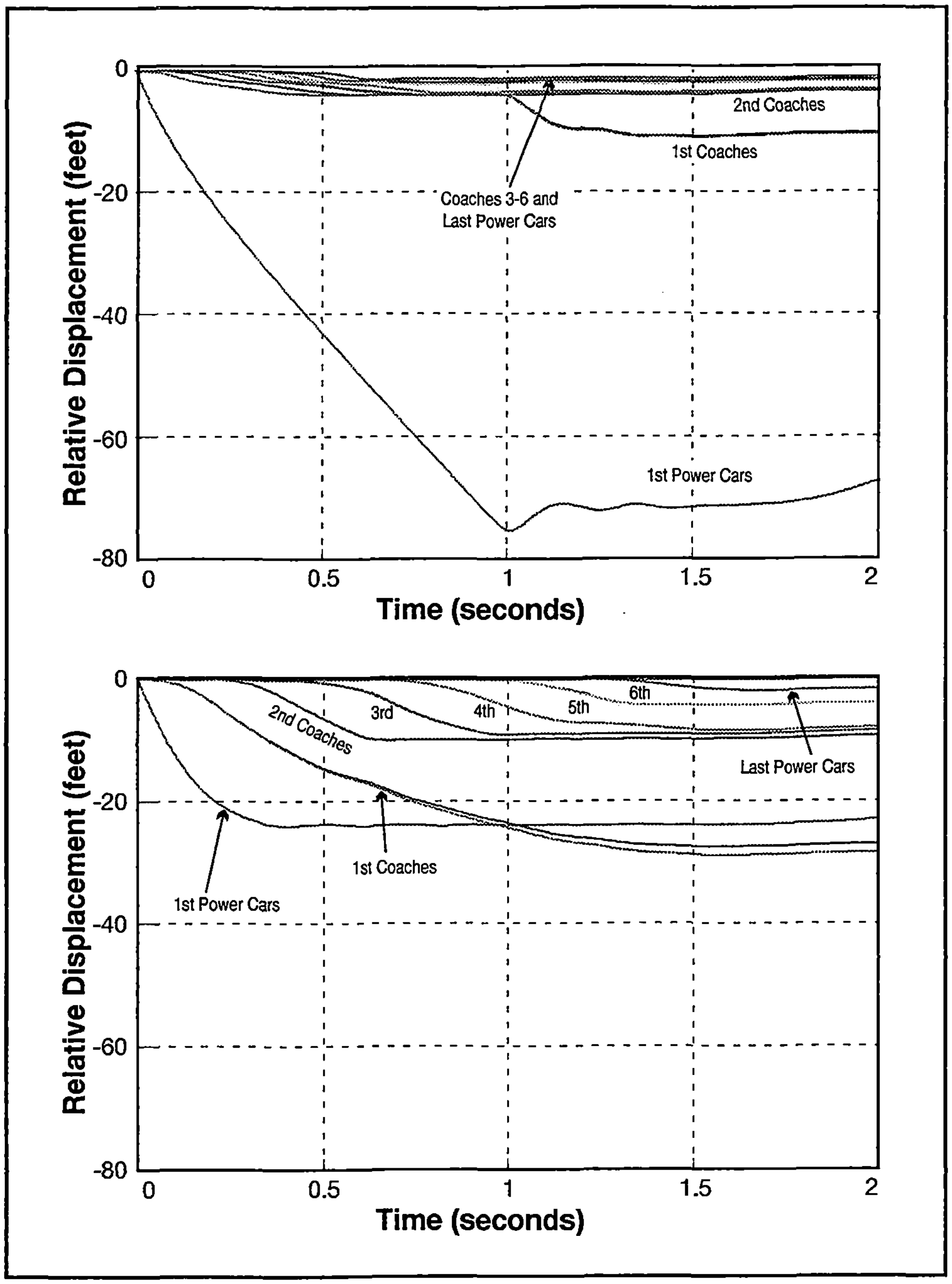

Note: Conventional Design (top), Crash-Energy Management Design (bottom)

Figure 2-13. Relative Displacement Time Histories, Each Car in the Consist, 100 mph Closing Speed

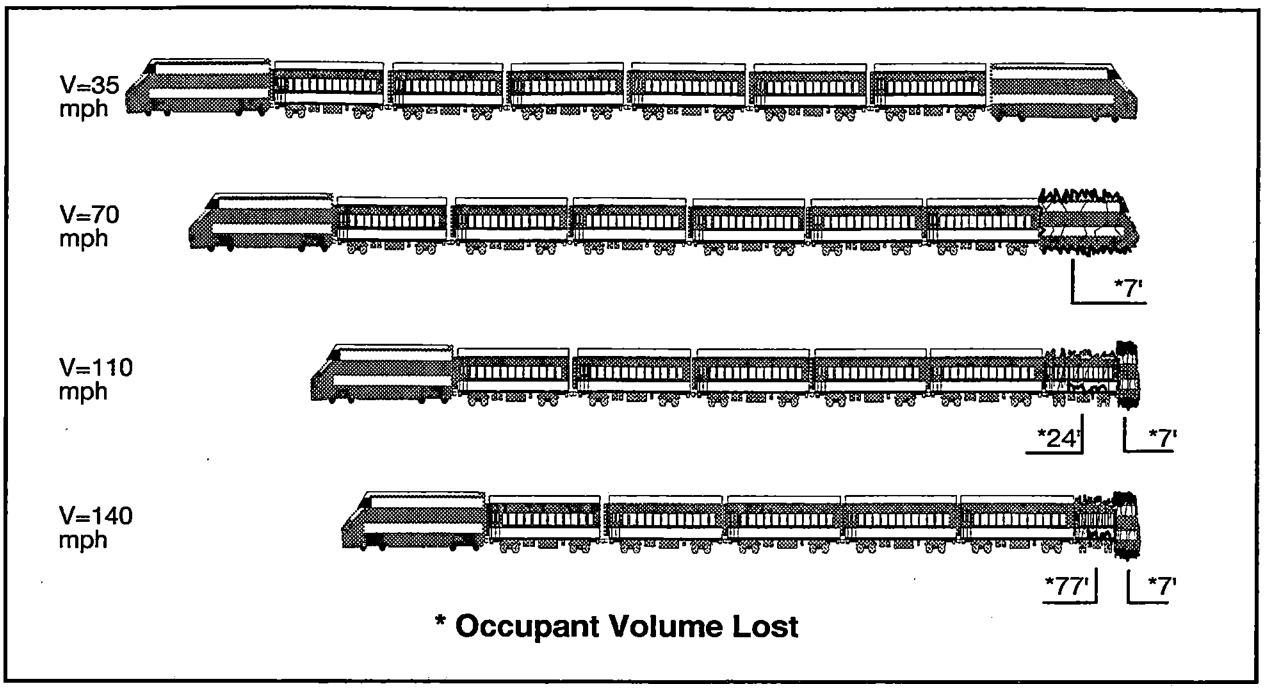

Figure 2-14. Occupant Volume Loss for a Range of Closing Speeds, Power Car to Power Car Collision, Initially Moving Consist, Conventional Design

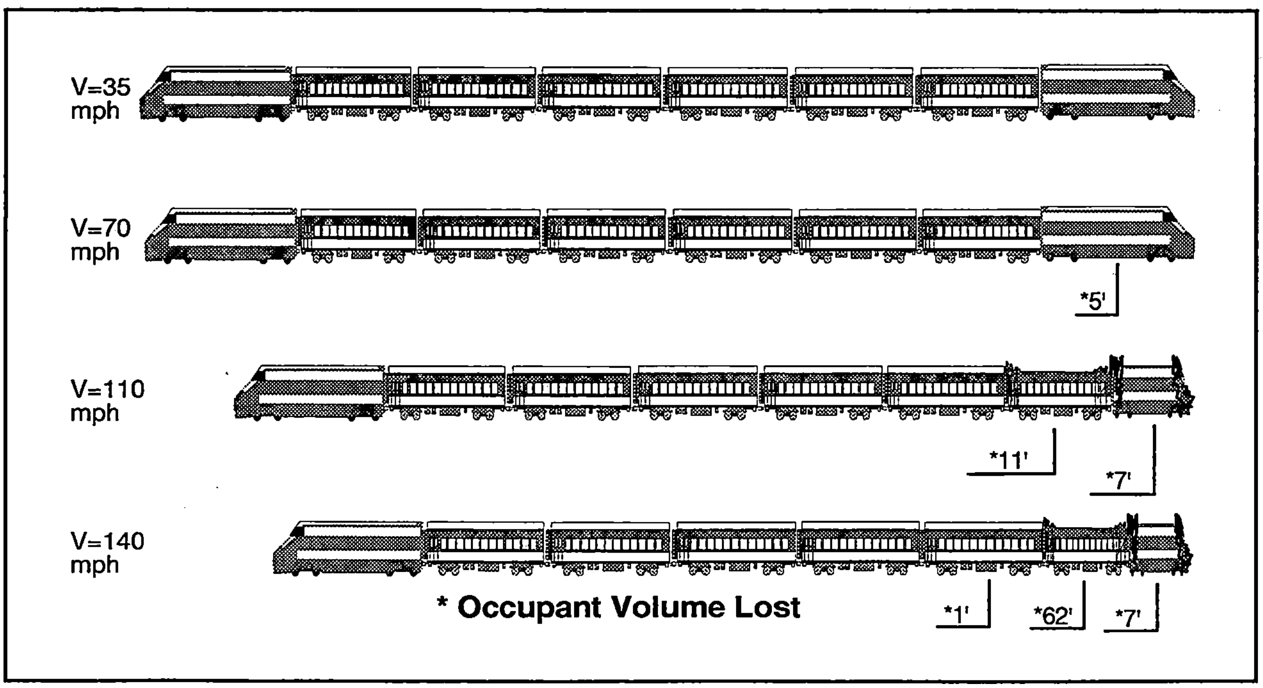

Figure 2-15. Occupant Volume Loss for a Range of Closing Speeds, Power Car to Power Car Collision, Initially Moving Consist, Crash-Energy Management Design

mph. The additional occupant volume lost for closing speeds above 70 mph is much greater for the conventional design than the constrained crash-energy management design.

Occupant Deceleration - Figure 2-16 shows plots of occupant velocity relative to the vehicle as a function of displacement relative to the vehicle for both the constrained crash-energy management design and conventional design at 100 mph. The distance from the occupant's nose to the seat back ahead of him is assumed to be 2 1/2 feet — the seat pitch (longitudinal distance between two seats one row apart) is assumed to be 42 inches, the occupant's head is assumed to be 8-inches deep, and the padding on the seat is assumed to be 4-inches thick. The secondary impact velocity for the power car occupant in the crash-energy management design is greater than that in the conventional design. Increased protection of the power car occupant volume is achieved in the crash-energy management design at the expense of increased secondary impact velocity. The assumption is that increased protection against secondary collision (such as seat belts, or increased interior padding) can be provided for the occupants in the power car. The secondary impact velocity in the first coach car is the same for both designs, while for all remaining cars, the crash-energy management design provides substantially lower secondary collision velocities than the conventional design.

Figure 2-17 shows the secondary impact velocities for each of the cars in the initially moving consists, for both the crash-energy management design and the conventional design trains, for primary collision speeds of 140, 110, 70, and 35 mph. The secondary impact speed does not change significantly for primary collision speeds above 35 mph for the conventional design while they do not change significantly for primary collision speeds above 70 mph for the crash-energy management design. Secondary impact velocities are not strongly influenced by the primary collision speed because the secondary impact speed is principally a function of the first portion of the deceleration crash pulse, i.e., the secondary collision occurs soon after the primary collision starts and well before the primary collision ends. Increasing primary collision closing speed has a greater influence on the final portion of the crash pulse than on the initial portion.

Fatalities - Table 2-5 lists the range of Head Injury Criteria (HIC) values expected on the moving train for several collision speeds, for both the crash-energy management and conventional design trains. The crash-energy management design results in substantially lower HIC values. This is a result of the lower secondary collision velocities for most of the cars in the consist.

Table 2-6 lists the predicted fatalities owing to occupant volume loss and secondary impacts for a train with the power car leading colliding with the power car of a standing train. Most of the fatalities are predicted to be due to loss of occupant volume; this prediction is consistent with the outcomes of actual collisions [8]. The crash-energy management design provides significant benefits in this scenario for all speeds considered; this design is consistently more effective in preserving occupant volume and limiting fatalities due to secondary impacts.

2.3.2 Power Car, Five Coach, Cab Car Collision With Similar Train

2.3.2.1 Power Car to Power Car Collision

Occupant Volume - Figure 2-18 illustrates the occupant volume lost in each of the cars for the conventional design train for four closing speeds ranging from 35 mph to 140 mph. Most of the occupant volume lost is in the first coach car. The figure shows that the crushing of the train

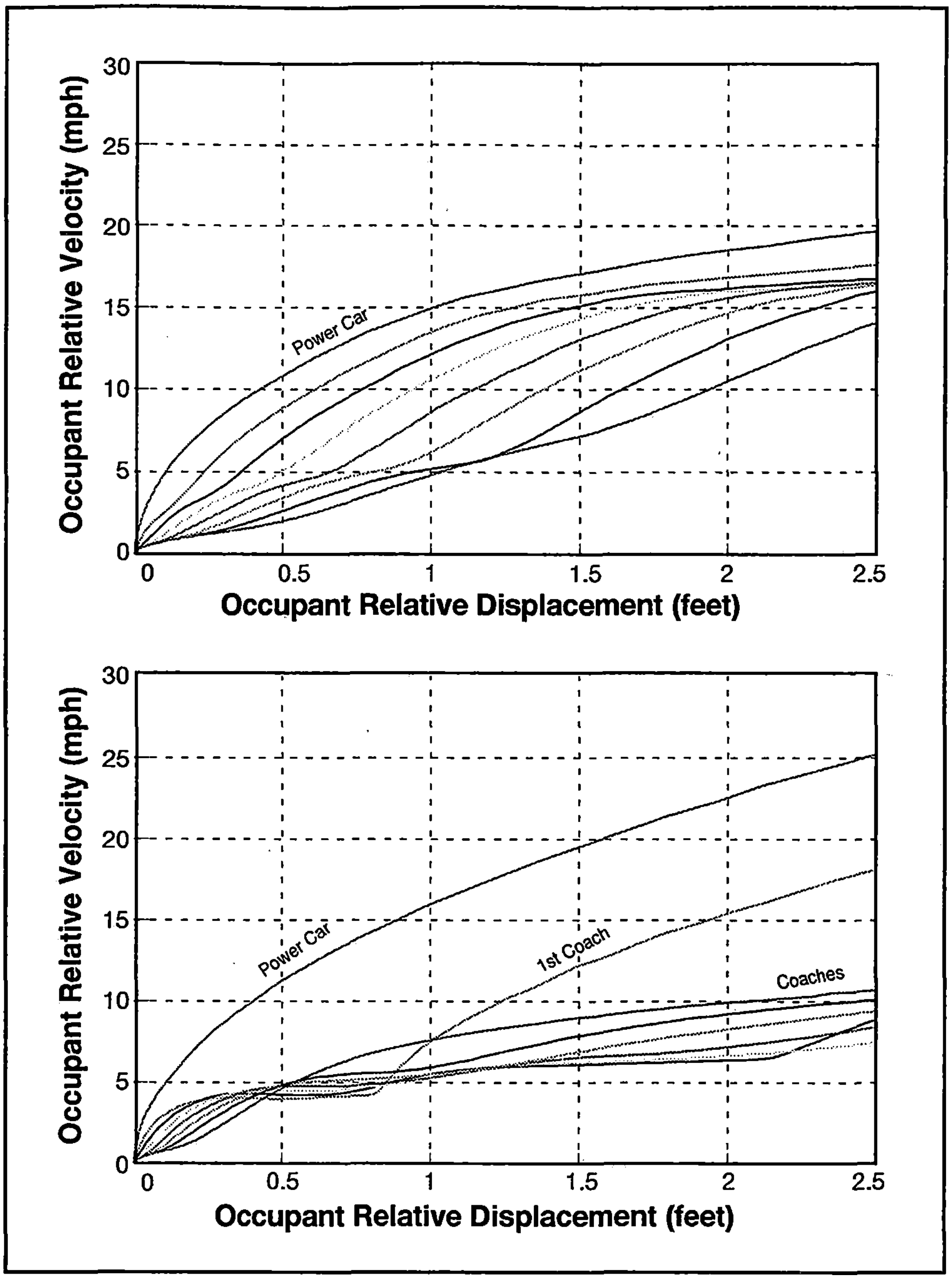

Note: Conventional Design (top), Crash-Energy Management Design (bottom)

Figure 2-16. Occupant Relative Displacement versus Occupant Relative Velocity, Cab Car to Power Car Collision, Initially Moving Consist

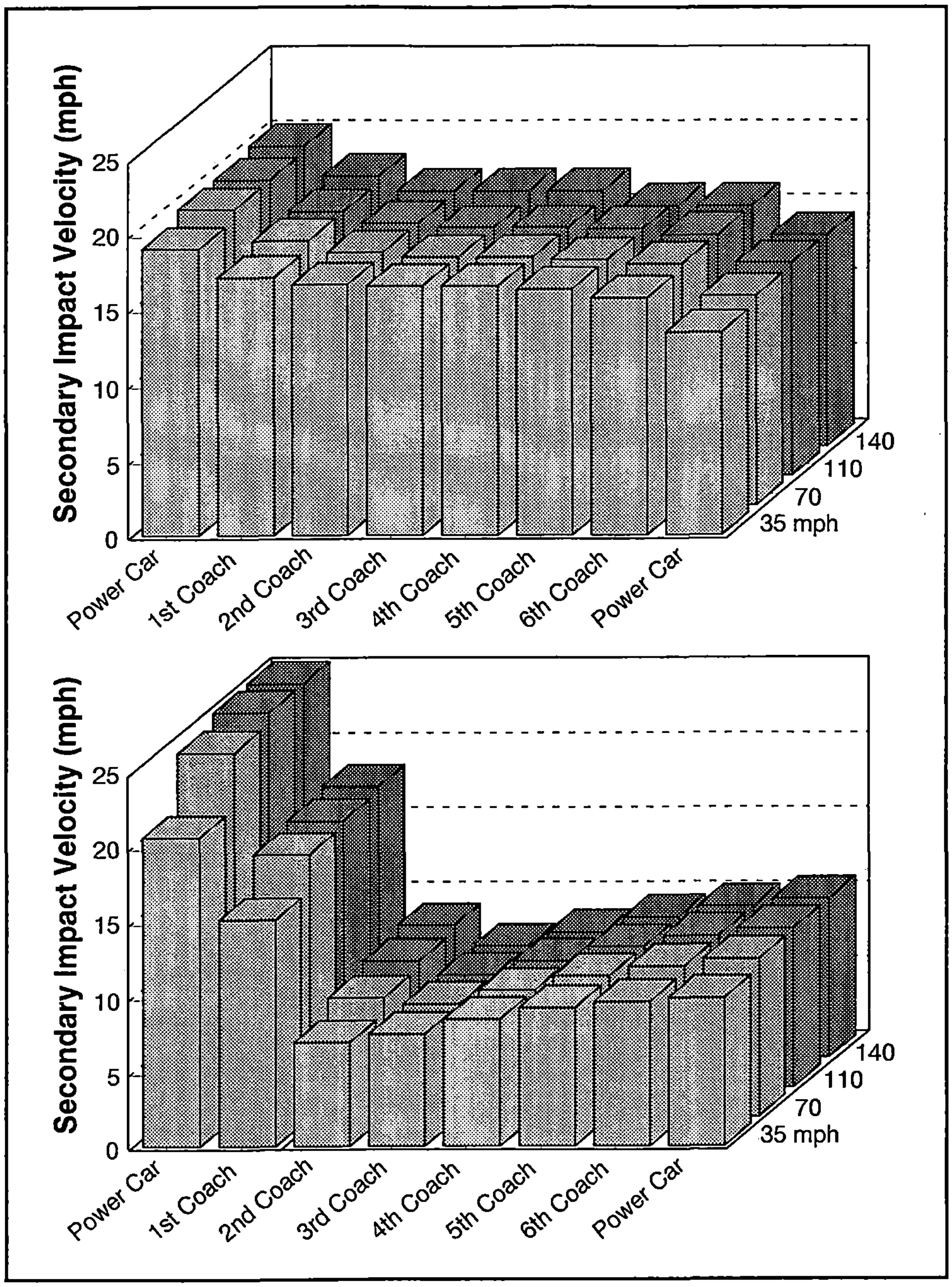

Note: Conventional Design (top), Crash-Energy Management Design (bottom)

Figure 2-17. Occupant Secondary Impact Velocities, Initially Moving Consist

Table 2-5. HIC, Cab Car to Power Car Collision, Initially Moving Consist, Conventional and Crash-Energy Management Designs

Primary Collision Speed (MPH)		HIC Coaches					
		1	2	3	4	5	6
Conventional Design	140	220-475	195-420	185-405	185-400	180-395	175-375
	110	215-470	195-420	185-405	185-400	180-390	170-370
	70	215-470	195-420	185-405	185-400	180-390	170-370
	35	200-440	185-405	185-400	185-400	185-385	165-355
Crash-Energy Management Design	140	235-505	40-85	25-55	35-75	45-100	55-120
	110	225-485	35-75	25-55	35-75	45-100	55-115
	70	215-465	30-65	25-55	35-75	45-100	55-115
	35	150-325	20-45	25-55	35-75	45-95	50-105

Table 2-6. Fatalities, Conventional and Crash-Energy Management Designs

Speed (MPH)	Conventional Design			Crash-Energy Management Design		
	Seats Lost	Secondary Impact Fatalities	Total	Seats Lost	Secondary Impact Fatalities	Total
140	54	0-5	54-59	47	0	47
110	18	0-6	18-24	10	0-1	10-11
70	4	0-6	4-10	2	0-1	2-3
35	0	0-5	0-5	0	0	0

starts at the front and proceeds toward the rear of the train. Figure 2-19 illustrates the occupant volume lost in each of the cars for the constrained crash-energy management design train for four closing speeds ranging from 35 mph to 140 mph. The figure shows that this design approach is successful in distributing the crush throughout the train.

Secondary Impact - Figure 2-20 shows bar charts of the secondary impact velocities for each of the cars in the initially moving consists, for both the crash-energy management design and the conventional design trains, for primary collision speeds of 140, 110, 70, and 35 mph. As shown in the bar chart, the secondary impact speed does not change significantly for collision speeds above 35 mph for the conventional design while they do not change significantly for speeds above 70 mph for the crash-energy management design. Increasing primary collision

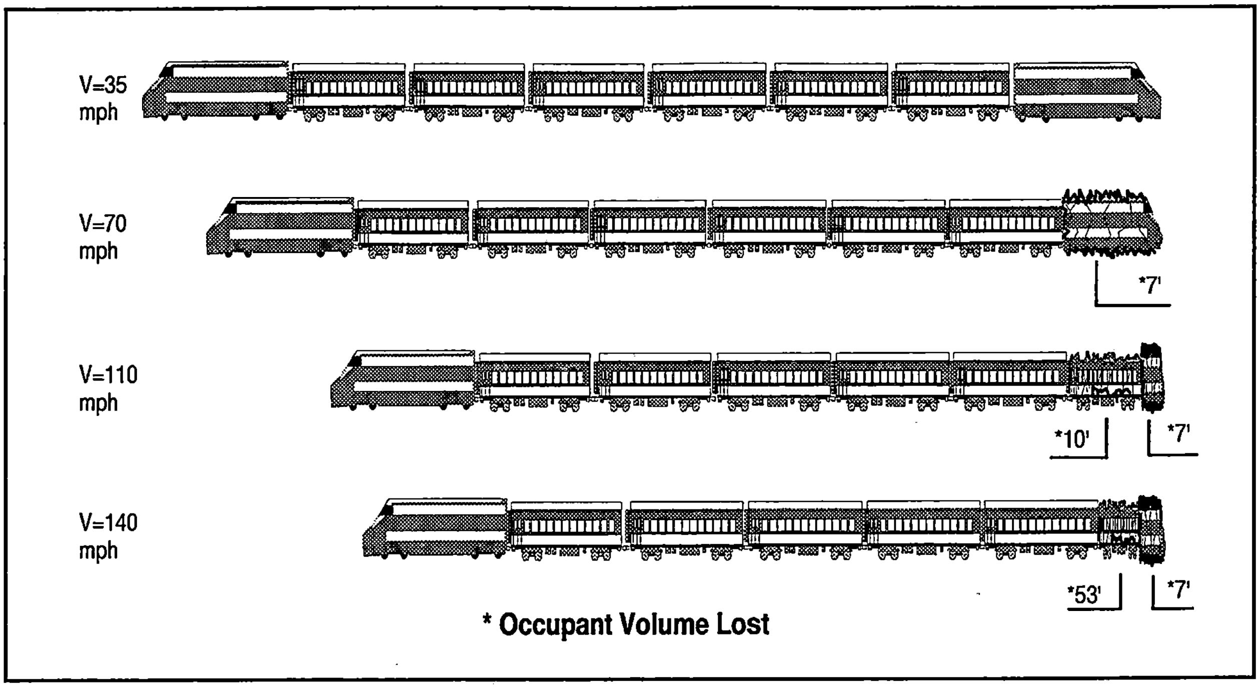

Figure 2-18. Occupant Volume Loss for a Range of Closing Speeds, Power Car to Power Car Collision, Initially Moving Consist, Conventional Design

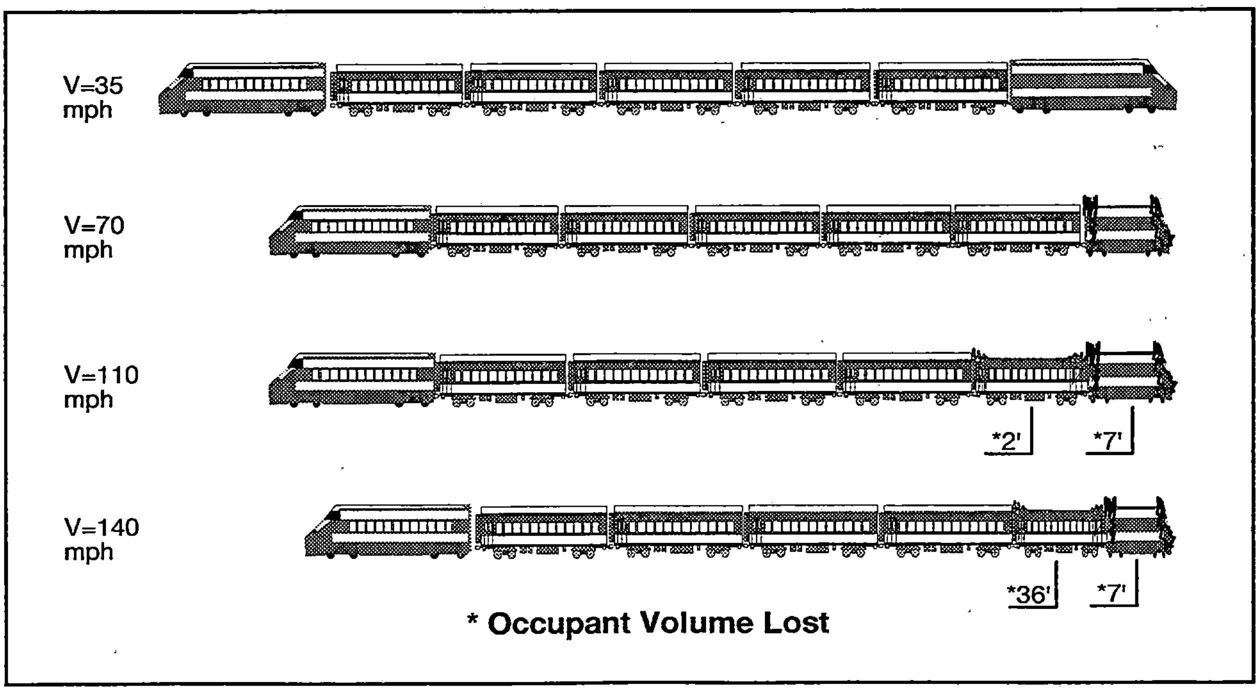

Figure 2-19. Occupant Volume Loss for a Range of Closing Speeds, Power Car to Power Car Collision, Initially Moving Consist, Constrained Crash-Energy Design

speed principally influences the duration of the crash pulse, rather than its maximum value. The secondary impact starts during the initial portion of the primary collision (crash pulse). As a consequence, primary collision speed has little influence on secondary impact velocity.

Fatalities - Table 2-7 lists the predicted fatalities owing to occupant volume loss and secondary impacts for a train with the power car leading colliding with the power car of a standing train. Most of the fatalities are predicted to be due to loss of occupant volume. The crash-energy management design provides significant benefits in this scenario for all speeds considered. This design is consistently more effective in preserving occupant volume and limiting fatalities due to secondary impacts.

Table 2-7. Fatalities, Conventional and Crash-Energy Management Designs, Power Car to Power Car Collision

Speed (MPH)	Conventional Design			Crash-Energy Management Design		
	Seats Lost	Secondary Impact Fatalities	Total	Seats Lost	Secondary Impact Fatalities	Total
140	52	0-5	52-57	37	0-1	37-38
110	11	0-5	11-16	4	0-2	4-6
70	2	0-1	2-3	0	0-3	0-3
35	0	0	0	0	0	0

2.3.2.2 Power Car to Cab Car Collision

In this scenario, a moving train with the cab car leading collides with the power car of an identical consist which is stationary on the track. The cab car is substantially lighter than the power car and the cab car also carries passengers while the power car does not.

Occupant Volume - Figure 2-21 illustrates the occupant volume lost in each of the cars of the car cab leading consist for the conventional design train for four closing speeds ranging from 35 to 140 mph. Most of the occupant volume lost is in the cab car and the first coach car. Figure 2-22 illustrates the occupant volume lost in each of the cars for the constrained crash-energy management design train for four closing speeds ranging from 35 to 140 mph.

Secondary Impact - Figure 2-23 shows bar charts of the secondary impact velocities for each of the cars in the initially moving consists, for both the crash-energy management design and the conventional design trains, for primary collision speeds of 140, 110, 70, and 35 mph. As shown in the bar chart, the secondary impact speed does not change significantly for collision speeds above 35 mph for the conventional design, while they do not change significantly for speeds above 70 mph for the crash-energy management design. Increasing primary collision speed principally influences the duration of the crash pulse rather than its maximum value. The secondary impact starts during the initial portion of the primary collision (crash pulse). As a consequence, primary collision speed has little influence on secondary impact velocity.

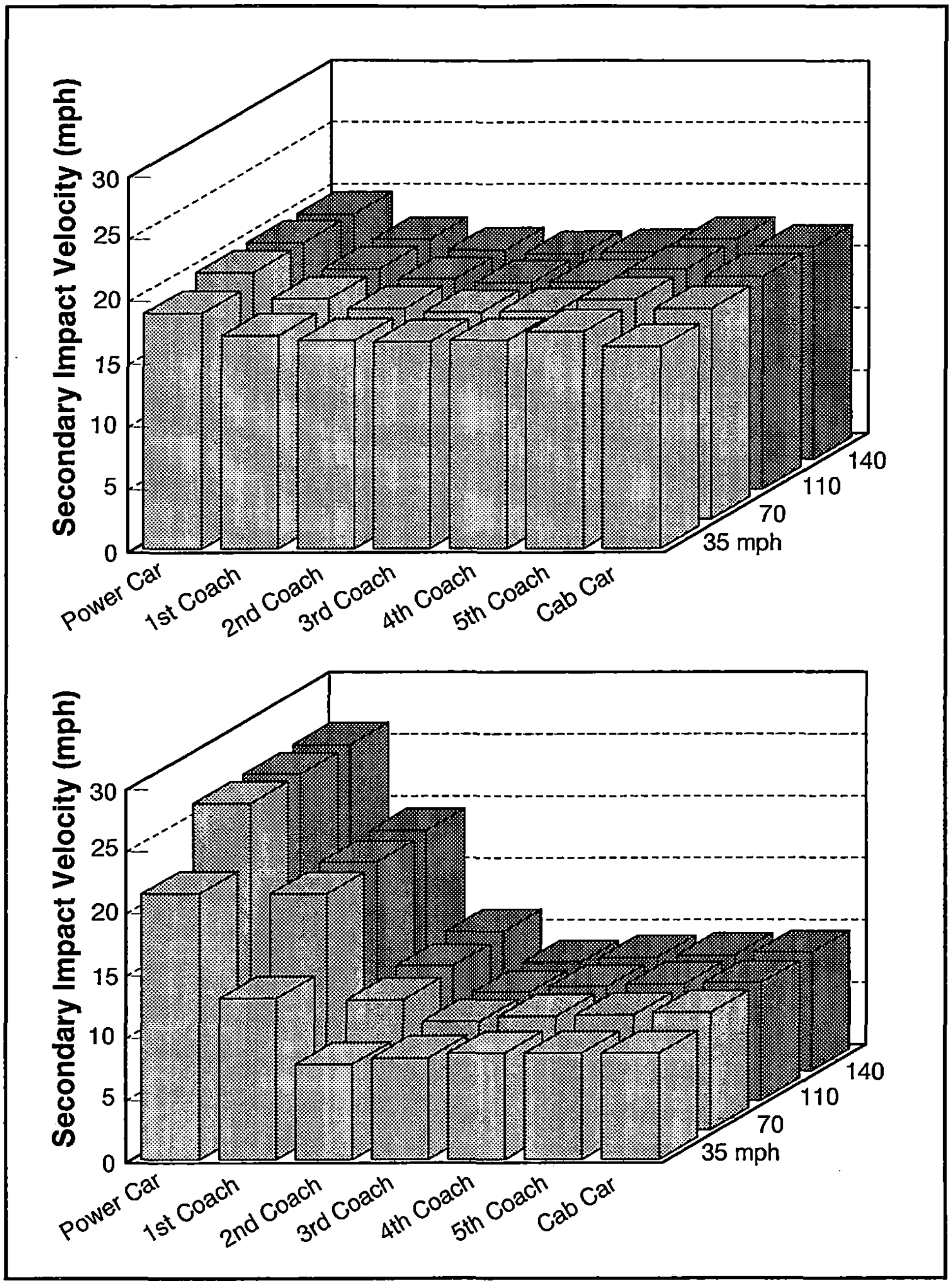

Note: Conventional Design (top), Crash-Energy Management Design (bottom)

Figure 2-20. Occupant Secondary Impact Velocities, Initially Moving Consist

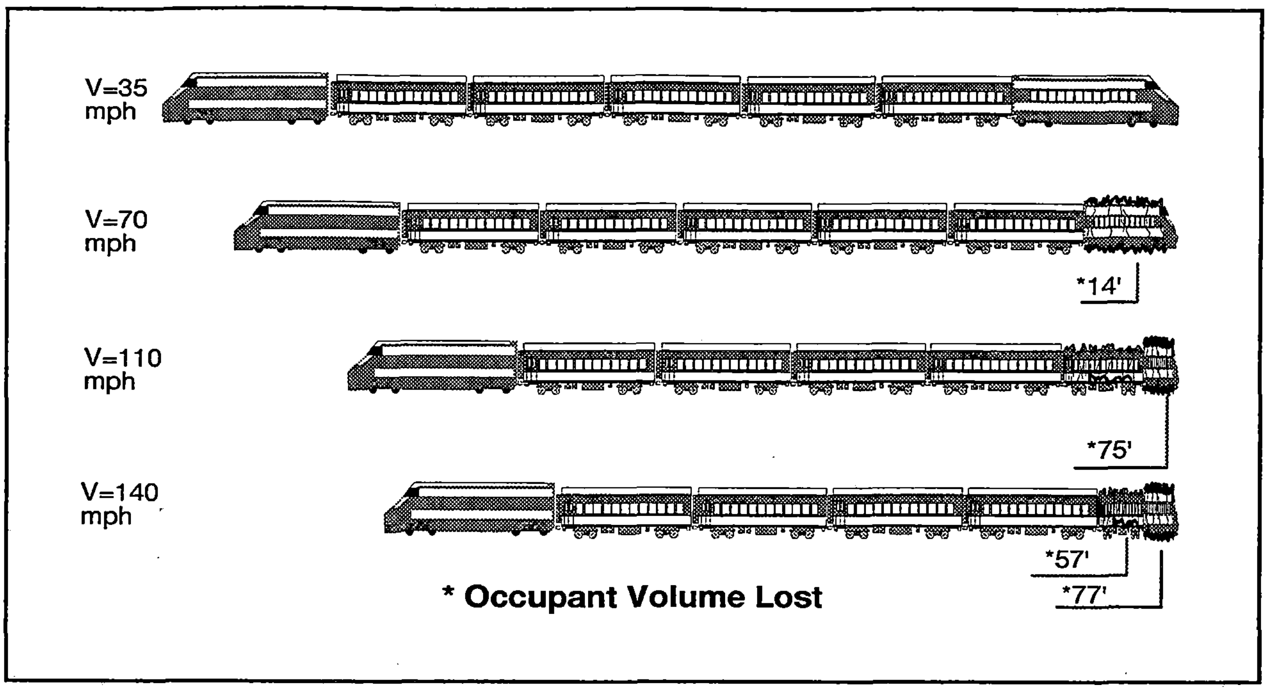

Figure 2-21. Occupant Volume Loss for a Range of Closing Speeds, Cab Car to Power Car Collision, Initially Moving Consist, Conventional Design

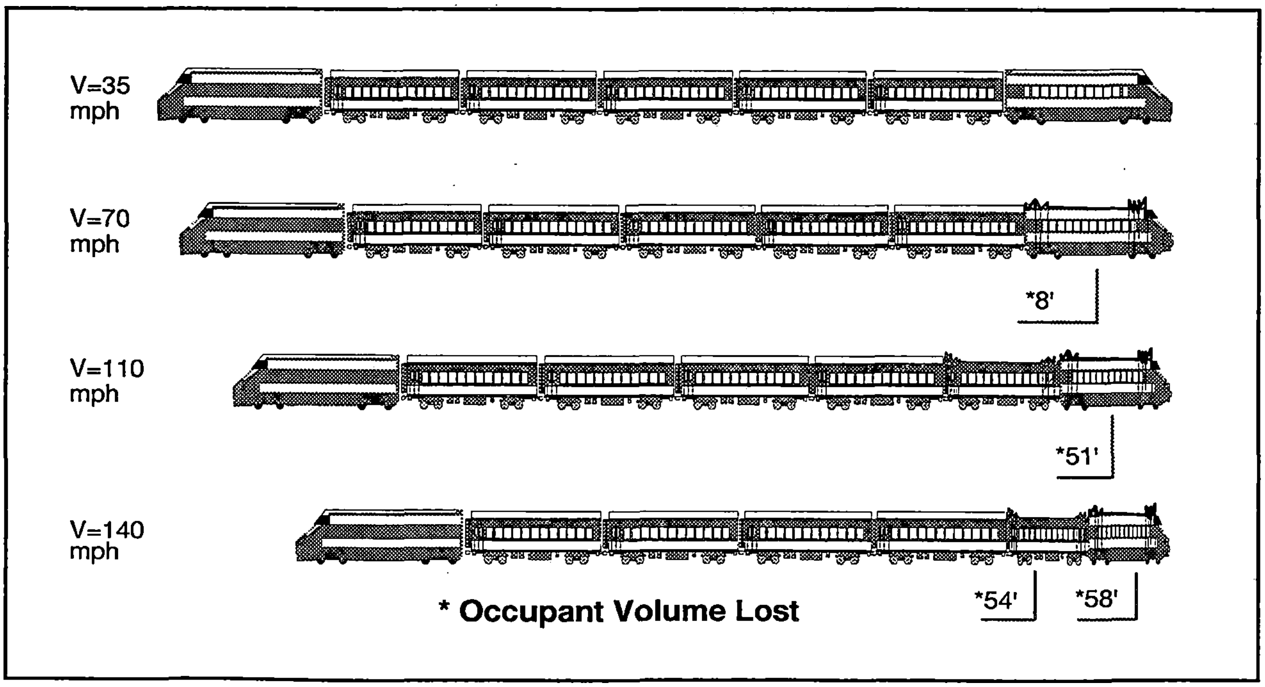

Figure 2-22. Occupant Volume Loss for a Range of Closing Speeds, Cab Car to Power Car Collision, Initially Moving Consist, Crash-Energy Management Design

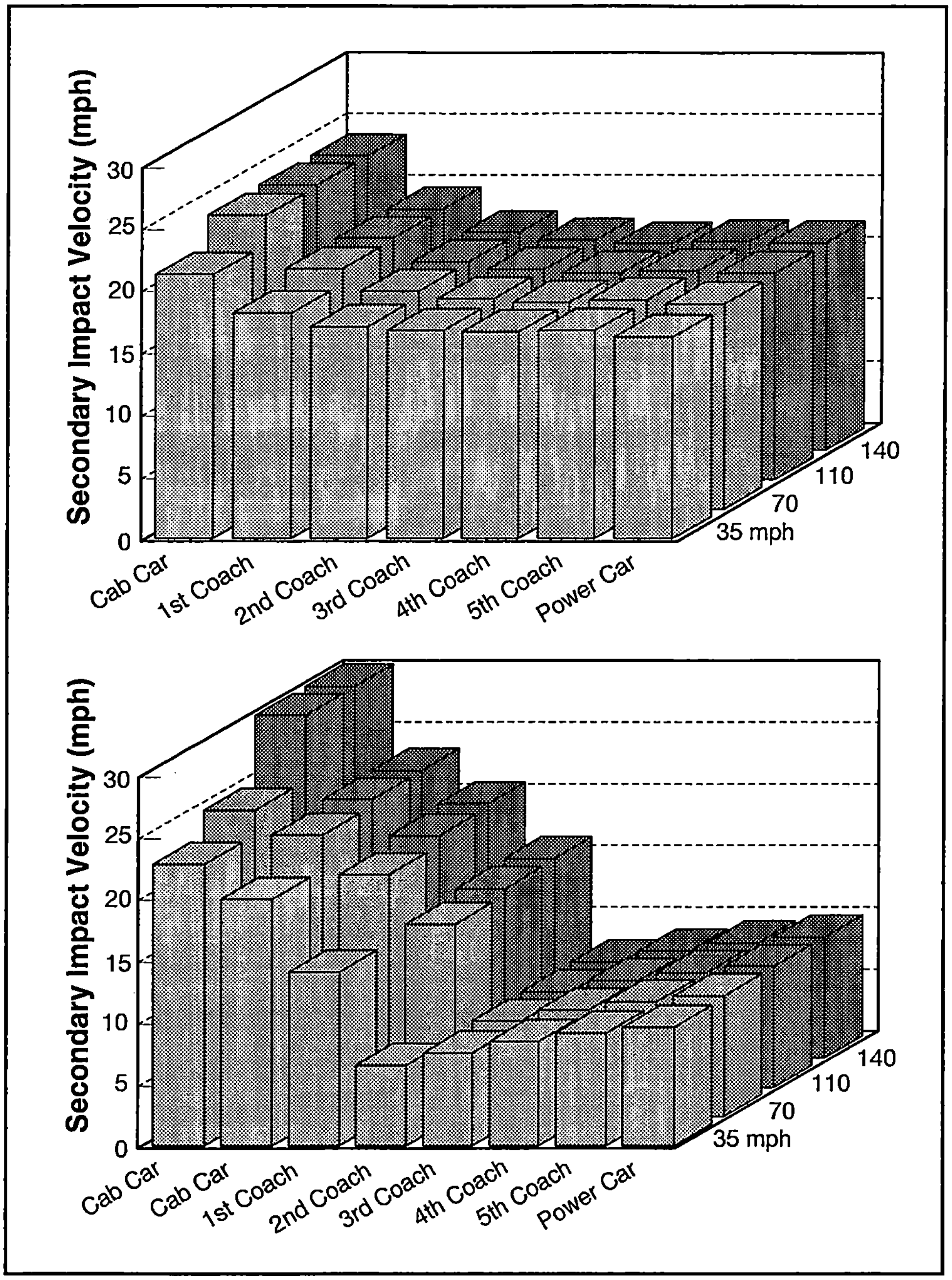

Note: Conventional Design (top), Crash-Energy Management Design (bottom)

Figure 2-23. Occupant Secondary Impact Velocities, Initially Moving Consist

Fatalities - Table 2-8 lists the predicted fatalities owing to occupant volume loss and secondary impacts for a train with the power car leading colliding with the power car of a standing train. This collision scenario results in substantially more fatalities than the power car to power car collision scenario for the same closing speed. This is principally a result of the cab car, with 46 passenger seats, leading in the collision. For the 140 mph collision, the cab car is essentially demolished for both designs. Again, the crash-energy management design is consistently more effective in preserving occupant volume and limiting fatalities due to secondary impacts than the conventional design.

Table 2-8. Fatalities, Conventional and Crash-Energy Management Designs, Power Car to Cab Car Collision

Speed (MPH)	Conventional Design			Crash-Energy Management Design		
	Seats Lost	Secondary Impact Fatalities	Total	Seats Lost	Secondary Impact Fatalities	Total
140	79	0-4	79-83	81	0-2	81-83
110	47	0-5	47-52	42	0-4	42-46
70	8	0-11	8-19	2	0-8	2-10
35	0	0-8	0-8	0	0-2	0-2

2.3.2.3. Cab Car to Cab Car Collision

In this scenario, a moving train with the cab car leading collides with the cab car of an identical consist which is stationary on the track. In this scenario, the heaviest car in each consist — the power car — is furthest from the collision.

Occupant Volume - Figure 2-24 illustrates the occupant volume lost in each of the cars for the conventional design train for four closing speeds ranging from 35 to 140 mph. Most of the occupant volume lost is in the cab car and the first coach car. Figure 2-25 illustrates the occupant volume lost in each of the cars for the constrained crash-energy management design train for four closing speeds ranging from 35 to 140 mph.

Secondary Impacts - Figure 2-26 shows bar charts of the secondary impact velocities for each of the cars in the initially moving consists, for both the crash-energy management design and the conventional design trains, for primary collision speeds of 140, 110, 70, and 35 mph. As shown in the bar chart, the secondary impact speed does not change significantly for collision speeds above 35 mph for the conventional design, while they do not change significantly for speeds above 70 mph for the crash-energy management design. Secondary impact velocities are not strongly influenced by the primary collision speed because the secondary impact speed is principally a function of the first portion of the deceleration crash pulse, i.e., the secondary collision occurs soon after the primary collision starts and well before the primary collision ends. Increasing primary collision closing speed has a greater influence on the final portion of the crash pulse than on the initial portion.

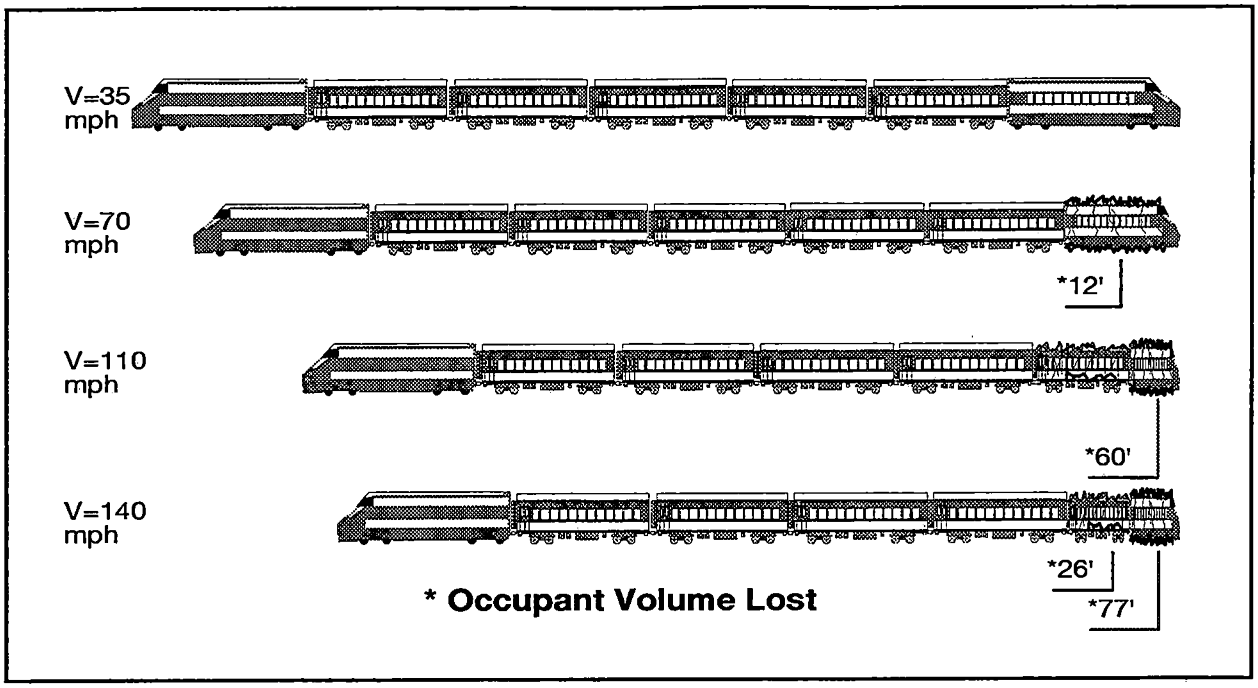

Figure 2-24. Occupant Volume Loss for a Range of Closing Speeds, Cab Car to Cab Car Collision, Initially Moving Consist, Conventional Design

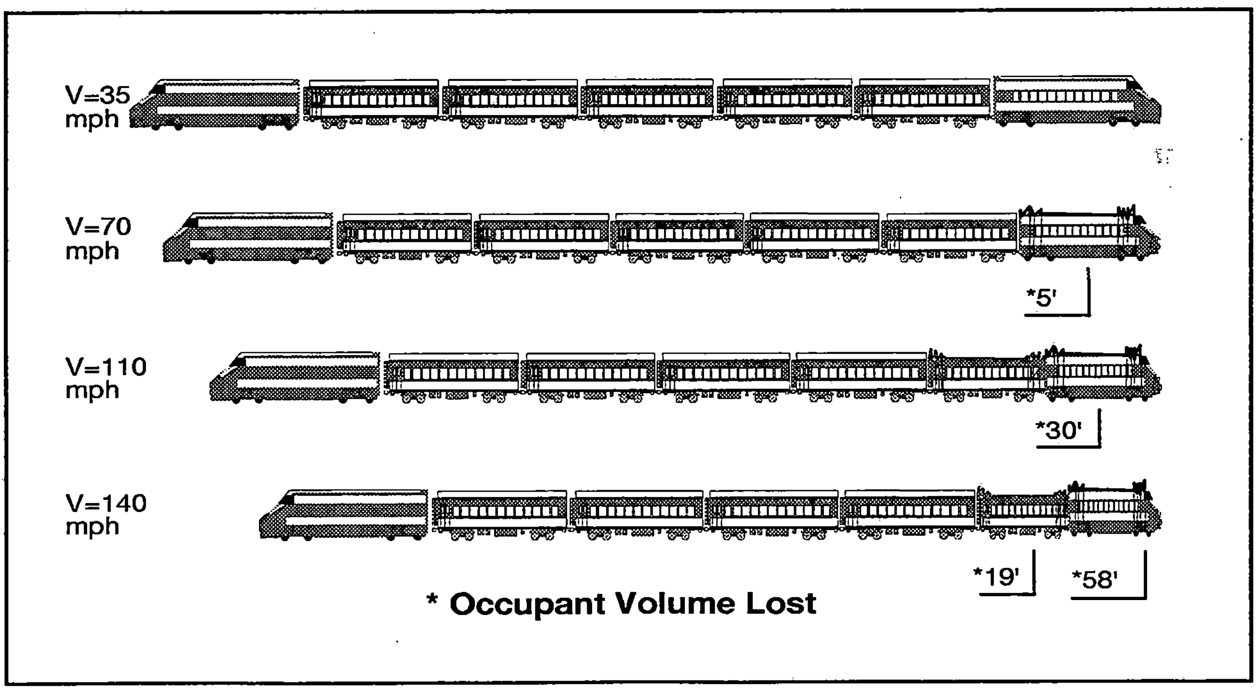

Figure 2-25. Occupant Volume Loss for a Range of Closing Speeds, Cab Car to Power Car Collision, Initially Moving Consist, Crash-Energy Management Design

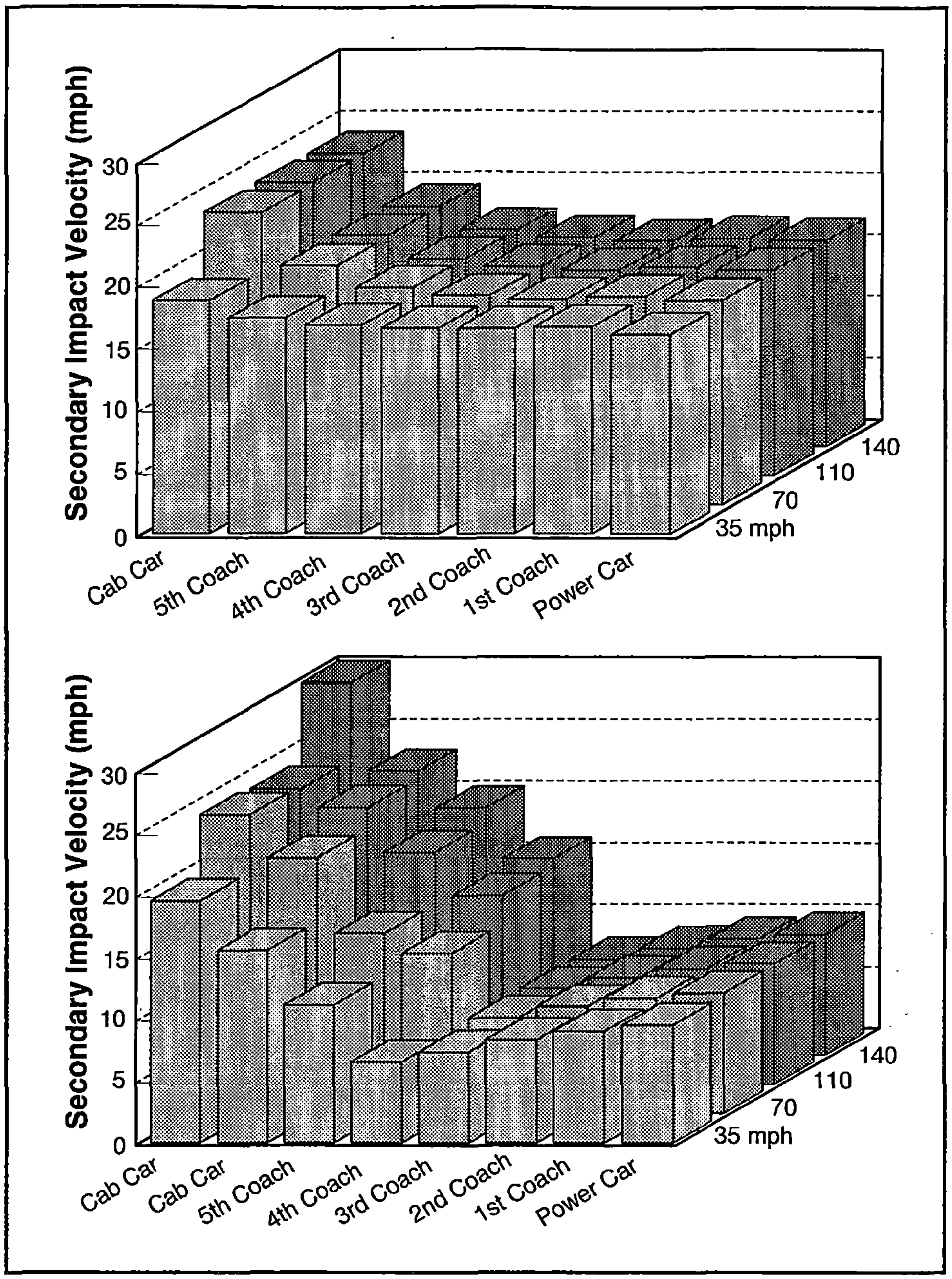

Note: Conventional Design (top), Crash-Energy Management Design (bottom)

Figure 2-26. Occupant Secondary Impact Velocities, Initially Moving Consist

Fatalities - Table 2-9 lists the predicted fatalities owing to occupant volume loss and secondary impacts for a train with the cab car leading colliding with the cab car of a standing train. Again, the crash-energy management design is consistently more effective in preserving occupant volume and limiting fatalities due to secondary impacts than the conventional design.

Table 2-9. Fatalities, Conventional and Crash-Energy Management Designs, Cab Car to Cab Car Collision

Speed (MPH)	Conventional Design			Crash-Energy Management Design		
	Seats Lost	Secondary Impact Fatalities	Total	Seats Lost	Secondary Impact Fatalities	Total
140	63	0-5	63-68	60	0-2	60-62
110	37	0-7	37-44	23	0-5	23-28
70	7	0-12	7-19	2	0-3	2-5
35	0	0-6	0-6	0	0	0

2.3.3 Power Car, Five Coach, Cab Car Collision With Commuter Train

In these scenarios, a moving power car propelled train collides with a stationary commuter mu train. The high-speed consist is made up of a power car, five coach, cab car. The interior of the commuter train is assumed to be less friendly than the interior of the power car propelled train, with the seatbacks of the commuter car stiffer than the seatbacks of the power car propelled train, as discussed in Appendix A. Two scenarios with commuter cars have been analyzed: one with the power car leading the high-speed consist and the second with the cab car leading the consist.

2.3.3.1 Power Car to Commuter MU

Occupant Volume - Figure 2-27 illustrates the occupant volume lost in each of the cars for the conventional design train for four closing speeds ranging from 35 to 140 mph. Most of the occupant volume lost is in the first coach car. Figure 2-28 illustrates the occupant volume lost in each of the cars for the constrained crash-energy management design train. For speeds up to and including 70 mph, the crash-energy management is effective in distributing the crush throughout the train. Somewhere between 70 and 110 mph the crash-energy management design is no longer effective in distributing the crush. This loss in effectiveness is due to the crash-energy management design being optimized for a symmetric collision at 90 mph.

Figures 2-29 and 2-30 show the occupant volume lost in each of the commuter cars, for collisions with the conventional design power car propelled train and the crash-energy management design power car propelled train, respectively. For all the collision speeds, the crash-energy management design power car propelled train results in a smaller loss of occupant volume for the commuter train. This is principally due to the crash-energy management design train appearing softer to the commuter train than the conventional design power car propelled train. As a result, the crash-energy management train is more compatible with the commuter in a collision

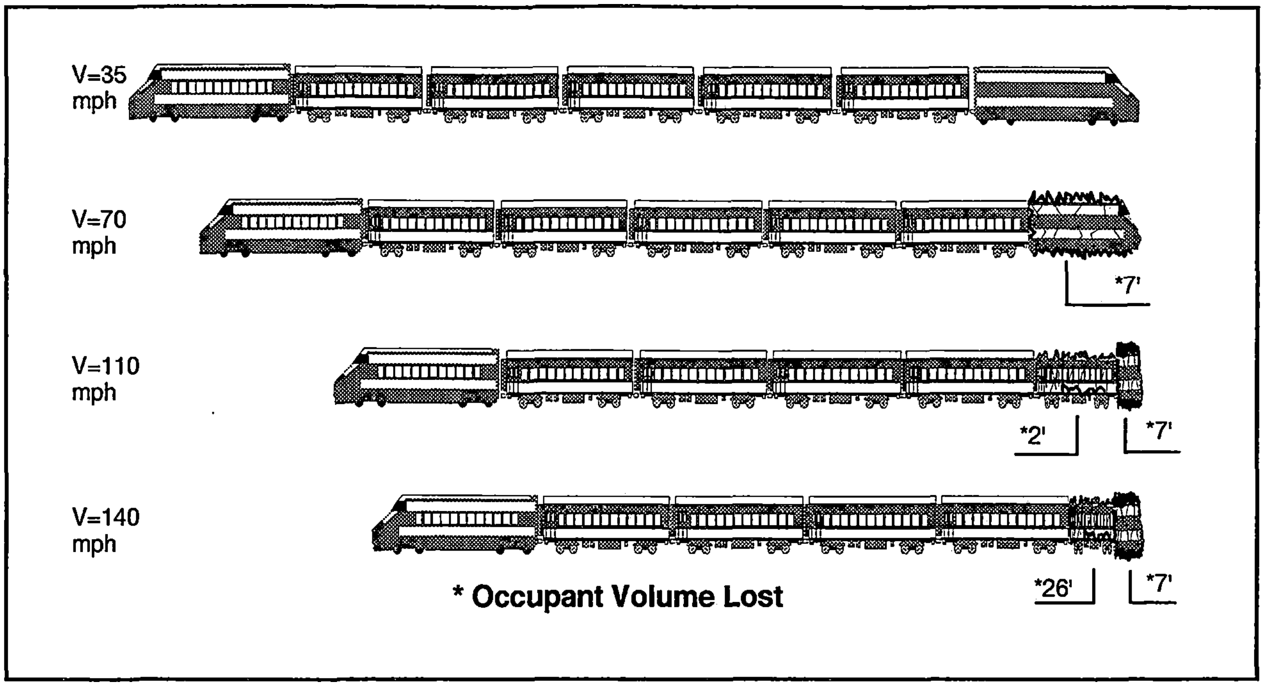

Figure 2-27. Occupant Volume Loss for a Range of Closing Speeds, Power Car to Commuter MU, Power Car Propelled Passenger Train, Conventional Design

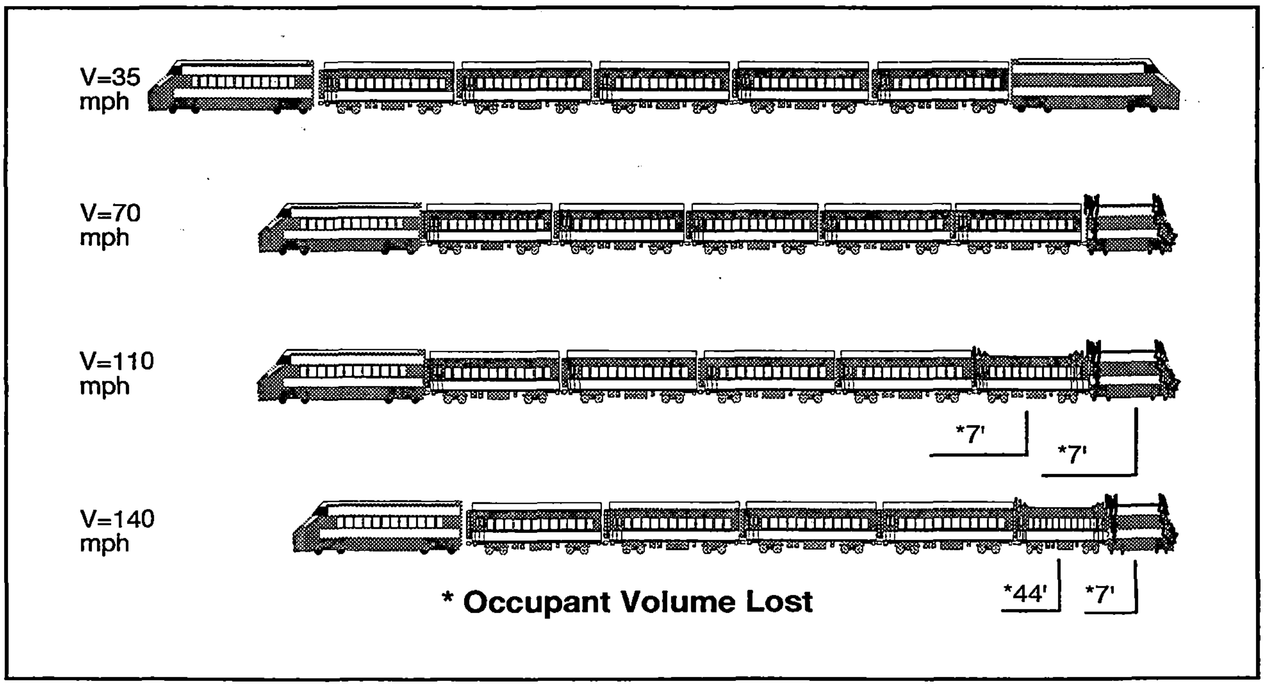

Figure 2-28. Occupant Volume Loss for a Range of Closing Speeds, Power Car to Commuter MU, Power Car Propelled Passenger Train, Crash-Energy Management Design

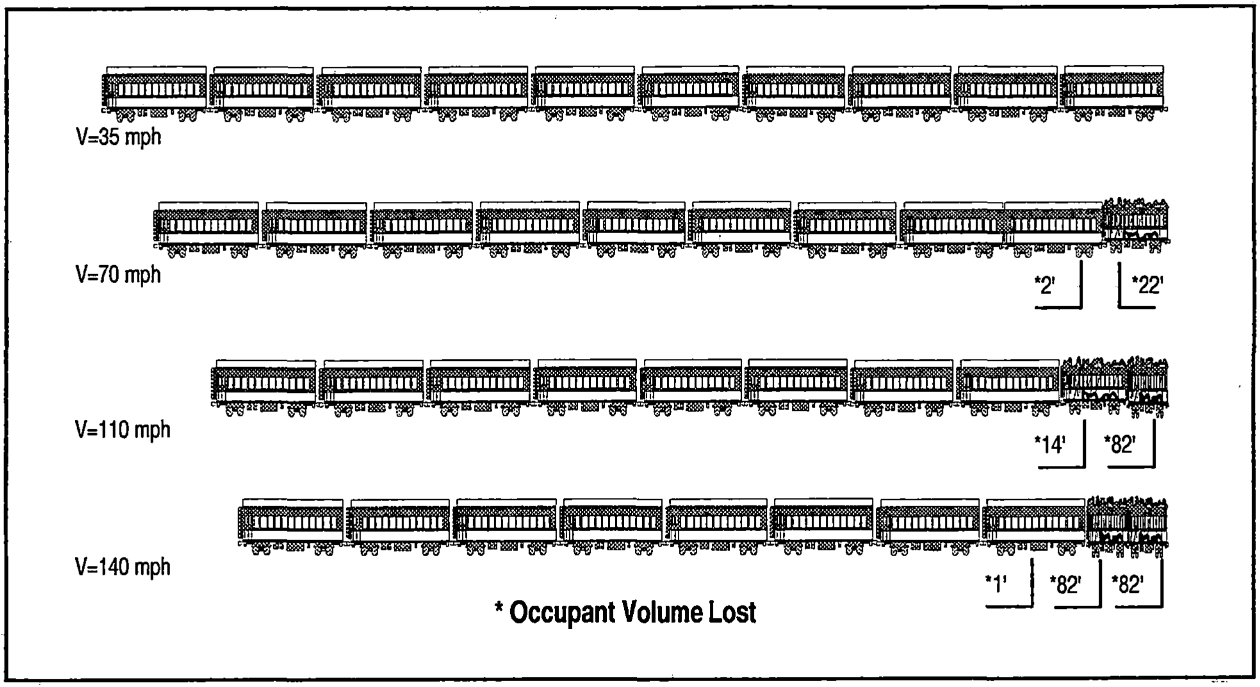

Figure 2-29. Occupant Volume Loss for a Range of Closing Speeds, Power Car to Commuter MU, Conventional Design

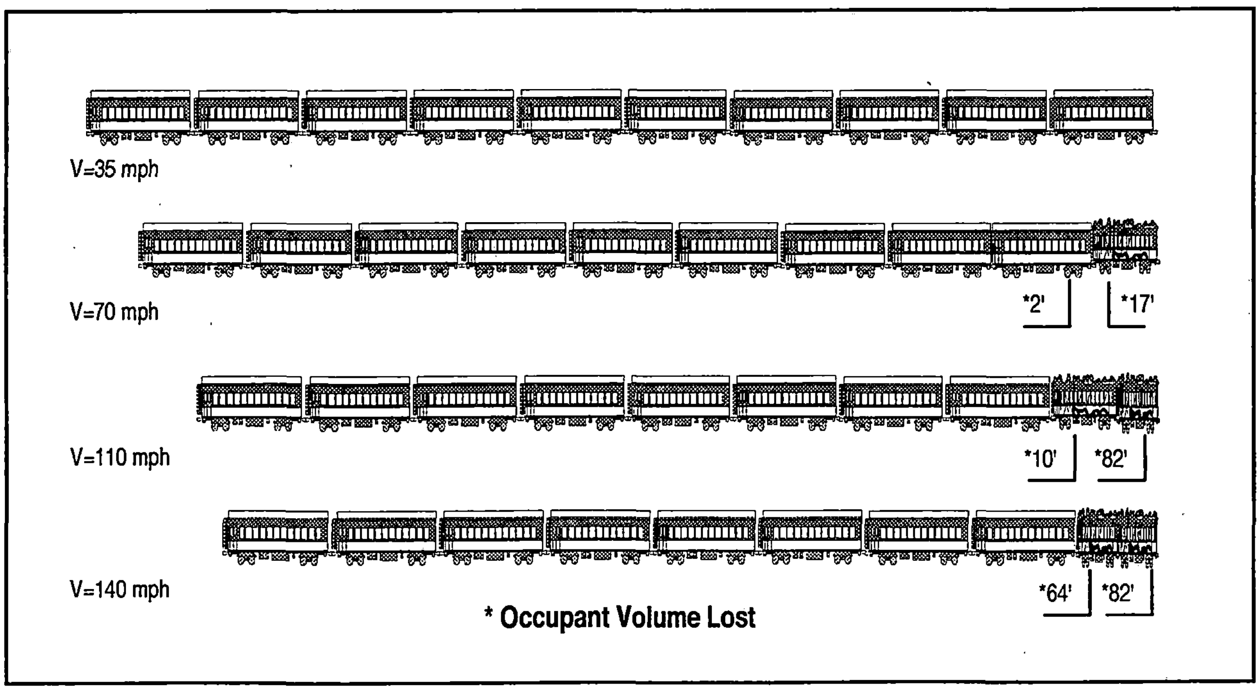

Figure 2-30. Occupant Volume Loss for a Range of Closing Speeds, Power Car to Commuter MU, Crash-Energy Management Design

than the conventional design train.

Secondary Impacts - The secondary impact velocities in each of the cars in both the crash-energy management design and the conventional design power car propelled trains are shown in Figure 2-31. The crash-energy management design results in higher secondary impact velocities in the operator's cab of the power car, essentially the same as the secondary impact velocity in the first coach car, and substantially lower secondary impact velocities in the remaining coach cars. This behavior is consistent with the assumptions made in developing the crash-energy management, particularly that greater secondary impact speeds could be tolerated in the operator's cab owing to the assumption that greater interior crashworthiness measures can be taken for the operator than for the passengers. In the crash-energy management design, the operator's cab was strengthened in order to better preserve sufficient volume for the operator to survive, at the cost of increasing the deceleration imparted to the cab.

The secondary impact velocities in each of the cars in the commuter train are shown in Figure 2-32, for collisions with a conventional design and a crash-energy management design power car propelled train. For train-to-train closing speeds of 70 mph and above, the secondary impact velocities are essentially the same for the two power car propelled train designs. For the 35 mph train collision, however, the secondary impact velocities are significantly lower for the collision with the crash-energy management design power car propelled train. This is principally due to the crash-energy management design power car propelled train appearing softer to the commuter train than the conventional design train. When a mass runs into a stationary mass of the same size, the deceleration of the initially moving mass is equal to the acceleration of the initially stationary mass. If the force/crush characteristics are initially stiff, the deceleration and acceleration will be rapid. If one of the masses has a soft initial force/crush characteristic, then the initial deceleration and acceleration will be gentler. The deceleration and acceleration of the masses is controlled by the weaker force/crush characteristic.

Fatalities - Fatalities reflect the consequences of the loss of occupant volume and the secondary impacts. Table 2-10 lists the total fatalities (fatalities on both the commuter train and the power car propelled train) for commuter train collisions with a conventional design power car propelled train and a crash-energy management design train. For speeds up to and including 70 mph, the crash-energy management design is more effective in preserving occupant volume than the conventional design. At some point between 70 and 110 mph, all the effective crush zones are collapsed and the two designs perform essentially the same in preserving occupant volume.

Table 2-11 lists the fatalities on the power car propelled train for a commuter train collision with a power car propelled train. For speeds up to and including 70 mph, the crash-energy management design is effective in preserving all the occupant volume. Somewhere between 70 and 110 mph, the crash-energy management design is no longer effective in preserving the occupant volume. This loss in effectiveness is due to the crash-energy management design being optimized for a symmetric collision at 90 mph.

Table 2-12 lists the fatalities on the commuter train for a commuter train collision with a power car propelled train. The crash-energy management design consistently results in fewer fatalities, principally due to better preservation occupant volume, for the entire speed range considered.

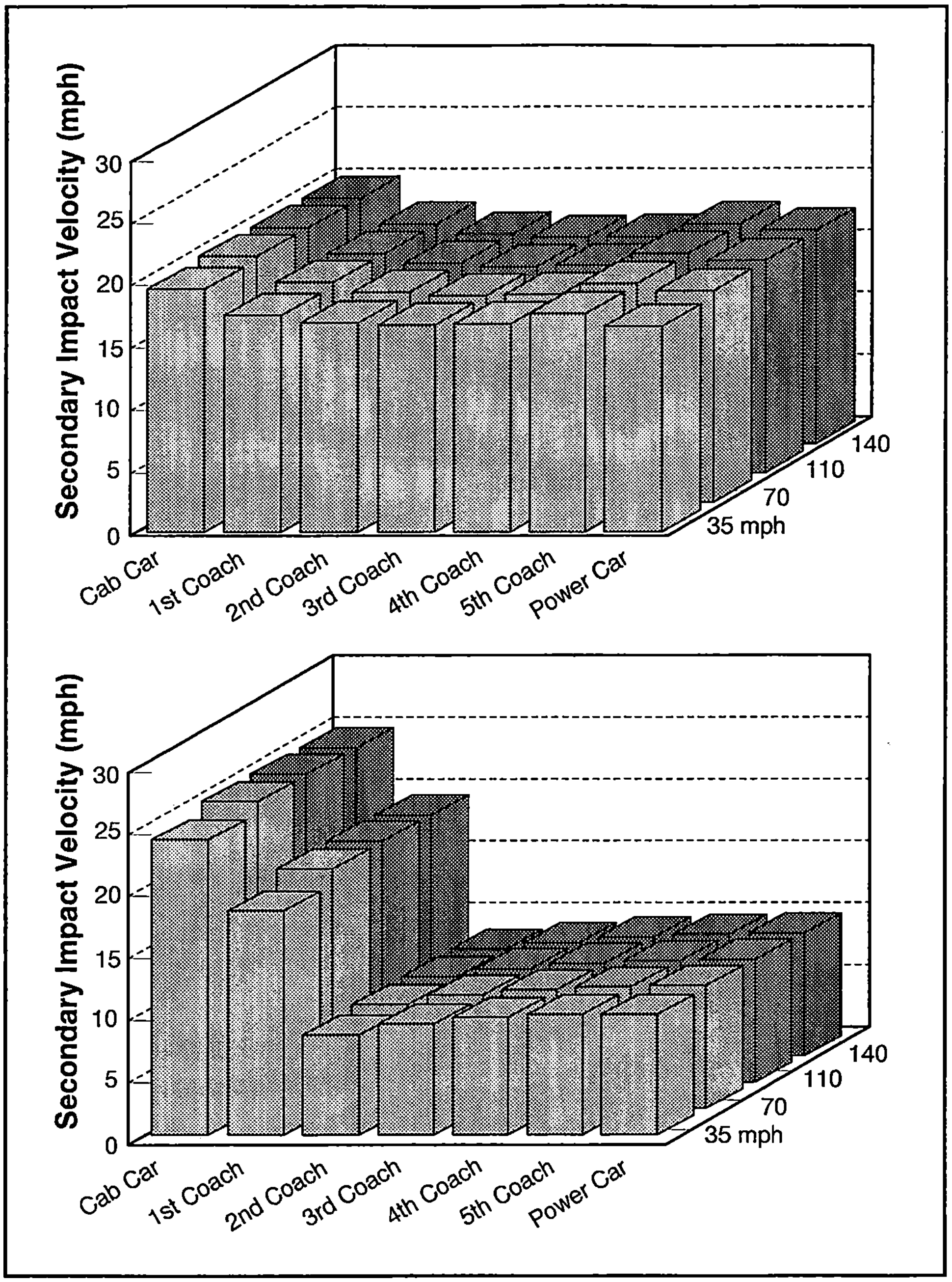

Note: Conventional Design (top), Crash-Energy Management Design (bottom)

Figure 2-31. Bar Chart of Occupant Secondary Impact Velocity, Power Car to Commuter MU, Power Car Propelled Passenger Train

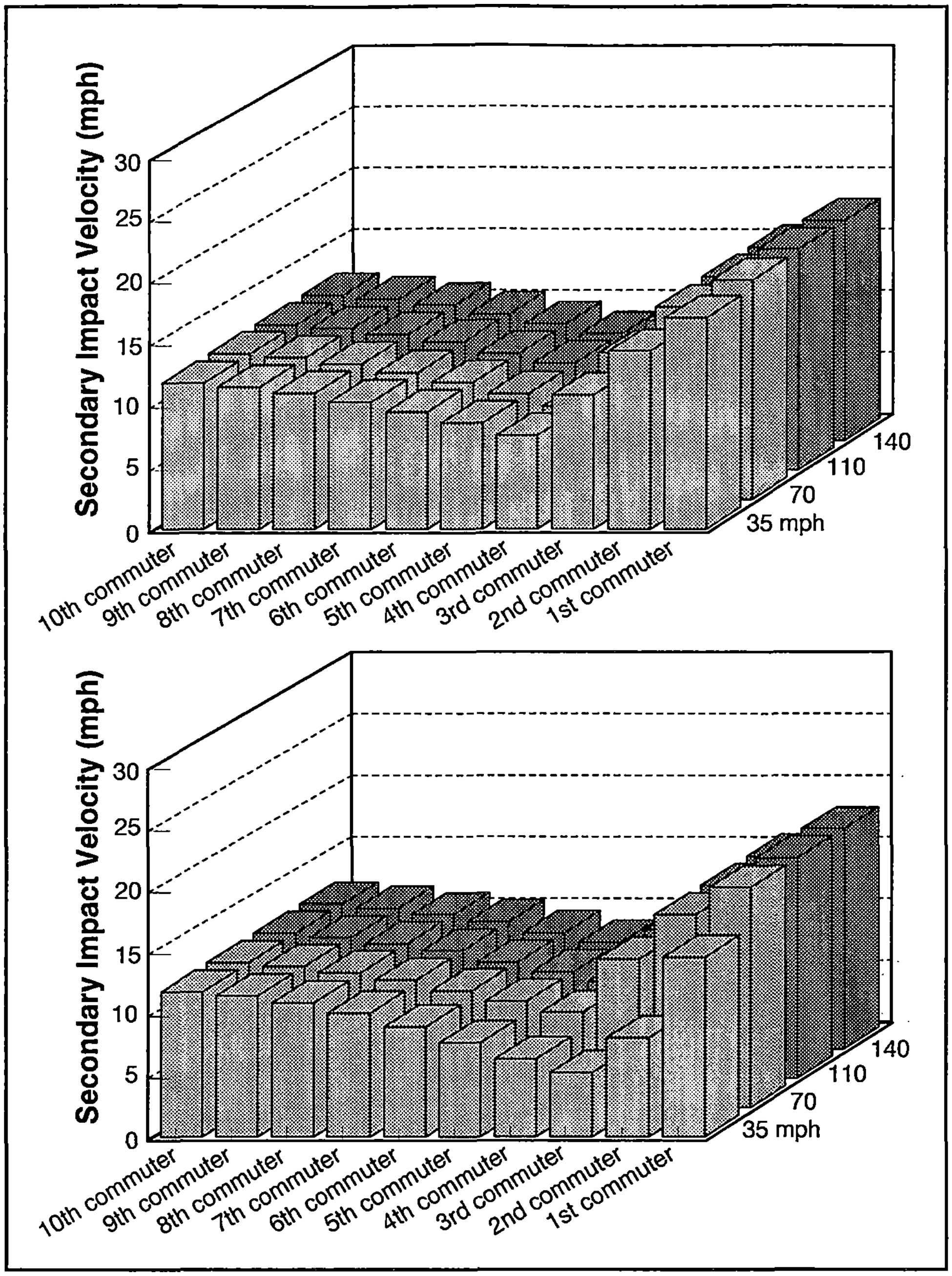

Note: Conventional Design (top), Crash-Energy Management Design (bottom)

Figure 2-32. Bar Chart of Occupant Secondary Impact Velocity, Power Car to Commuter MU

Table 2-10. Total Fatalities, Power Car to Commuter MU Collision

Speed (MPH)	Conventional Design Train and Commuter Train			Crash-Energy Management Design and Commuter Train		
	Seats Lost	Secondary Impact Fatalities	Total	Seats Lost	Secondary Impact Fatalities	Total
140	278	12-117	290-395	270	16-127	286-397
110	150	19-171	169-321	151	20-171	171-322
70	39	28-246	67-285	29	34-253	63-282
35	0	2-230	25-230	0	15-137	15-137

Table 2-11. Power Car Propelled Passenger Train Fatalities, Power Car to Commuter MU Collision

Speed (MPH)	Conventional Design			Crash-Energy Management Design		
	Seats Lost	Secondary Impact Fatalities	Total	Seats Lost	Secondary Impact Fatalities	Total
140	27	0-5	27-32	47	0-1	47-48
110	4	0-6	4-10	10	0-1	10-11
70	2	0-4	2-6	0	0-1	0-1
35	0	0-4	0-4	0	0-1	0-1

Table 2-12. Commuter Train Fatalities, Power Car to Commuter MU Collision

Speed (MPH)	Commuter Train (Collision with Conventional Design)			Commuter Train (Collision with Crash-Energy Management Design)		
	Seats Lost	Secondary Impact Fatalities	Total	Seats Lost	Secondary Impact Fatalities	Total
140	251	12-112	290-395	223	16-126	239-349
110	146	16-19	169-321	141	20-170	161-310
70	37	28-242	67-285	29	34-252	63-281
35	0	25-226	25-230	0	15-136	15-136

2.3.3.2 Cab Car to Commuter MU

Occupant Volume - Figure 2-33 illustrates the occupant volume lost in each of the cars for the conventional design train for four closing speeds ranging from 35 to 140 mph. Most of the occupant volume lost is in the cab car and the first coach car. Figure 2-34 illustrates the occupant volume lost in each of the cars for the constrained crash-energy management design train. For speeds up to and including 110 mph, the crash-energy management is effective in distributing the crush throughout the train. Somewhere between 110 and 140 mph the crash-energy management design is no longer effective in distributing the crush. This loss in effectiveness is due to the crash-energy management design being optimized for a symmetric collision at 60 mph.

Figures 2-35 and 2-36 show the occupant volume lost in each of the commuter cars, for collisions with the conventional design power car propelled train and the crash-energy management design power car propelled train, respectively. For all the collision speeds, the crash-energy management design power car propelled train results in a smaller loss of occupant volume for the commuter train. This is due principally to the crash-energy management design train appearing softer to the commuter train than the conventional design power car propelled train.

Secondary Impacts - The secondary impact velocities in each of the cars in both the crash-energy management design and the conventional design power car propelled trains are shown in Figure 2-37. The cab car is split into two occupant volumes: the operator's cab and the passenger volume. The secondary impact velocities in these areas is relatively high, due to the choice made to preserve occupant volume at the expense of increased secondary impact velocity. The secondary impact velocities in these occupant volumes are nearly the same as the secondary impact velocity in the cab car of the conventional train. The secondary impact velocity in the first coach of the crash-energy management design is slightly greater than in the first coach of the conventional design. The crash-energy management design does result in substantially lower secondary impact velocities in the remaining coach cars.

The secondary impact velocities in each of the cars in the commuter train are shown in Figure 2-38, for collisions with a conventional design and crash-energy management design power car propelled train. The secondary impact velocities are essentially the same for the two power car propelled train designs.

Fatalities - Fatalities reflect the consequences of the loss of occupant volume and the secondary impacts. Table 2-13 lists the total fatalities (fatalities on both the commuter train and the power car propelled train) for commuter train collisions with a conventional design power car propelled train and a crash-energy management design power car propelled train. For all speeds considered, the crash-energy management design is more effective in preserving occupant volume than the conventional design. The crash-energy management design provides consistently gentler secondary impacts, resulting in fewer secondary fatalities for the speed range considered.

Table 2-14 lists the fatalities on the power car propelled train for a commuter train collision with a power car propelled train. For speeds up to and including 70 mph, the crash-energy management is effective in preserving all the occupant volume. Somewhere near 110 mph the crash-energy management design is no longer effective in preserving the occupant volume.

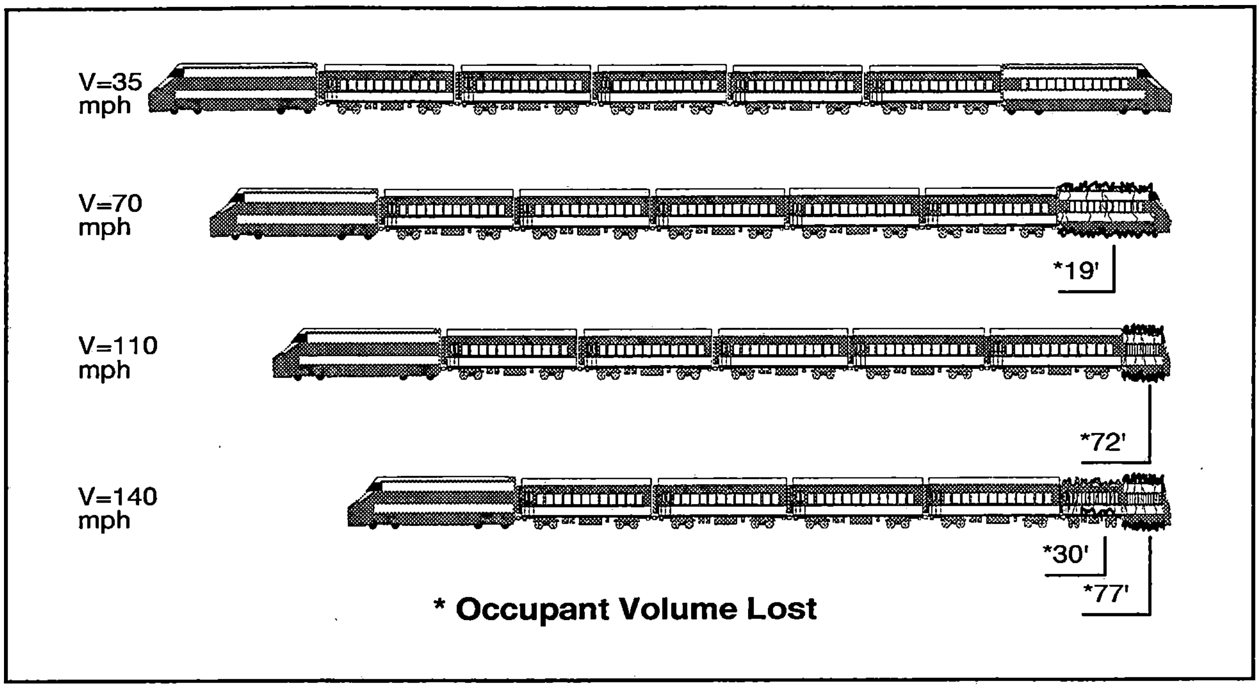

Figure 2-33. Occupant Volume Loss for a Range of Closing Speeds, Cab Car to Commuter MU, Power Car Propelled Passenger Train, Conventional Design

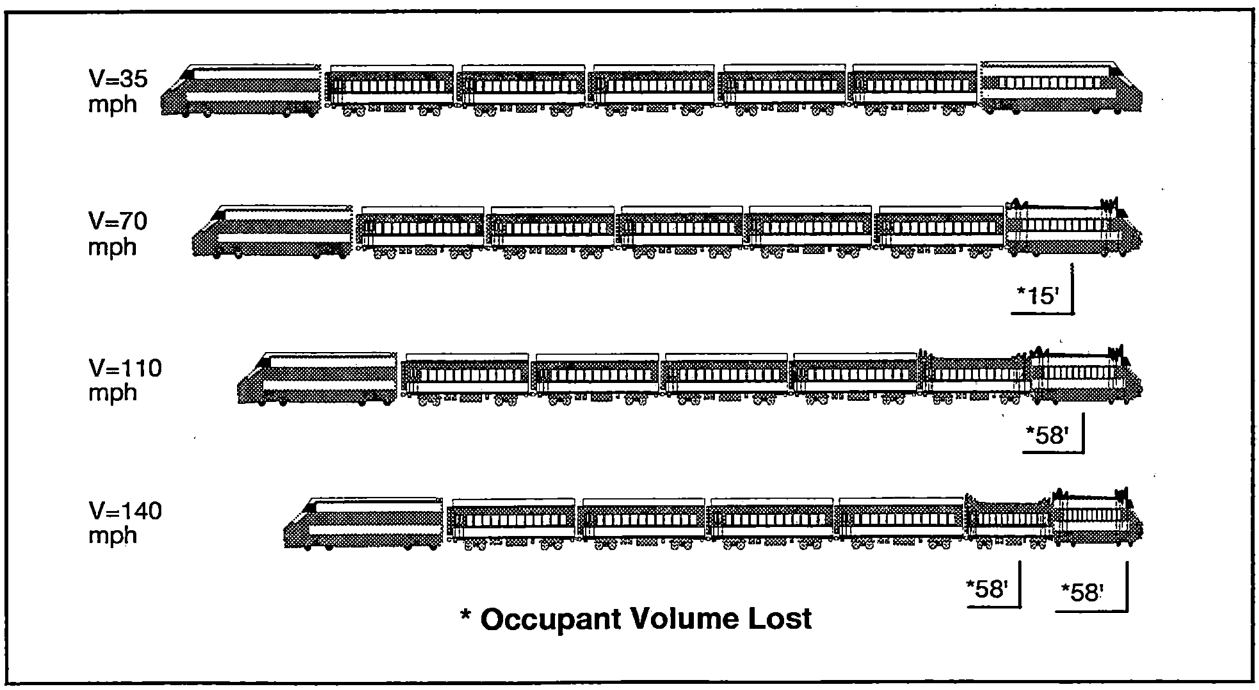

Figure 2-34. Occupant Volume Loss for a Range of Closing Speeds, Cab Car to Commuter MU, Power Car Propelled Passenger Train, Crash-Energy Management Design

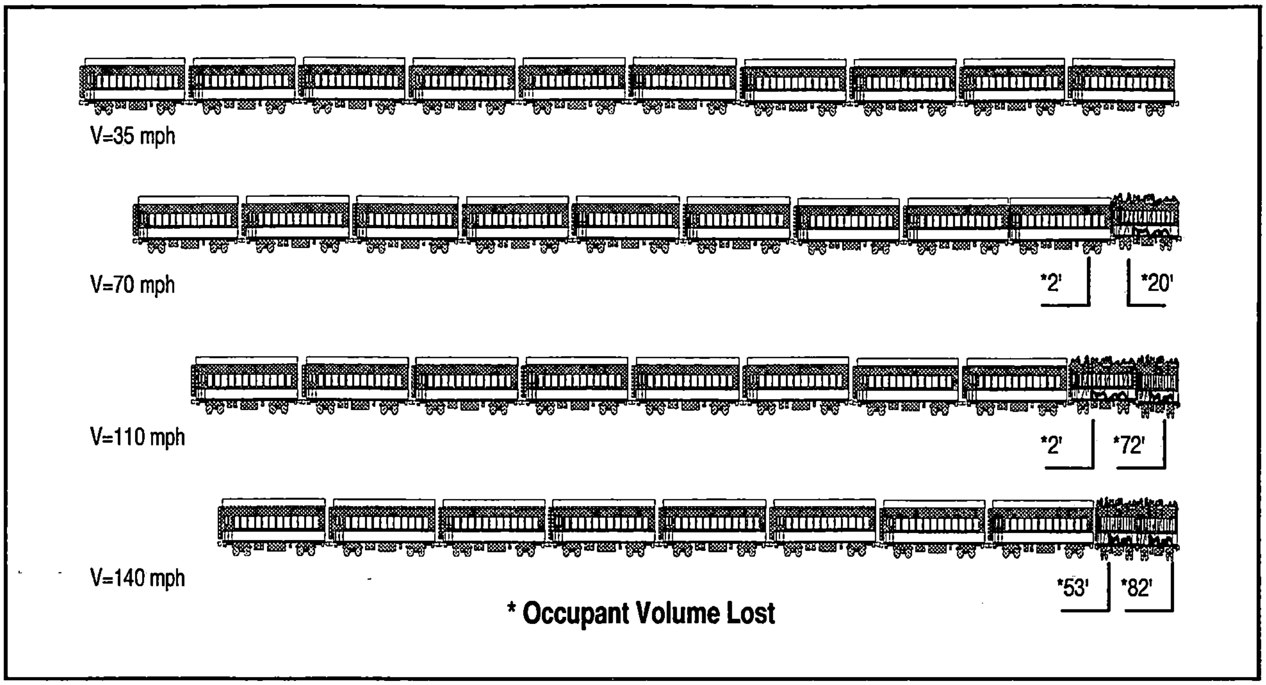

Figure 2-35. Occupant Volume Loss for a Range of Closing Speeds, Cab Car to Commuter MU, Commuter Train, Conventional Design

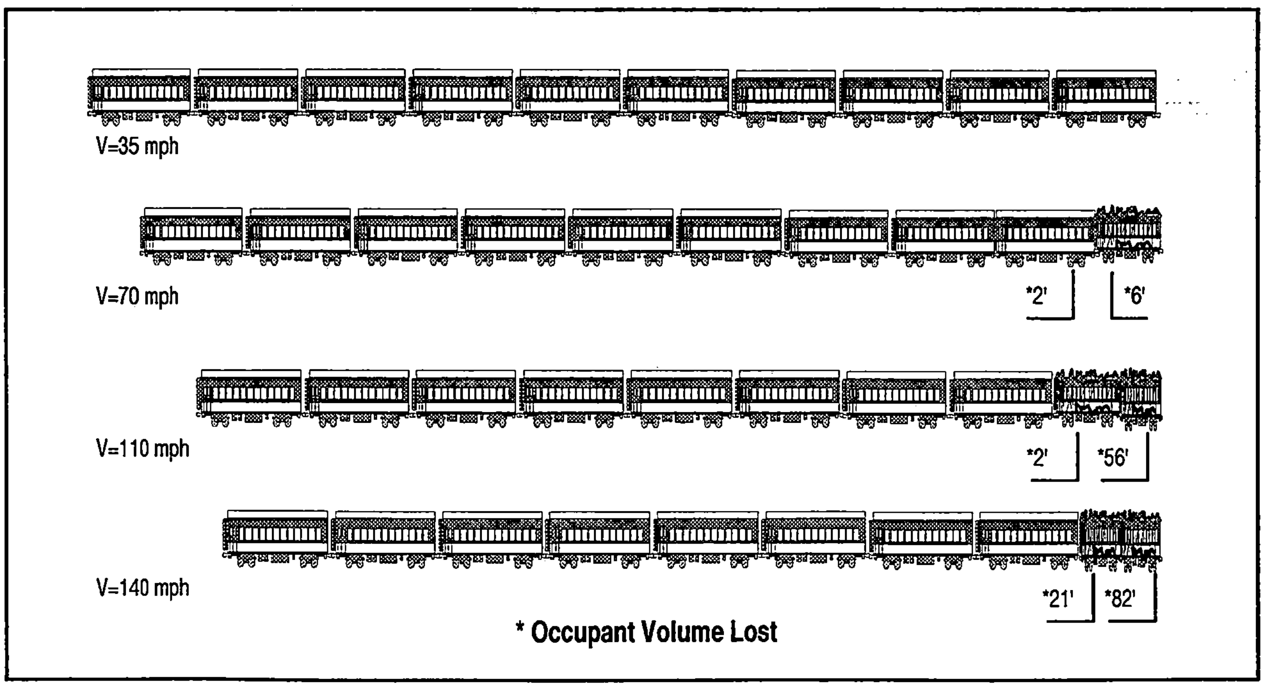

Figure 2-36. Occupant Volume Loss for a Range of Closing Speeds, Cab Car to Commuter MU, Commuter Train, Crash-Energy Management Design

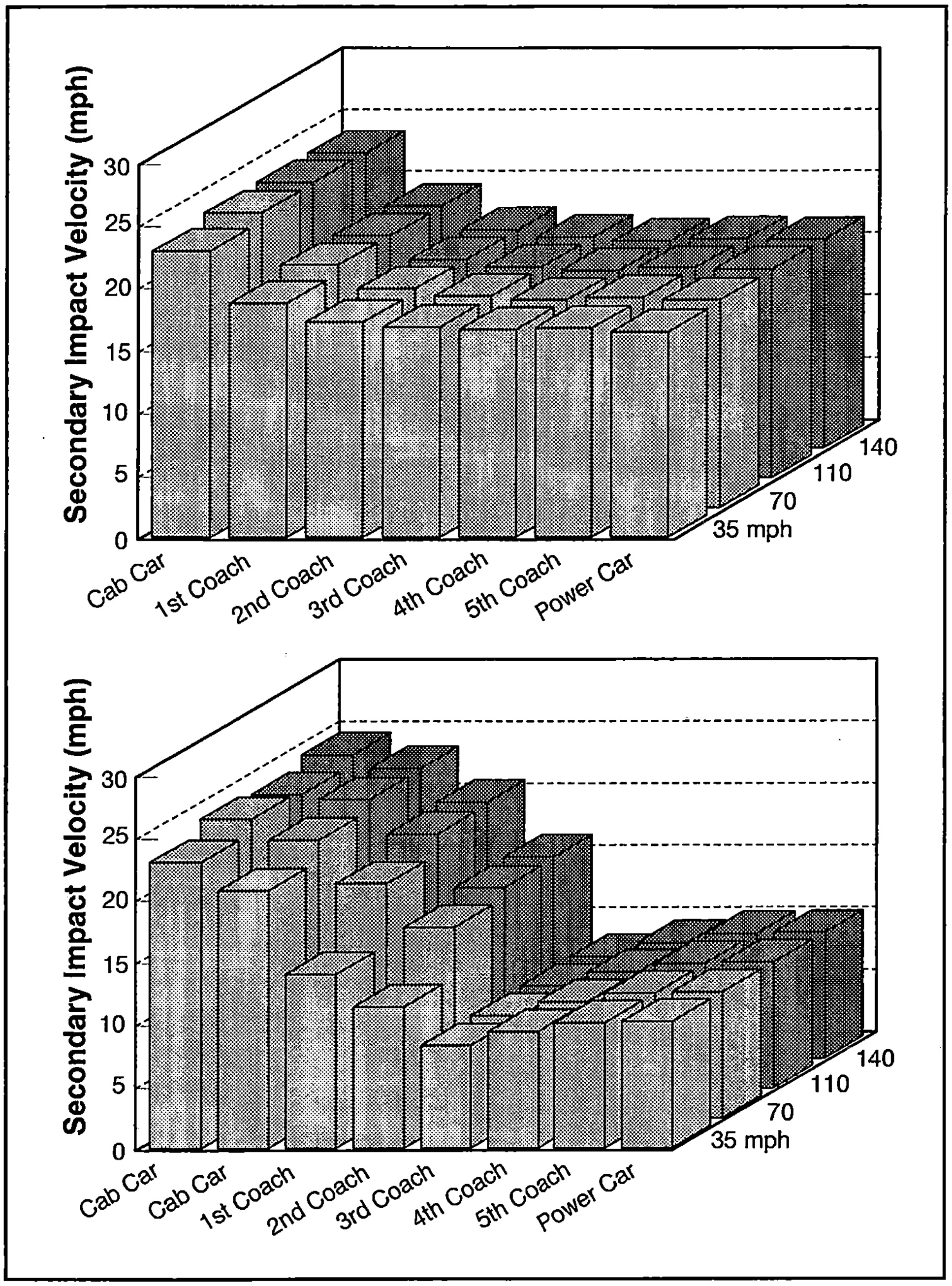

Note: Conventional Design (top), Crash-Energy Management Design (bottom)

Figure 2-37. Bar Chart of Occupant Secondary Impact Velocity, Cab Car to Commuter MU, Power Car Propelled Passenger Train

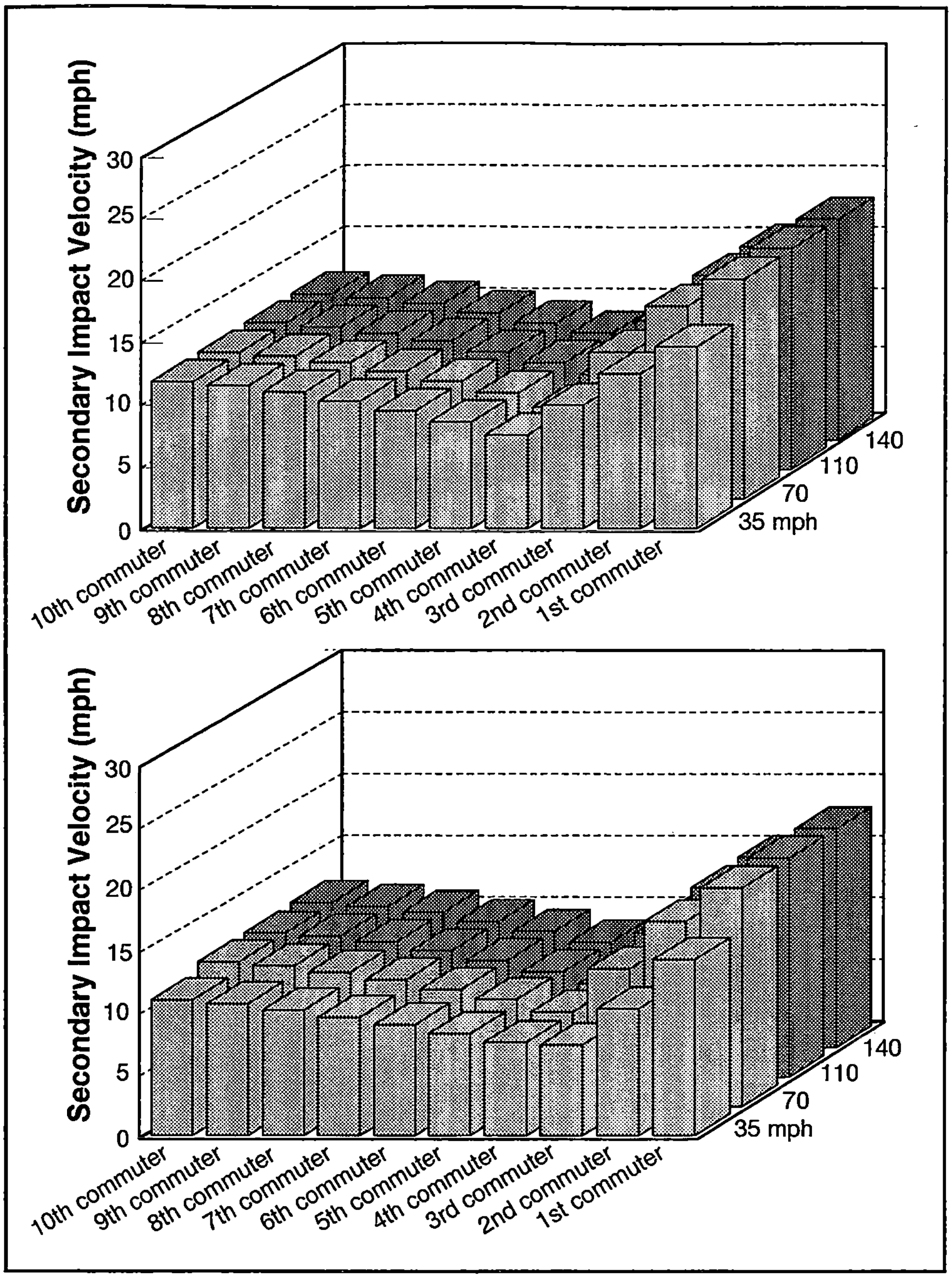

Note: Conventional Design (top), Crash-Energy Management Design (bottom)

Figure 2-38. Bar Chart of Occupant Secondary Impact Velocity, Cab Car to Commuter MU, Commuter Train

Table 2-13. Total Fatalities, Cab Car to Commuter MU Collision

Speed (MPH)	Conventional Design Train and Commuter Train			Crash-Energy Management Design and Commuter Train		
	Seats Lost	Secondary Impact Fatalities	Total	Seats Lost	Secondary Impact Fatalities	Total
140	272	16-139	288-411	240	18-156	28-396
110	158	22-191	180-349	138	25-199	163-337
70	46	28-255	74-301	21	29-248	50-269
35	0	19-184	19-184	0	12-129	12-129

Table 2-14. Power Car Propelled Passenger Train Fatalities, Cab Car to Commuter MU Collision

Speed (MPH)	Commuter Train (Collision with Conventional Design)			Commuter Train (Collision with Crash-Energy Management Design)		
	Seats Lost	Secondary Impact Fatalities	Total	Seats Lost	Secondary Impact Fatalities	Total
140	65	0-4	65-69	83	0-1	83-84
110	45	0-6	45-51	49	0-3	49-52
70	12	1-11	12-23	8	0-6	8-14
35	0	0-11	0-11	0	0-2	0-2

Table 2-15 lists the fatalities on the commuter train for a commuter train collision with a power car propelled train. The crash-energy management design consistently results in fewer fatalities, both due to loss of occupant volume and to secondary impacts, for the entire speed range considered.

2.4 Analysis Conclusions

For power car propelled train to power car propelled train collision speeds below 70 mph, both the crash-energy management design and the conventional design preserve sufficient volume for the occupants to survive. For collisions above 70 mph, the crash-energy management approach is significantly more effective than the conventional approach in preserving occupant volume. For the full range of collision speeds, the crash-energy management design provides a significantly gentler initial deceleration than the conventional design.

The collision in which the cab car is the leading car results in substantially more fatalities on the power car propelled train than in the collisions in which the power car leads.

Table 2-15. Commuter Train Fatalities, Cab Car to Commuter MU Collision

Speed (MPH)	Commuter Train (Collision with Conventional Design)			Commuter Train (Collision with Crash-Energy Management Design)		
	Seats Lost	Secondary Impact Fatalities	Total	Seats Lost	Secondary Impact Fatalities	Total
140	207	16-135	223-342	157	18-155	175-312
110	113	22-185	135-298	89	25-196	114-285
70	34	28-244	62-278	13	29-242	42-255
35	0	19-173	19-173	0	12-127	12-127

The crash-energy management design power car propelled train is more compatible with existing equipment than conventional design. The analysis results indicate that there are fewer casualties on the commuter train in a collision with a crash-energy management designed power car propelled train than in a collision with a conventional design train. The results also indicate fewer casualties on the power car propelled train for collision up to the speed for which the crash-energy management design was intended.

The crash-energy management design presented in this report was designed for a particular collision scenario and should not be considered a universal or global optimum. The crash-energy management design was not fully optimized for a collision with a commuter train, however, any change which causes a decrease in power car propelled train fatalities may increase commuter train fatalities. The optimum force/crush characteristics will depend upon the details of all the collision scenarios which must be survived. If a range of collisions must be survived (i.e., collisions with freight trains, with maintenance of way equipment, with highway vehicles, etc.) a number of force crush characteristics should be evaluated for this range of collisions in order to determine the overall optimum design for a particular application.

3. INTERIOR OCCUPANT PROTECTION STRATEGIES IN TRAIN COLLISIONS

3.1 INTRODUCTION

A secondary collision occurs when the train rapidly decelerates due to the primary collision of the train with an obstruction, and the occupant continues to travel, in free flight, until he or she collides with an interior fixture, such as the seat back ahead. An occupant can be expected to survive if the forces and accelerations he or she experience are within human tolerance levels.

The means of protecting occupants and keeping the forces and accelerations they experience within human tolerance levels include controlling the deceleration of the vehicle, compartmentalization to provide a "friendly" interior, and passenger restraint such as seat and shoulder belts. The gentler the initial deceleration of the vehicle, the lower the speed at which the occupant will strike the interior. (Section 2 discusses structural crashworthiness measures at length, including strategies for controlling the initial deceleration of the cars in a train during a collision.) Compartmentalization is a strategy for providing occupant protection during a collision by limiting the occupant's range of motion and by ensuring that interior surfaces are sufficiently soft to limit forces imparted to the occupant during the secondary collision. By limiting the occupant's range of motion, the occupant's speed relative to the interior can be limited, resulting in a gentler secondary impact. By making the interior surfaces sufficiently soft, the maximum forces and decelerations experienced by the occupant can be limited to human tolerance levels. Occupant restraints act to constrain impacts with the interior and to tie the occupant to the center of gravity of the car. By constraining the motion of the occupant, occupant impacts with interior surfaces can be avoided or limited to particular surfaces, which can be specifically designed to provide a gentle impact.

The influence of the vehicle deceleration, the effectiveness of compartmentalization, lap belts, and lap belts and shoulder harnesses has been evaluated for three different interior configurations: seated rows with consecutive rows of forward-facing seats; facing seats with alternating rows of forward and rearward facing seats; and facing seats with a table.

The model used to perform the analysis is implemented in the computer program MADYMO [9]. MADYMO models the human body as a series of lumped-masses connected with force- and moment-deflection characteristics representative of the human body. This model has been developed principally for evaluating occupant response in automobile collisions.

3.2 ANALYSIS APPROACH

3.2.1 Secondary Impact Model

Figure 3-1 shows a schematic of the model seated in a train interior with consecutive rows of forward-facing seats. The analysis uses the deceleration time history of the vehicle predicted from the analyses of the dynamics and structural deformation under collisions described in Section 2. This deceleration is applied to the floor of the interior and causes the occupant to

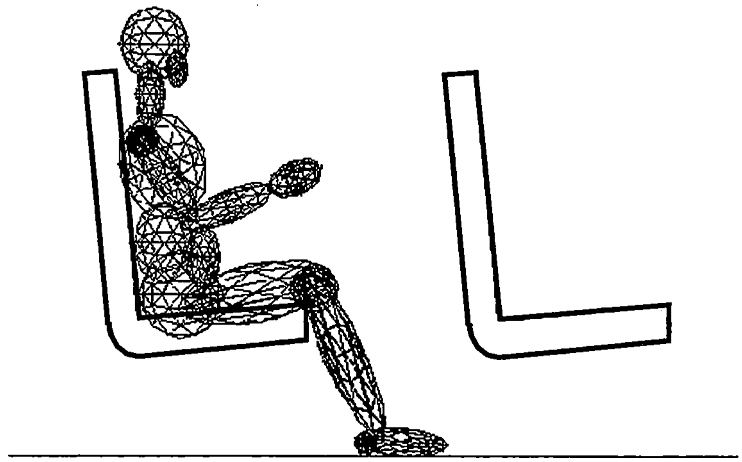

Figure 3-1. MADYMO Human Body Model

move. At some time during the vehicle deceleration, an unrestrained occupant will impact an interior fixture, such as a seat back, a partition, or the floor.

In the simulation, the occupant is modeled as a system of inter-connected, elliptically-shaped masses (ellipsoids) with the parameters chosen to approximate the characteristics of a human body. For this study, the parameters used correspond to a 50th percentile U.S. male. The 50th percentile male has a height which is just greater than half the male population of the U.S. and a weight which is just greater than half that population, etc.

The model generates time histories for the displacement, velocity, and acceleration for all the ellipsoids, including those corresponding to the head, and the forces and torques at the connections between the ellipsoids. Based on these motions and forces, injury criteria are calculated. Program outputs include data files for computer animations which depict the occupant motion during the collision. This animation allows the user to observe how different interiors, restraint systems, and structural train designs affect the occupant motion. MADYMO has been shown to simulate accurately the results of sled testing of automobile interiors with instrumented dummies [9].

The model assumes the occupant is passive during the collision. The increased duration of a train collision over an automobile collision allows the train occupants more time to react to the collision, increasing the likelihood that the occupant will respond during the collision. Such reactions may influence the outcome of the secondary collisions, however, it is likely that such reactions are specific to particular individuals. It would be difficult to model these reactions and their potential influences on the outcome of the secondary collision.

The program does not account for failure of interior components, i.e., seats and tables are assumed to remain intact. For the purpose of determining the occupant motion, the seats and tables are represented by plane surfaces with defined force/crush characteristics.

3.2.2 Interior Arrangements

The interior configuration is the geometric arrangement and physical characteristics (stiffness, damping) of the seats, tables, and other fixtures in the occupant compartment of a passenger train. The three interior arrangements modeled — forward-facing seats in rows, seats facing each other, and seats with tables — are shown in Figure 3-2.

The dimensions for the three seating configurations are shown in Figure 3-3.

a. Seats in Rows

b. Seats Facing

c. Seats and Table

* Seat dimensions are the same in all configurations

For the study, the seat backs were assumed to be in the fully-upright position. Occupant response may be influenced by details of the interior geometry, including the recline angle of the seat back, the distance between the seats (seat pitch), and the pitch angle of the seat bottom.

3.2.3 Occupant Protection Strategies

Compartmentalization - Compartmentalization is a strategy for providing occupant protection during a collision. The principal objectives of this strategy are to limit the occupant's range of motion and to ensure that the interior surfaces are sufficiently soft to limit injury during occupant impact. If an occupant is not protected by a forward seat back, a restraining barrier must be provided that is sufficiently flexible, yet strong enough to maintain its integrity. This strategy provides occupant protection independent of any action taken by the occupant. The concept of compartmentalization was used by the National Highway Traffic Safety Administration (NHTSA) to justify the absence of safety belt requirements on large school buses [10].

The regulations governing compartmentalization for school buses with a Gross Vehicle Weight Rating (GVWR) in excess of 10,000 lbs are contained in 49CFR571.222 - School Bus Seating and Crash Protection [11]. Figure 3-4, taken from this CFR, is a plot illustrating the required force/deflection characteristic for seat backs and partitions. When a sufficient amount of cushion and flexibility is provided in the surface of impact, the forces exerted on the occupant remain within a survivable level. For this study, the seat backs were assumed to have the softest force/deflection curve allowed in Figure 3-4.

Occupant Restraint - The two occupant restraint systems modeled consist of a lap belt alone and a lap belt with a shoulder harness. Occupant motions in the seats in rows and the seats-facing interiors were evaluated with a lap belt alone, and also with a lap belt and shoulder harness. The occupant motions in the interior with seats and table were evaluated only for the unrestrained occupant.

A readily available model of the seat and shoulder belts for an intermediate-sized automobile was utilized [12]. The belt model accounts for initial belt slack or pre-tension and for the potential rupture of belt segments if the force is greater than the strength of the belt. In the

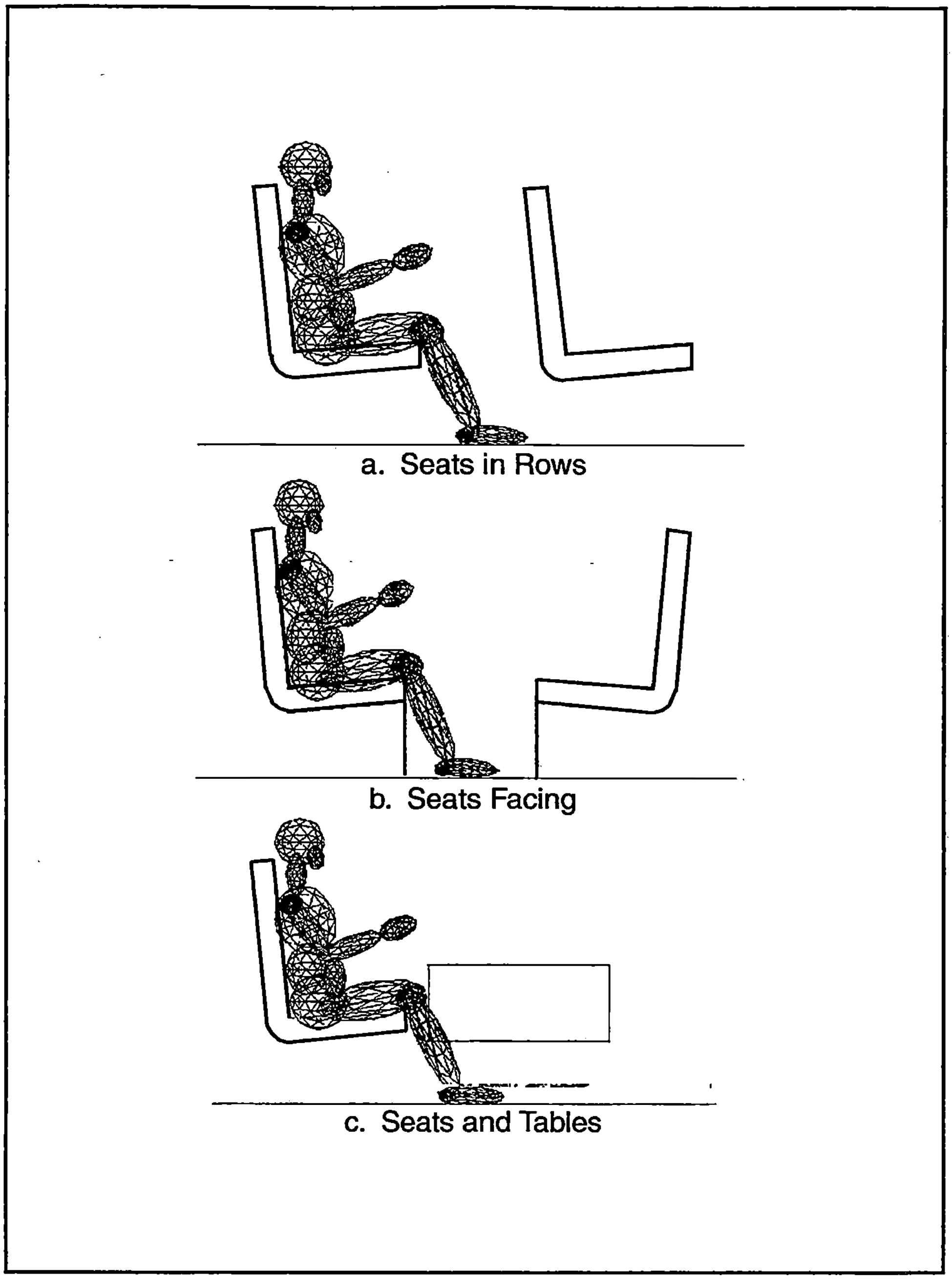

Figure 3-2. Interior Configurations

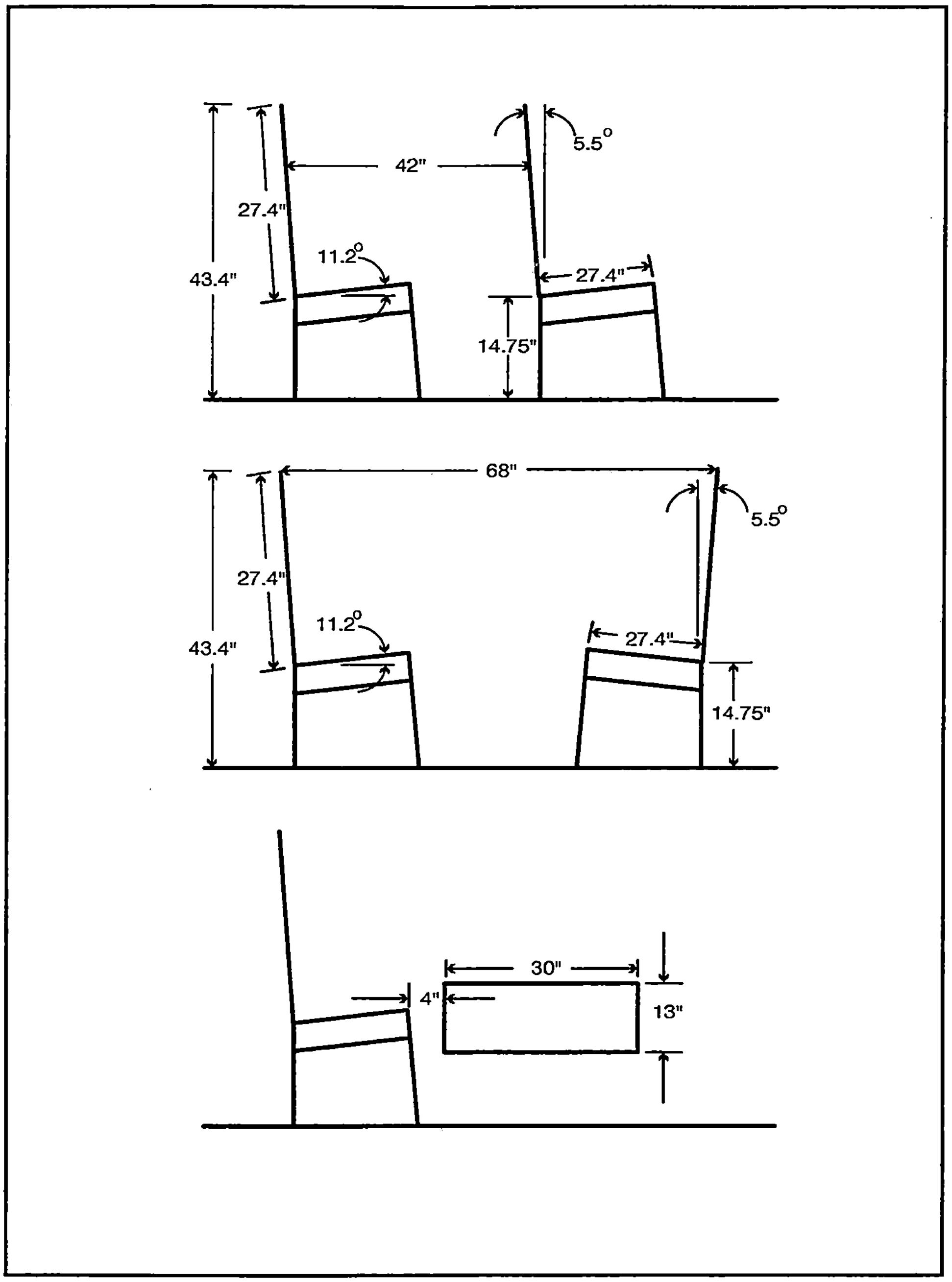

Figure 3-3. Interior Dimensions (not drawn to scale)

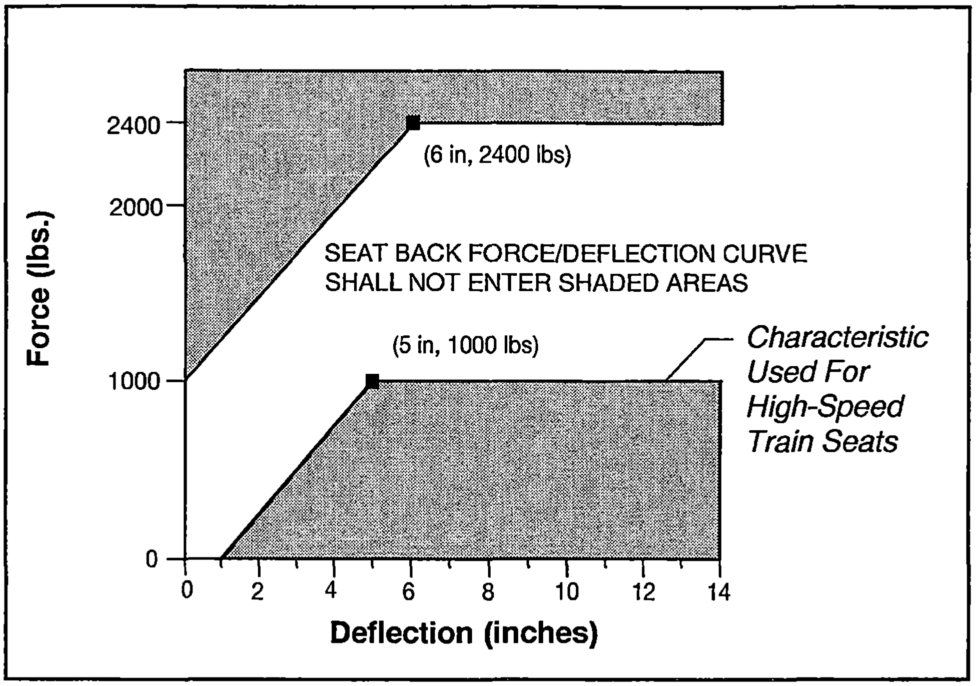

Figure 3-4. Force/Deflection Characteristic of Seat Back

model, the anchorage for the upper end of the shoulder harness is defined as a fixed point in the interior space.

There may be substantial difficulties in designing an appropriate upper attachment point for the shoulder harness. Owing to similar difficulties, NHTSA does not require a shoulder harness in the center (inboard) position of automobile seats [13].

3.2.4 Vehicle Deceleration Time Histories (Crash Pulses)

Occupant response to a range of crash pulses (primary collision deceleration time histories) was analyzed to determine the influence of car position, primary collision impact speed, and structural crashworthiness. Crash pulses from two primary collision conditions were used in this study. The primary collision conditions were a locomotive-to-locomotive collision and cab car-to-locomotive collision. The consist makeup includes a locomotive, five coach cars, and a cab car as illustrated in Figure 3-5. The train collision model used to calculate the deceleratio-time histories is described in detail in Section 2.

The crash pulse of the car is influenced by the car's position within the trainset. Figure 3-6 shows the crash pulses for each of the cars in the initially moving consist in a head-to-head collision with a 140 mph impact speed, for both the crash-energy management design train and the conventional design train. (The crash-energy management design train and the conventional design train are trains with different structures which behave in markedly different manners during a collision. The behavior of each train design in a collision is described in detail in Section 1.) For the crash-energy management design train, the peak deceleration for each succeeding car occurs later (in time). For the conventional design train, the peak decelerations occur in rapid succession.

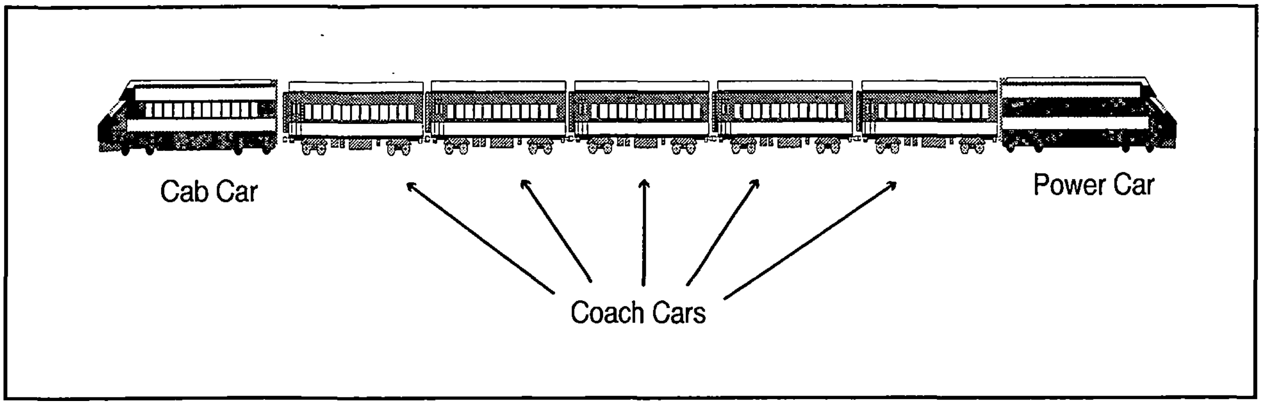

Figure 3-5. Basic Trainset Configuration

Figure 3-7 shows the influence of speed on the crash pulse. The principal characteristics of the crash pulse that are influenced by speed are its peak (maximum) value and its duration. For the crash-energy management design, the peak deceleration of the crash pulse increases as the primary collision speed is increased, up to speeds of about 70 mph. At primary collision speeds above 70 mph, the peak value no longer increases, but the duration of the crash pulse increases. This influence of primary collision speed is due to the nature of the force/crush characteristic of the car. After some amount of crushing of the car, the force required to cause further crushing no longer increases; this constant force/crush characteristic effectively limits the maximum deceleration the car can achieve. The conventional design reaches its maximum deceleration for a primary collision closing speed of about 35 mph. For primary collision speeds above 35 mph, the only influence on deceleration of the first coach in the conventional design train is to increase the duration of the crash pulse.

Six crash pulses were used in evaluating all the interiors. These are shown in Figure 3-8. These crash pulses were selected to represent the range of crash-pulse characteristics as described in Section 2, with particular attention to the peak deceleration and the time required to develop the peak deceleration.

The crash pulse input for MADYMO was calculated from the crash pulse predicted by the lumped mass train model to eliminate high frequency oscillations resulting from the computation method used in the lumped parameter model. Figure 3-9 shows an example of the lumped mass train model results and the input crash pulse used in the occupant simulation.

3.2.5 Injury Criteria

The HIC, chest deceleration, and neck injury criteria were used to evaluate the mode and severity of predicted injuries. The Abbreviated Injury Scale (AIS) [14], published by the American Association for Automotive Medicine, was used to provide a basis for comparison of HIC and chest deceleration. Table 3-1 lists the AIS Code and the corresponding values of HIC and chest deceleration.

The AIS is coded 0 through 6. AIS 0 indicates no injury, AIS 1 indicates minor injury, and so on. AIS 6 indicates the most severe injury which cannot be treated currently and is determined

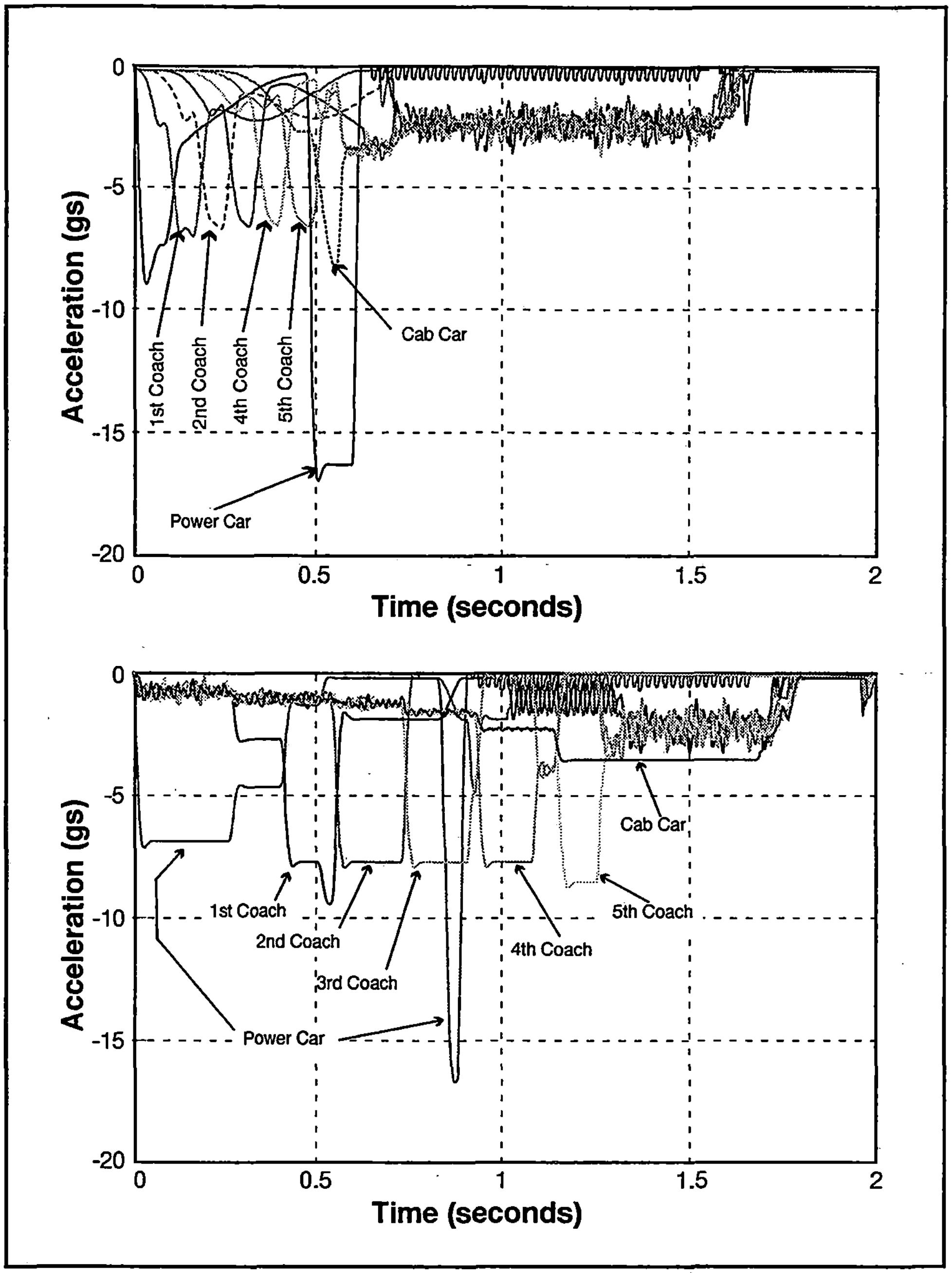

Note: Conventional Design (top), Crash-Energy Management Design (bottom)

Figure 3-6. Deceleration of Each Car in the Consist, Head-to-Head Collision With 140 mph Closing Speed

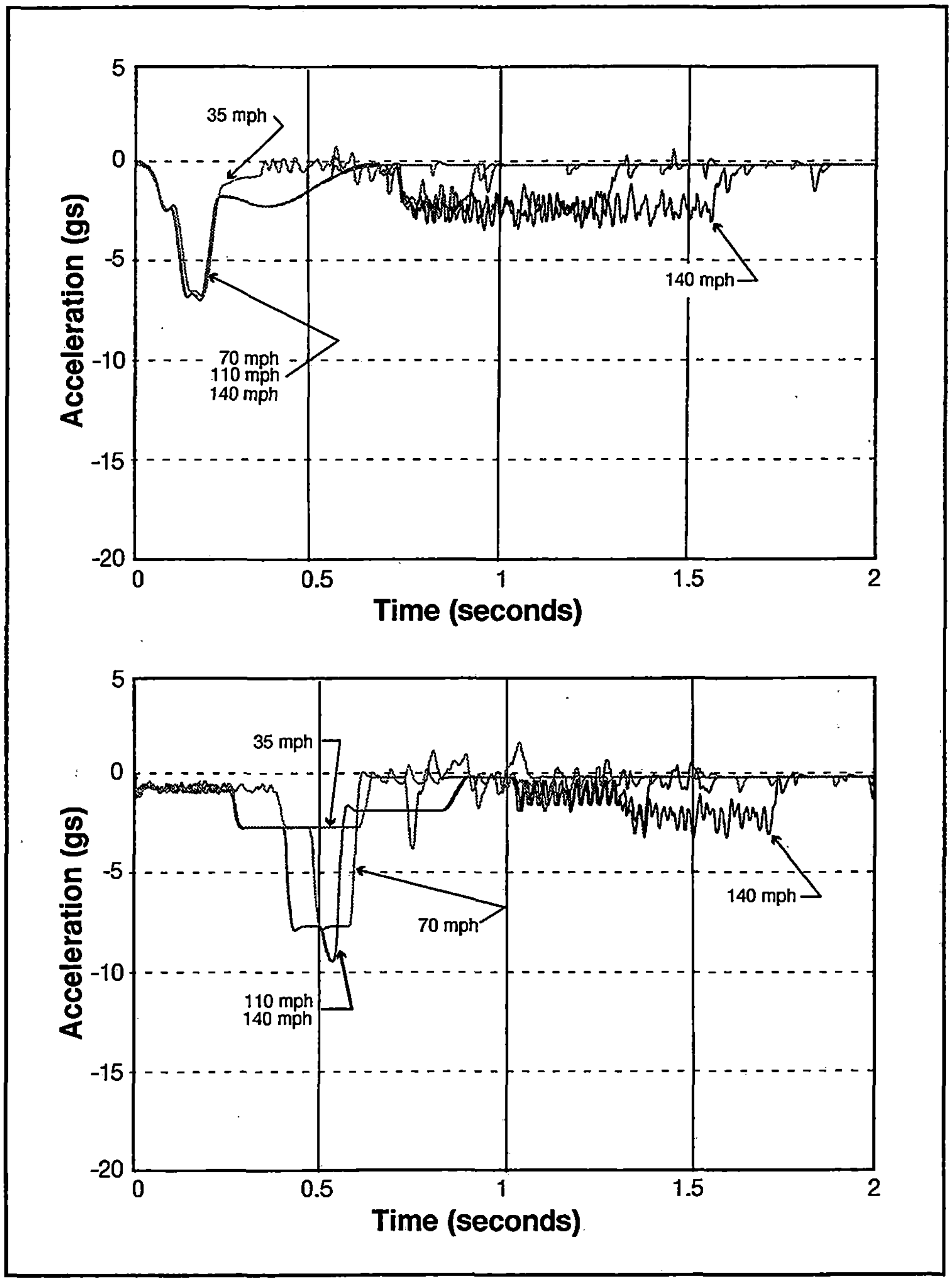

Note: Conventional Design (top), Crash-Energy Management Design (bottom)

Figure 3-7. Influence of Speed on First Coach Crash Pulse, 140 mph Head-to-Head Collision

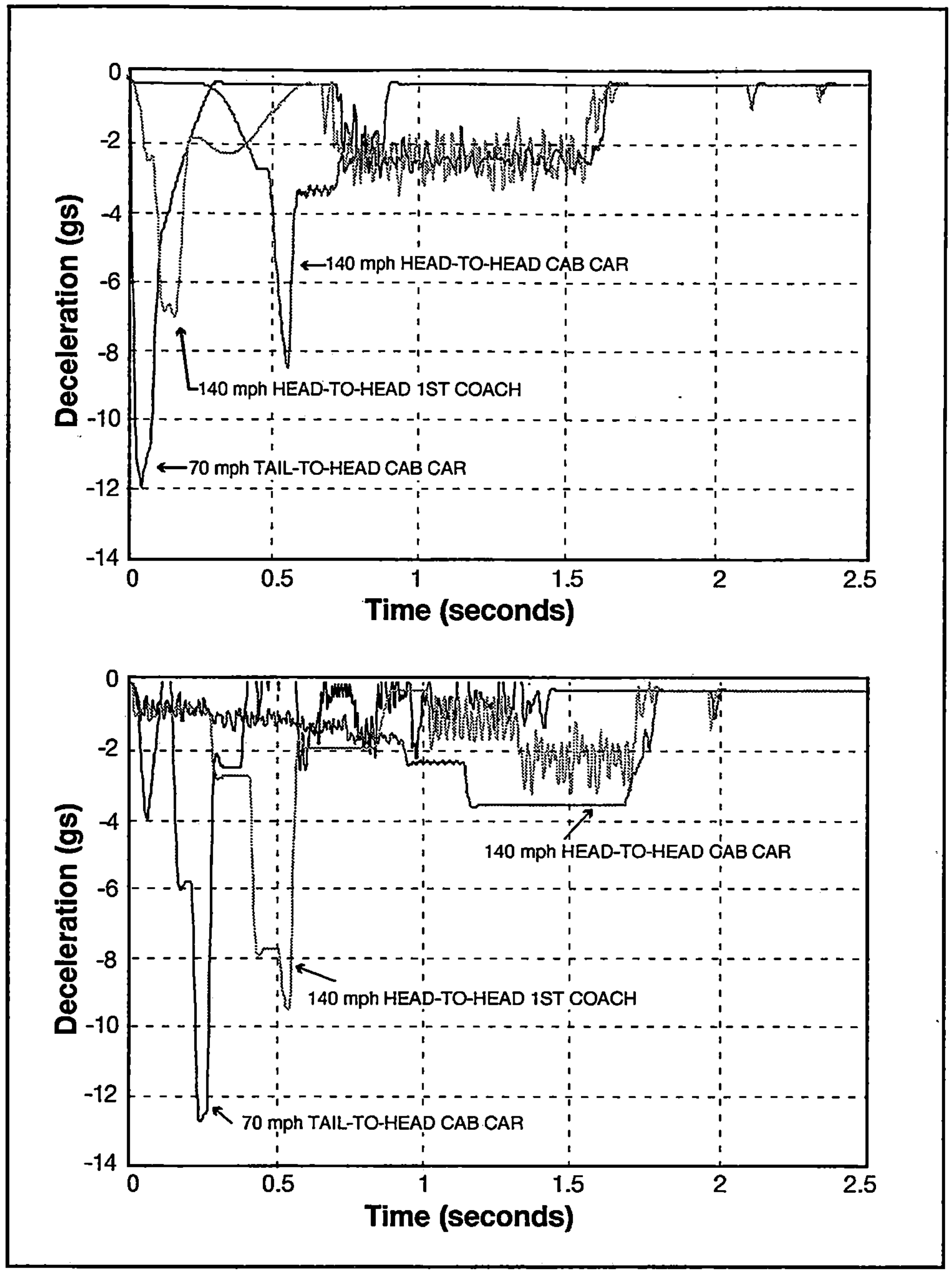

Note: Conventional Design (top), Crash-Energy Management Design (bottom)

Figure 3-8. Crash Pulses Used in Secondary Collision Analyses

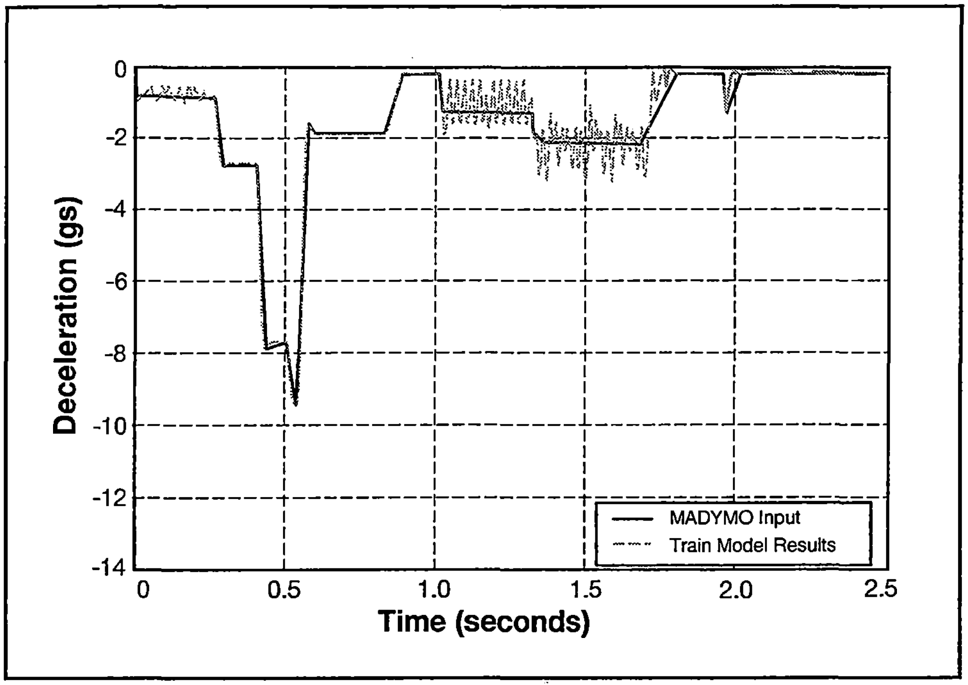

Figure 3-9. Crash Pulse, First Coach, 140 mph Head-to-Head Collision, Crash-Energy Management Design, MADYMO Input and Train Model Results

Table 3-1. AIS Code, HIC, and Chest Deceleration

AIS Code	HIC	Head Injury	Chest Deceleration	Chest Injury
1	135-519	Headache or dizziness	17-37 gs	Single rib fracture
2	520-899	Unconscious less than 1hour, linear fracture	38-54 gs	2 to 3 rib fractures; sternum fracture
3	900-1254	Unconscious 1 to 6 hours, depressed fracture	55-68 gs	4 or more rib fractures; 2 to 3 rib fractures with hemothorax or pneumothorax
4	1255-1574	Unconscious 6 to 24 Hours; open fracture	69-79 gs	Greater than 4 rib fractures with hemothorax or pneumothorax; flail chest
5	1575-1859	Unconscious more than 24 Hours; large hematoma	80-90 gs	Aorta laceration (partial transection)
6	>1860	Non-survivable	>90 gs	Non-survivable

to be virtually non-survivable. For instance, a HIC of 620 corresponds with AIS Code 2, where unconsciousness or linear skull fracture is possible due to head impact.

Figure 3-10, from reference [15], illustrates the relationship between injury criteria and the probability of fatality (percentage of life-threatening injury). If the HIC is determined to be 1000, this would be categorized as an AIS Code 3 and approximates an 18 percent risk of life-threatening injury. This means that for a group comprised of 50th percentile U.S. males subjected to the collision, 18 percent would not be expected to survive. This should not be interpreted to mean that the remaining 82 percent are unharmed; it is likely that the remaining 82 percent will have injuries, but their injuries are not expected to be life-threatening. AIS codes are superimposed on the HIC graph; a similar plot can be developed for chest deceleration.

Head Injury Criteria (HIC) - In reference [16], the Head Injury Criteria is defined as:

$$HIC = \left[\frac{1}{t_1 - t_2} \int_{t_1}^{t_2} a\,dt \right]^{2.5} (t_1 - t_2) \qquad (1)$$

(1)

where

a = resultant acceleration of the head in gs

$_1$ = start of time interval

t_2 = end of time interval

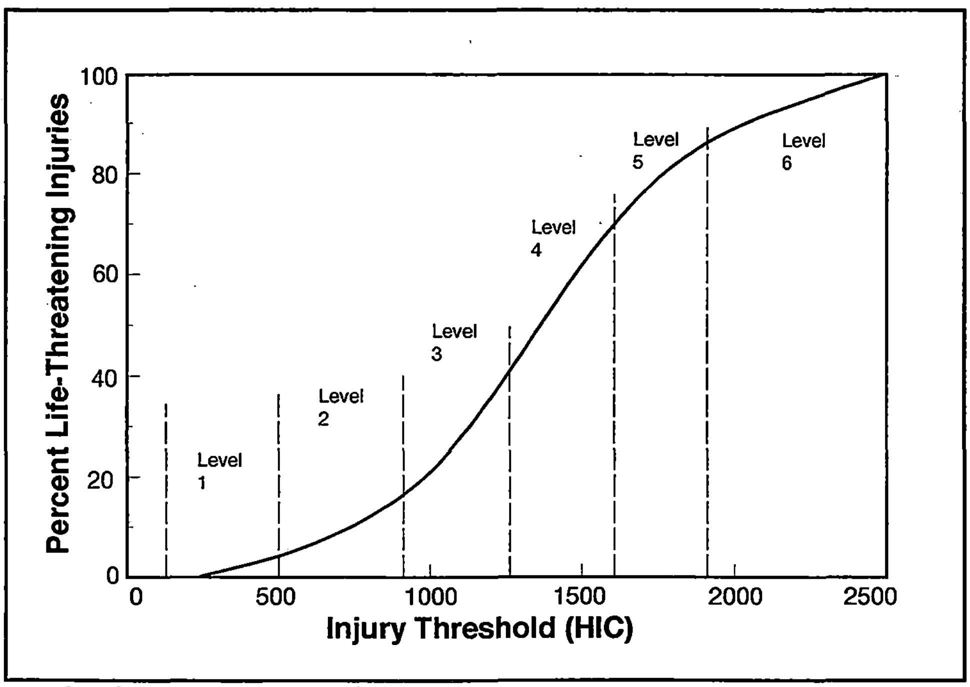

Figure 3-10. Probability of Fatality Versus Head Injury Criteria [15]

Using this HIC equation, the maximum HIC is calculated from the acceleration time history of the occupant's head, i.e., t_1 and t_2 are chosen to maximize the HIC calculation. Time intervals greater than 36 milliseconds are not employed. The HIC calculation includes the influence of the duration of the acceleration.

Chest Injury Criteria - The chest deceleration injury criteria is based on the maximum resultant deceleration of the chest. Spikes in the chest deceleration time history are discounted if they are less than 3 milliseconds in duration. For automobile crashworthiness testing, NHTSA specifies the maximum chest deceleration as 60 gs, which corresponds to a HIC of approximately 1000 for level of expected injury [16].

Neck Injury Criteria - Neck load criteria are used to assess injury when loads are imparted to the top of the head, in line with the spinal cord (a negative load represents compressive forces). In this study, this condition occurs when the unrestrained occupant in the facing rows of seats interior impacts the rearward facing seat. This particular seating configuration causes the occupant to dive head first into the seat, incurring large neck loads, even in cases with a gentle crash pulse.

This injury condition also may occur, in varying degrees, to occupants restrained with lap belts alone in the forward-facing seats in rows interior. While the occupant's body is restrained, the head builds up angular acceleration and strikes the seat back with the top of his head. The severity of the neck injury depends principally on the length of the occupant's torso and the distance separating the seats.

In collisions with no head impact (usually occurring when the occupant is restrained with a lap belt and shoulder harness), the tensile neck load can be used to assess injury.

Figures 3-11 and 3-12 illustrate the neck injury criteria for axial compressive and tensile neck loads, respectively, proposed but not implemented by NHTSA [14]. For the purpose of this paper, the criteria are used to compare the potential for neck injury between occupants involved in conventional and constrained crash-energy management train collisions. In both figures, the plots show the boundary between tolerance regions, i.e., neck loads for a given duration occurring below the boundary are survivable, while neck loads above the boundary are virtually non-survivable.

3.3 ANALYSIS RESULTS

3.3.1 Seats in Rows Interior

Compartmentalization - Figure 3-13 shows the computer-simulated occupant motions for the unrestrained occupant in the interior with forward-facing seats in rows.

Figures 3-14 and 3-15 show comparisons of the longitudinal velocity of the occupant's head as a function of distance, relative to the interior of the train, for the MADYMO model and the basketball model, and for the first coach car and the cab car. For the basketball model, it was assumed that the occupant's head goes into free flight (i.e., remains at the initial speed of the train) while the train slows down. The distance from the occupant's nose to the seat back ahead of him is 2 1/2 feet — the seat pitch is 42 inches, the occupant's head is assumed to be 8-inches deep,

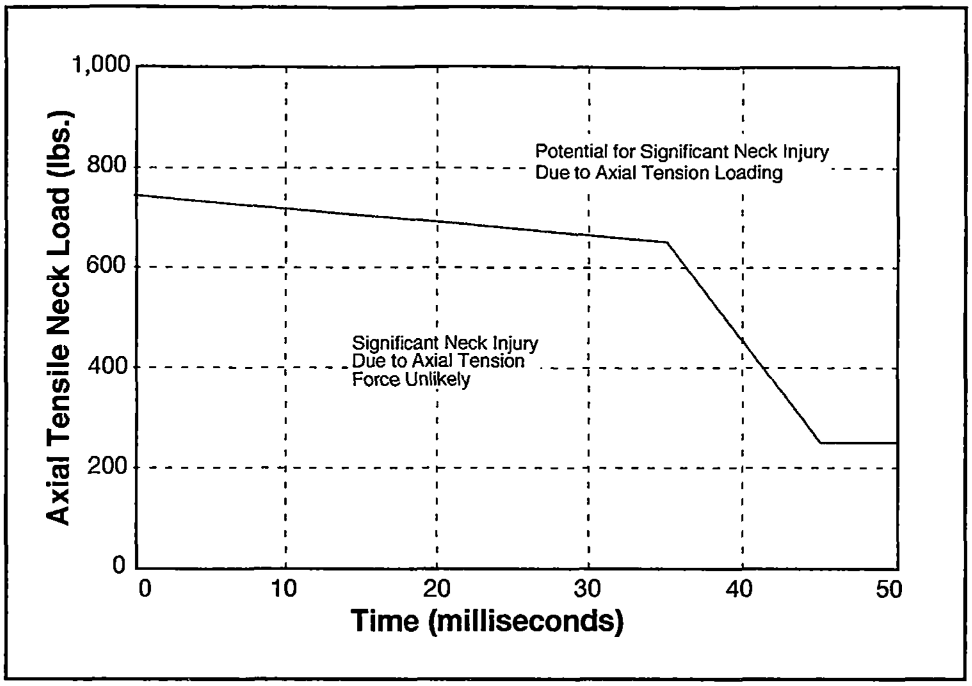

Figure 3-11. Injury Criteria for Tensile Neck Loads

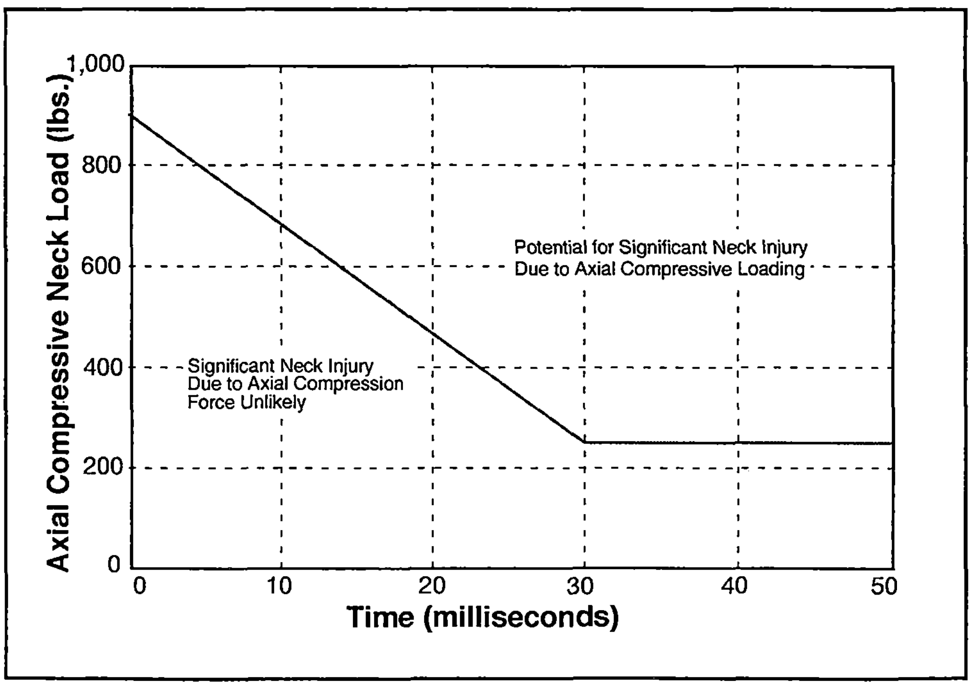

Figure 3-12. Injury Criteria for Compressive Neck Loads

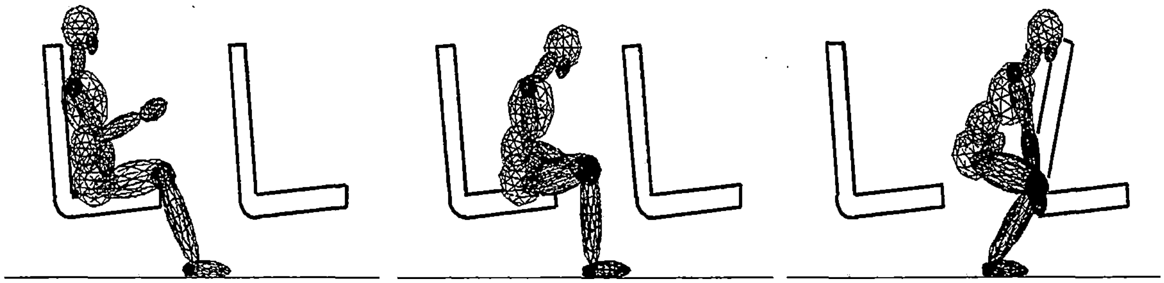

Figure 3-13. Occupant Motion, Unrestrained, Seats in Rows Interior

and the padding on the seat is assumed to be 4-inches thick. Comparisons are shown for head-to-head and tail-to-head collisions, for both the crash-energy management and conventional train structural designs. Figures 3-14 and 3-15 support the assumption that the unrestrained occupant goes into free flight during the collision and demonstrate that the representation in MADYMO is appropriate. In the constrained crash-energy management collisions, the velocity of the occupant's head begins to decrease gradually prior to the secondary impact, as shown graphically in Figures 3-19 and 3-21. Therefore, the free flight assumption is slightly less accurate for the constrained crash-energy management design.

Figure 3-16 shows the kinematic response of the unrestrained occupant in the seated rows interior during a 140 mph head-to-head collision for the conventionally designed train (left) and the constrained crash-energy management train (right). The initial portion of the constrained crash-energy management pulse is sufficiently gentle such that friction forces between the occupant's feet and the floor are large enough to keep the feet from sliding forward, causing the occupant to begin to stand up during the collision. The initial portion of the conventional pulse is sufficiently abrupt such that the occupants' feet slide on the floor.

Figure 3-17 plots the deceleration time histories for the unrestrained occupant's head and the first coach car during a 140 mph head-to-head collision. The occupant's peak deceleration is substantially greater than the car's and occurs shortly after the secondary impact, when the occupant is abruptly slowed.

Figure 3-18 shows plots of the unrestrained occupant's and the car's inertial velocity time histories for a 140 mph head-to-head collision. The more abrupt deceleration of the first coach

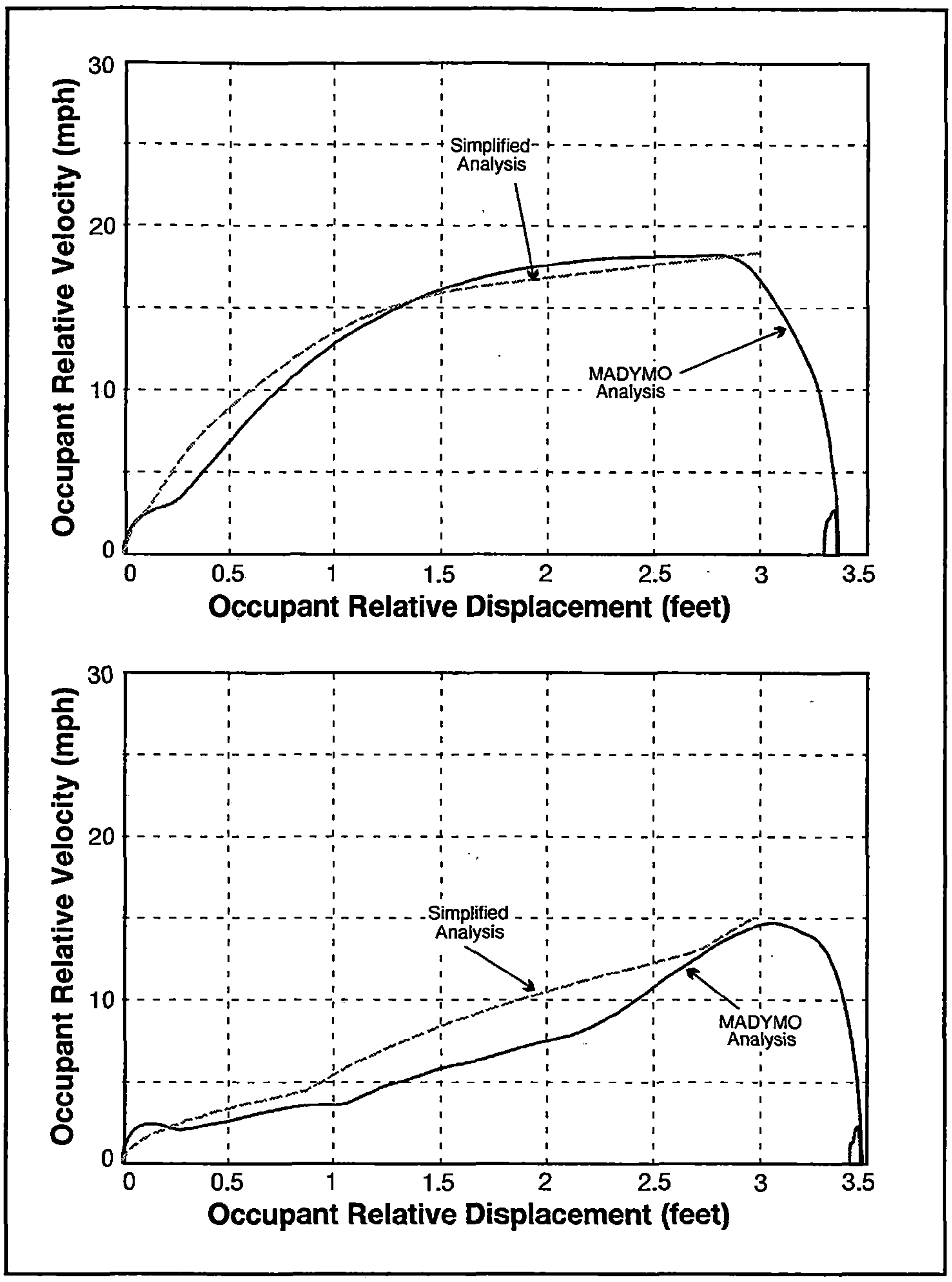

Note: Conventional Design (top), Crash-Energy Management Design (bottom)

Figure 3-14. Comparison of MADYMO and Simplified Model Analysis Predictions, Occupant Relative Velocity Versus Occupant Relative Displacement, First Coach Car, 140 mph Head-to-Head Collision

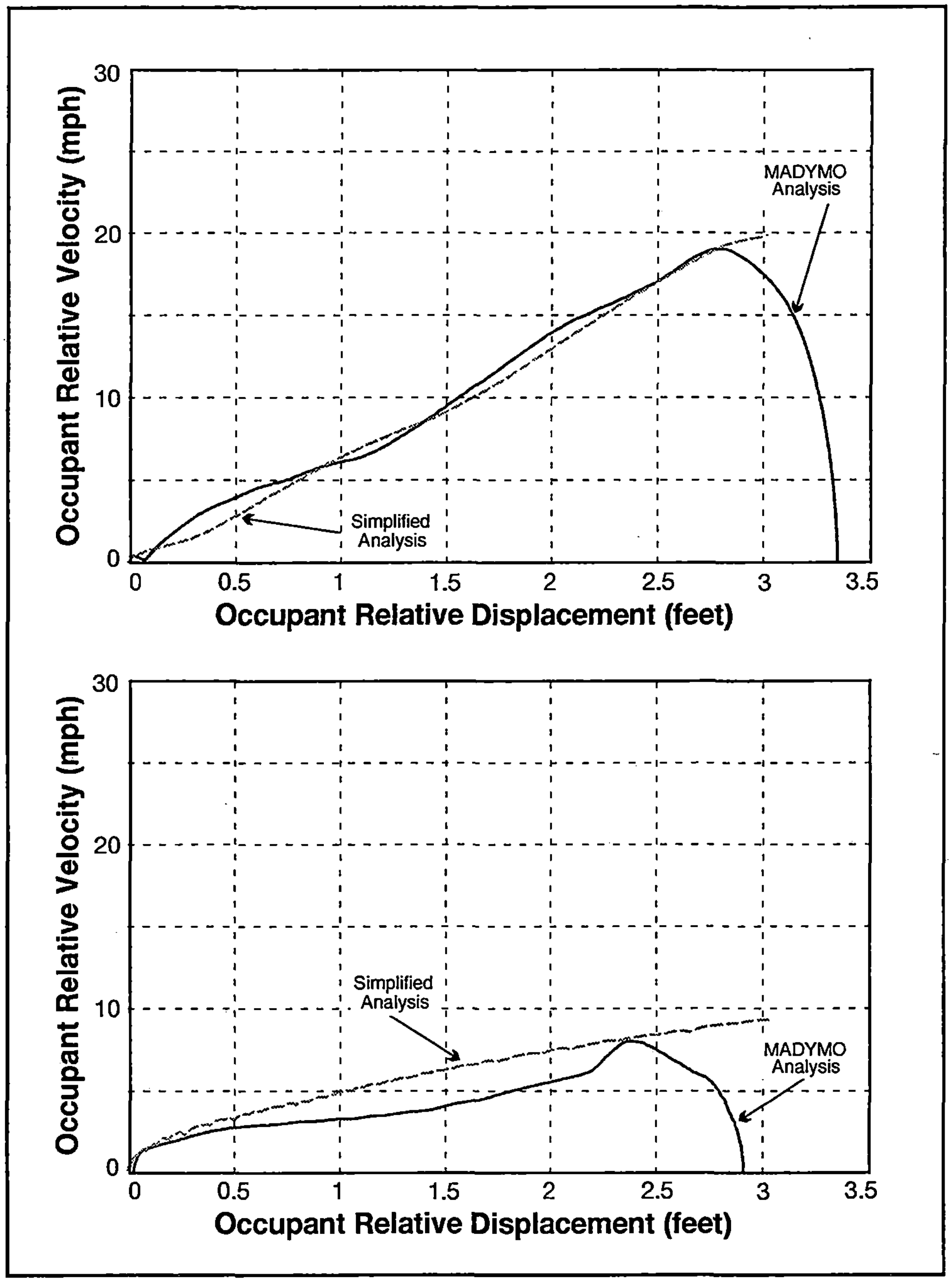

Note: Conventional Design (top), Crash-Energy Management Design (bottom)

Figure 3-15. Comparison of MADYMO and Simplified Model Analysis Predictions, Occupant Relative Velocity Versus Occupant Relative Displacement, Cab Car, 140 mph Head-to-Head Collision

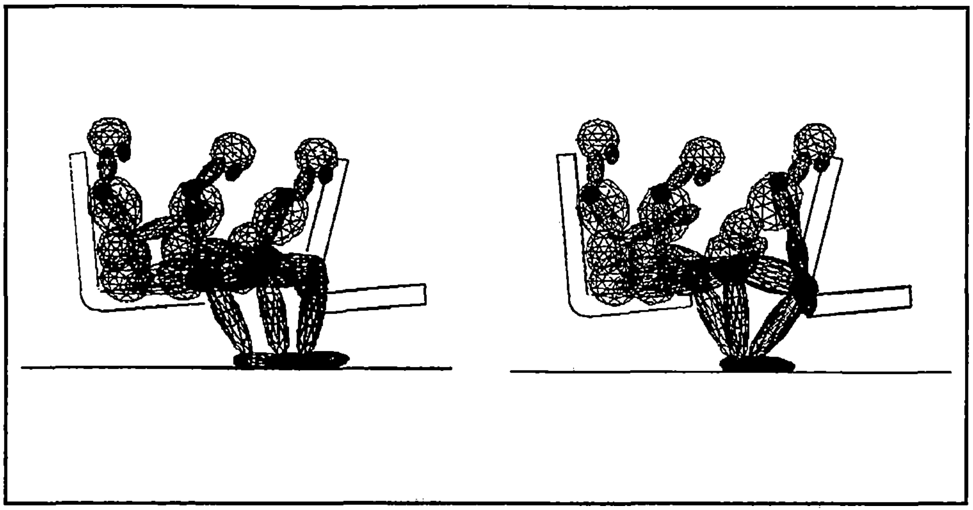

Figure 3-16. Human Body Kinematic Response to Initially Abrupt and Initially Gentle Crash Pulse, Seats in Rows Interior

car of the conventional design results in the occupant going into free flight, maintaining a speed of approximately 140 mph until the occupant impacts the forward seat. In general, this results in a more severe deceleration of the occupant's head. The initially gentle deceleration of the first coach car of the constrained crash-energy management design allows the occupant to begin to decelerate from 140 mph before impact with the seat. In general, this results in a less severe secondary impact.

In Figure 3-19, the relative velocity is plotted against the relative displacement for an occupant in a seated row interior in each car in a 140 mph head-to-head collision. The constrained crash-energy management design results in substantially lower secondary impact velocities as compared to the conventional design, especially for cars behind the second coach car.

Table 3-2 lists the corresponding injury criteria for an unrestrained occupant in the seats in rows interior in each of the passenger cars involved in a 140 mph head-to-head collision.

Occupant Restraint - Figure 3-20 shows how the occupant motion is influenced by the two restraint systems. The lap belt alone cannot prevent the head of a 50th percentile male from striking the forward seat with a 42-inch seat pitch. For taller occupants, or for the same occupant in an interior with the seats positioned closer together, an occupant restrained with only a lap belt could potentially suffer greater injuries than an unrestrained occupant, owing to head impact. The combined lap belt and shoulder harness are effective in preventing the occupant from striking the forward seat.

Figure 3-21 shows the deceleration time history of the occupant restrained with a lap belt, in addition to the unrestrained occupant and car deceleration time histories. The figure shows a substantial decrease in the head deceleration of the restrained occupant over the unrestrained occupant for the same collision conditions.

Figure 3-22 shows the velocity time history of the occupant restrained with a lap belt, in addition to the unrestrained occupant and car velocity time histories.

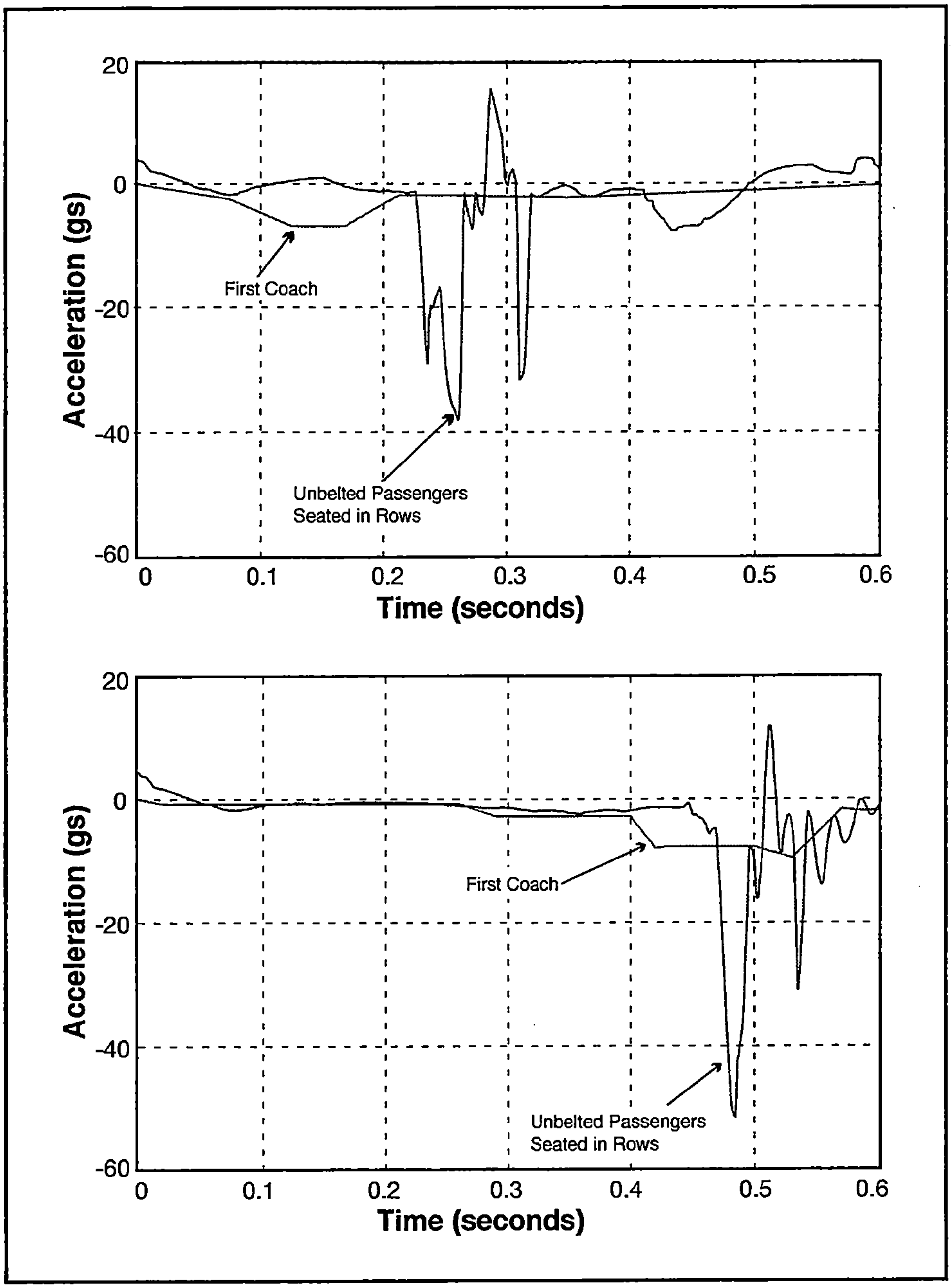

Note: Conventional Design (top), Crash-Energy Management Design (bottom)

Figure 3-17. Unrestrained Passenger and Vehicle Decelerations, 140 mph Head-to-Head Collision

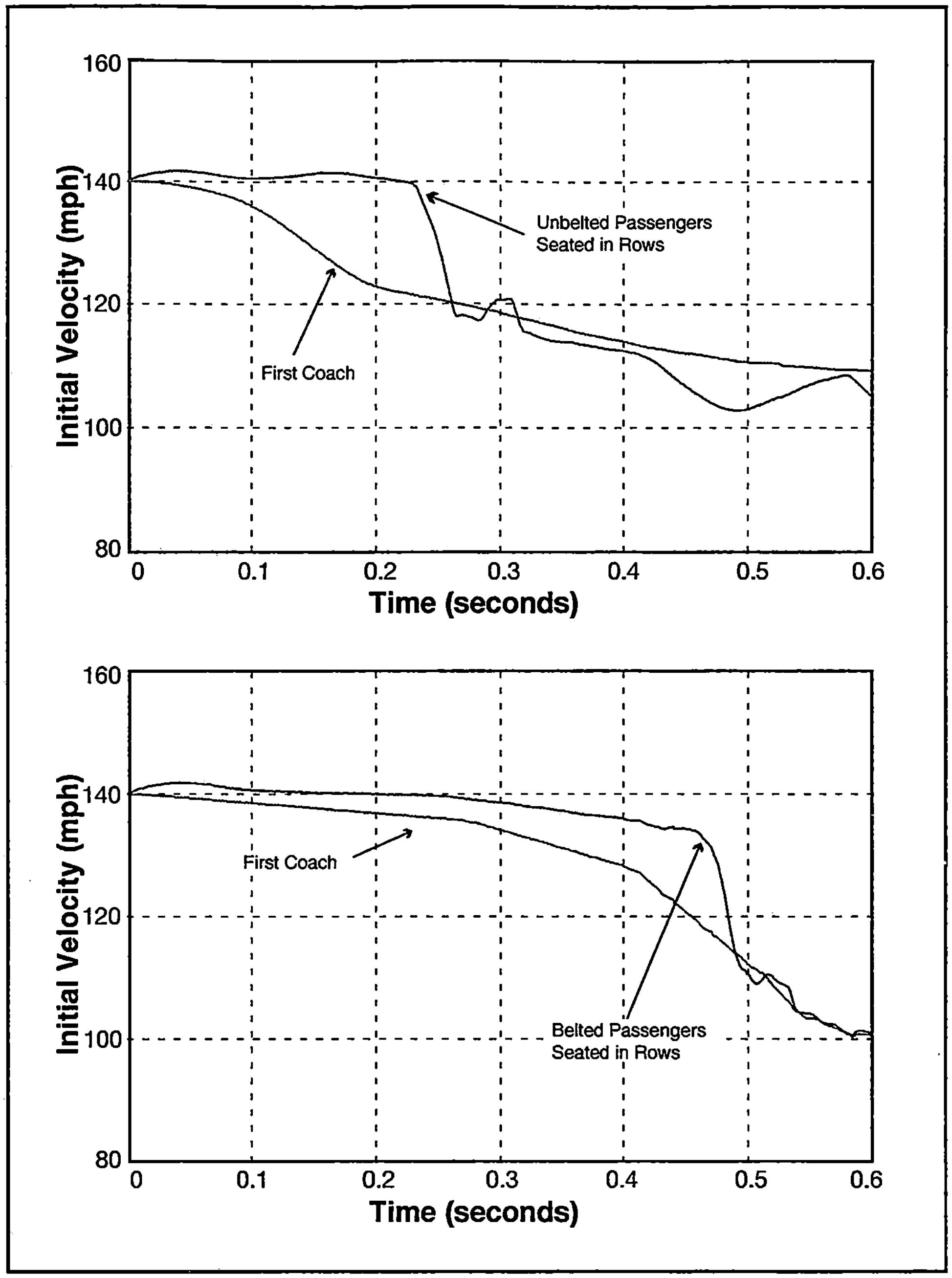

Note: Conventional Design (top), Crash-Energy Management Design (bottom)

Figure 3-18. Unrestrained Passenger and Vehicle Velocities, 140 mph Head-to-Head Collision

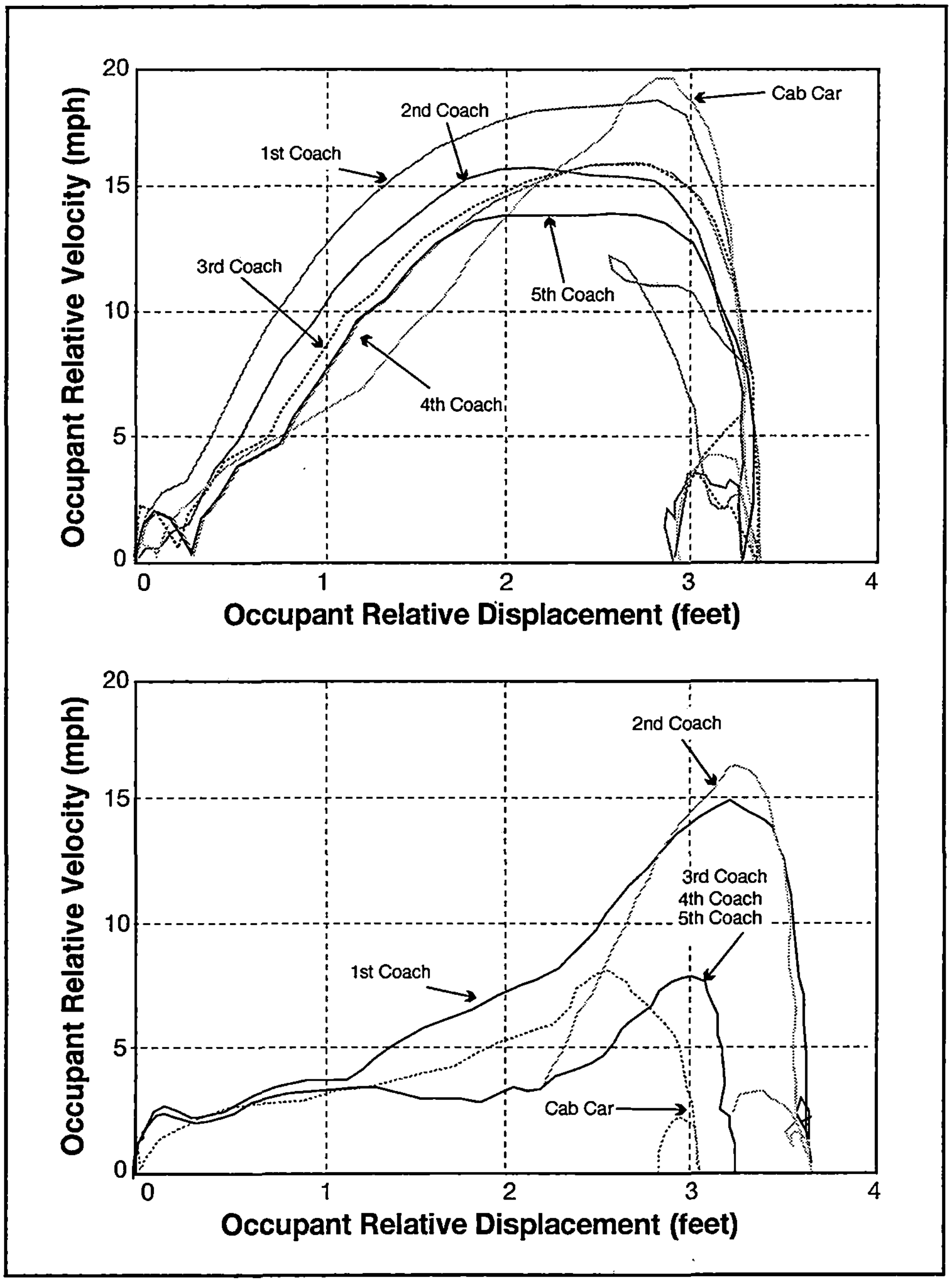

Note: Conventional Design (top), Crash-Energy Management Design (bottom)

Figure 3-19. Secondary Impact Velocities for Occupants by Passenger Car

Table 3-2. Injury Criteria for Secondary Collisions of Unrestrained Occupants, Seats in Rows Interior

		HIC	Chest gs	Neck Load (lbs)
		Unbelted	Unbelted	Unbelted
Conventional Design	1st Coach	167	24	-386
	2nd Coach	77	19	-454
	3rd Coach	109	25	-436
	4th Coach	59	16	-475
	5th Coach	135	28	-368
	Cab Car	223	36	-529
Constrained Crash-Energy Management Design	1st Coach	221	38	-536
	2nd Coach	313	33	-367
	3rd Coach	17	10	-301
	4th Coach	17	7	-244
	5th Coach	17	7	-244
	Cab Car	11	7	-229

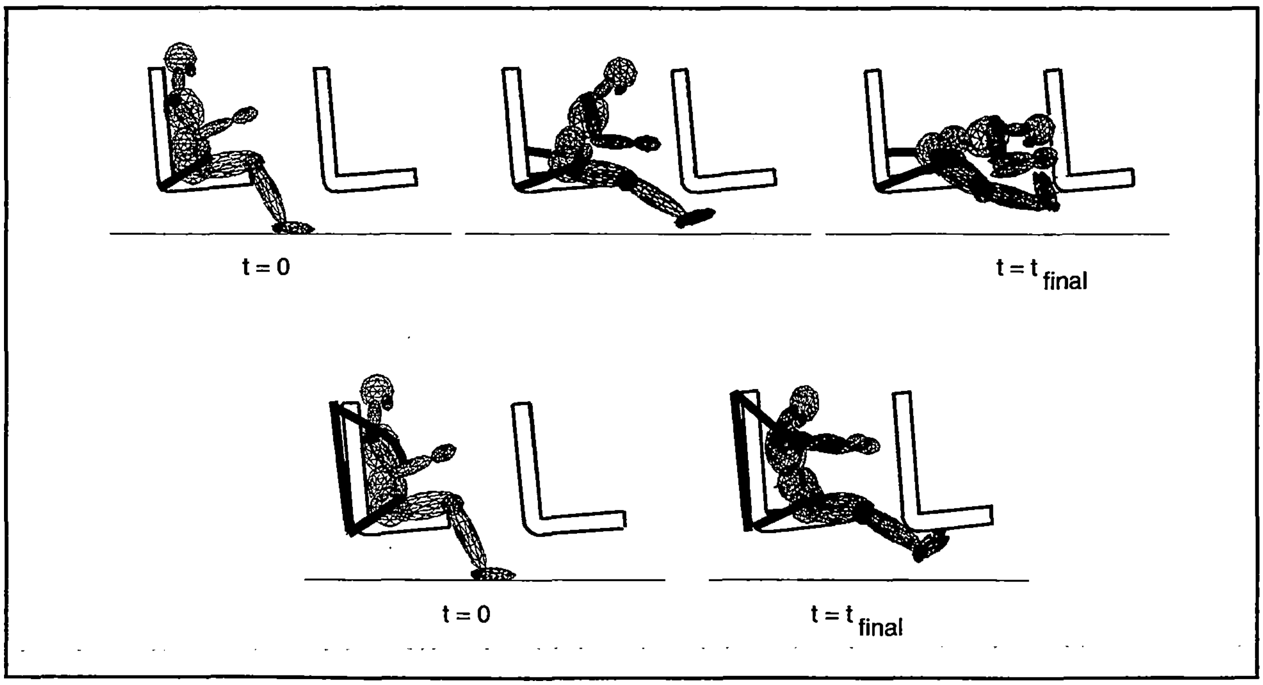

Figure 3-20. Occupant Motion, Restrained With Seat Belt and With Seat Belt and Shoulder Harness, Seats in Rows Interior

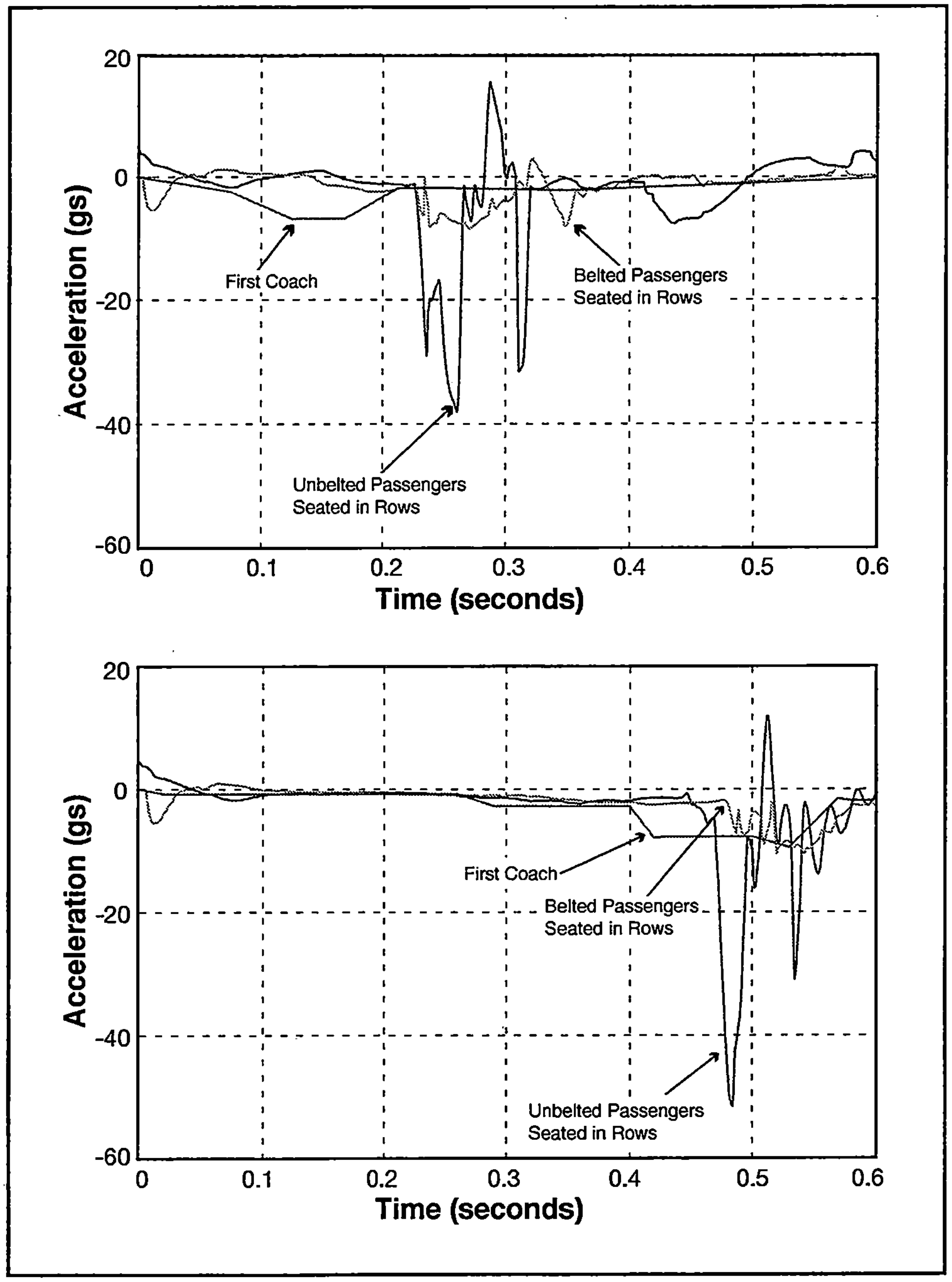

Note: Conventional Design (top), Crash-Energy Management Design (bottom)

Figure 3-21. Restrained Passenger and Vehicle Decelerations

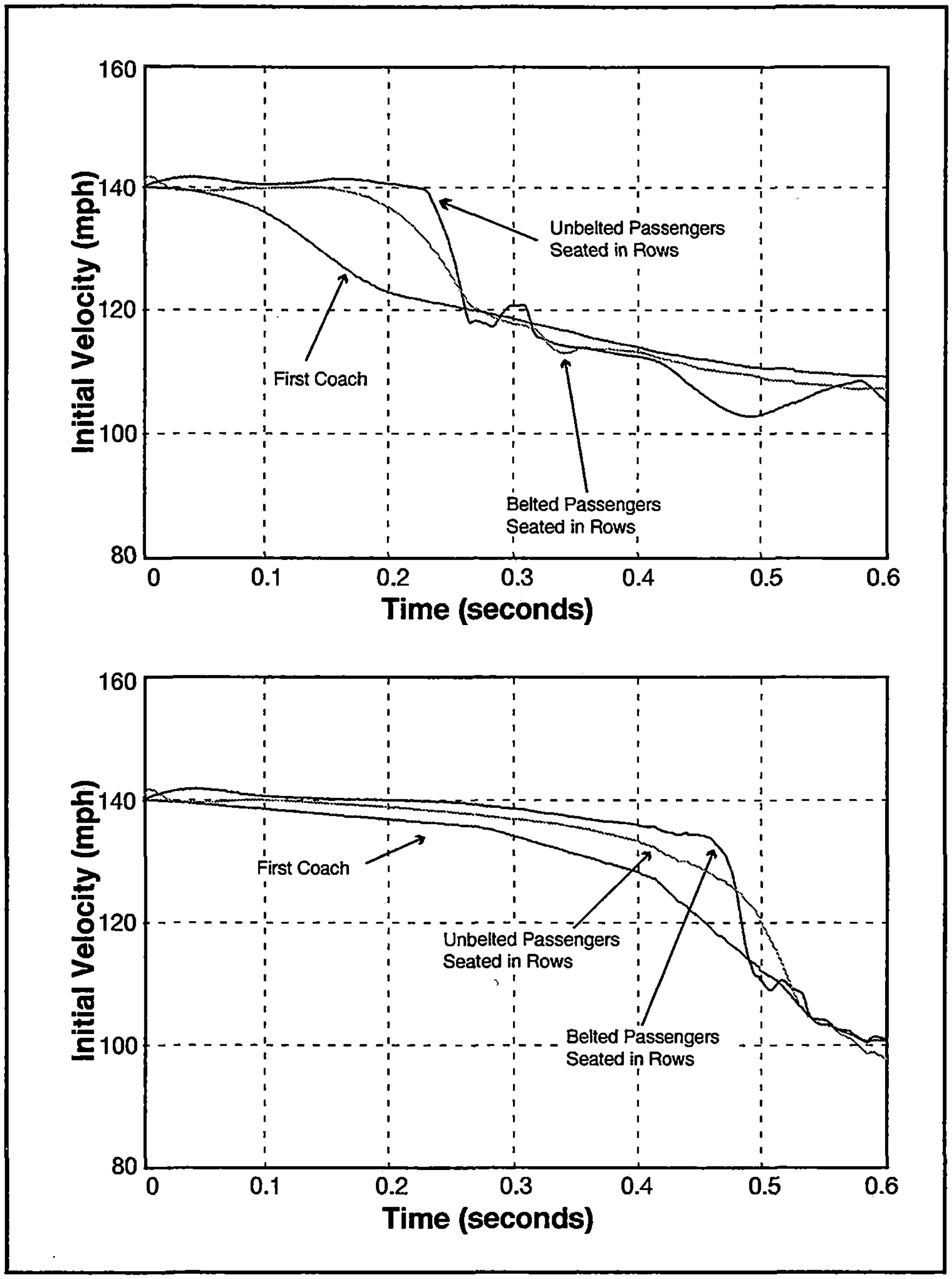

Note: Conventional Design (top), Crash-Energy Management Design (bottom)

Figure 3-22. Restrained Passenger and Vehicle Velocities

Calculation of Shear Forces and Moments on Seat Attachments - During the secondary impact, the occupant's inertial mass applies a load to the forward seat. The shear force and moment applied to the floor attachment of a passenger seat are engendered in two ways. In the case where an occupant is unrestrained, the applied load occurs when an occupant strikes the forward seat. In the case where an occupant is restrained with a lap belt, the load from the belted occupant is transferred to the seat via the seat belt. A passenger seat may experience both loads simultaneously if an unrestrained occupant strikes the seat back of a seat occupied by a belted passenger.

The shear forces and moments acting upon passenger seat floor attachments (see Figure 3-23) were evaluated for unrestrained occupants in the seats in rows interior in each passenger car. The shear forces and moments were evaluated for restrained passengers in the seats in rows interior only in the first coach car. In addition, calculations were made for the case in which an unrestrained occupant impacts a forward seat occupied by a restrained occupant.

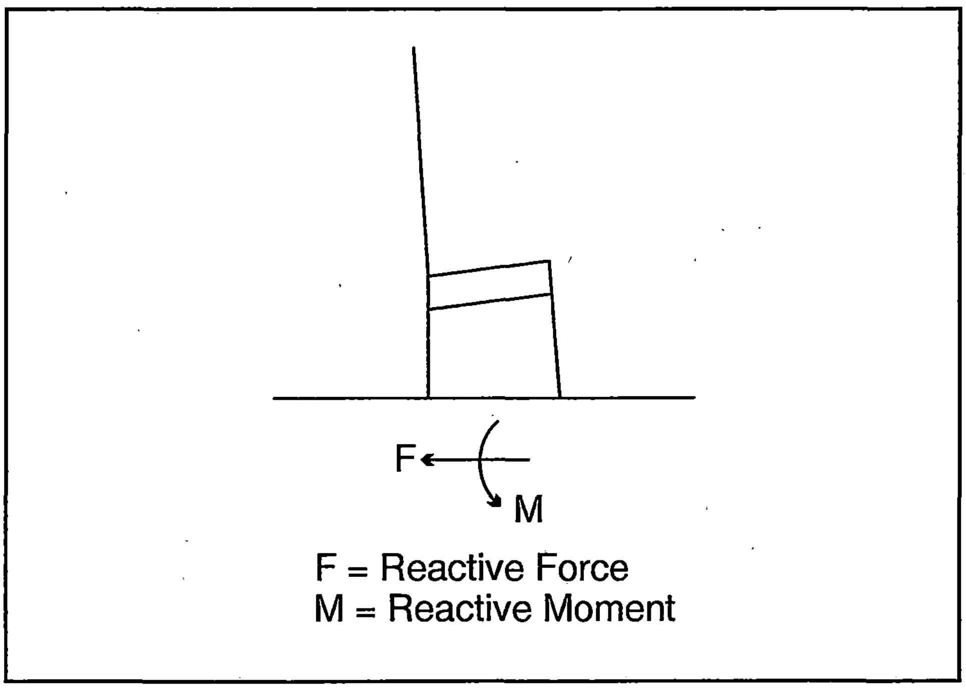

Figure 3-23. Shear Force and Moment Acting on Seat Attachment

Output from the simulation program included a data file containing the force time histories between the forward seat and each of the occupants' knees, head, neck, and upper torso in the unrestrained case, and forces between the occupied seat and the seat belt in the restrained case. The forces applied by each of the five body components (and the seat belt if applicable) were summed at each time step to represent the total shear force applied to the forward seat (or the occupied seat) by an unrestrained (or restrained) occupant during a collision. The sum of the moments acting about the seat's floor fixture was calculated from the five forces (left and right knees, head, neck, and upper torso). The height at which the five different forces were acting was estimated from the program's pictorial representation of the occupant's dynamic motion (see Figures 3-13 and 3-20).

Figures 3-24 and 3-25 show plots of the total forces and moments, respectively, acting on the forward seat due to an unrestrained occupant seated in each passenger car of the consist, for both a conventional train and a crash-energy management train.

Figures 3-26 and 3-27 show plots of the forces and moments, respectively, acting upon an occupied seat due to an occupant restrained with a lap belt, in the first coach car only. The components of the forces and moments are separated in these figures to show the portion attributed to the head acting on the forward seat back and the portion due to the seat belt acting on the occupied seat. The sum of the forces and moments due to the head and seatbelt represents the combined effects of two occupants in a row (both restrained with lap belts) applying loads to the same seat.

In Figures 3-24 and 3-25, the trends in forces and moments acting on seats by car resemble the trends seen in occupant injury data by car. In the constrained crash-energy management design, the severity of the forces applied to the seats is minimized away from the initial train-to-train collision. In the conventional train, the forces imparted to the passenger seats remain relatively high throughout all cars of the consist. The peak forces and moments applied to the passenger seats are summarized in Tables 3-3 and 3-4. The peak forces are normalized to the weight of a 175-pound occupant.

Summary of the Results of Seats in Rows Interior - Table 3-5 presents the injury criteria and the associated probability of fatal injury for unrestrained, belted, and belted and harnessed occupants in the seated rows interior. The table shows that the most severe crash pulse for this interior is for the cab car when it is leading during the collision, even at a lower impact speed. The table also shows that the nominal occupant is expected to survive the deceleration in all the collision scenarios evaluated if he or she is restrained with seat and shoulder belts.

3.3.2 Seats Facing

Figure 3-28 depicts the simulated motion for an occupant who is unrestrained, belted, and belted and harnessed in the seats facing interior. For this analysis, only the forward-facing seat is occupied. It is assumed that the addition of a rearward-facing occupant in the opposing seat would increase the level of injury.

The unrestrained occupant travels a substantial distance before impacting the seat back of the facing seat. This distance allows the occupant to build up speed relative to the interior, resulting in a severe impact. Due to the position of the body at impact, the inertial mass of the body follows the head into the seat, creating considerably large forces on the head and neck that are nearly unsurvivable.

Table 3-6 lists the probability of fatal injury for occupants that are unrestrained, belted, and belted and harnessed in the seats facing interior. This interior performed the worst among the interiors evaluated. There is near certain fatality for the unrestrained occupant in the seats facing interior for each crash pulse considered in this evaluation. The most severe crash pulse for this interior is also for the cab car in a tail-to-head collision. For this crash pulse, there is a substantial probability of fatality even for occupants with lap belts alone. The table also shows that the nominal occupant is expected to survive for each crash pulse evaluated if he or she is restrained with a lap belt and shoulder belt.

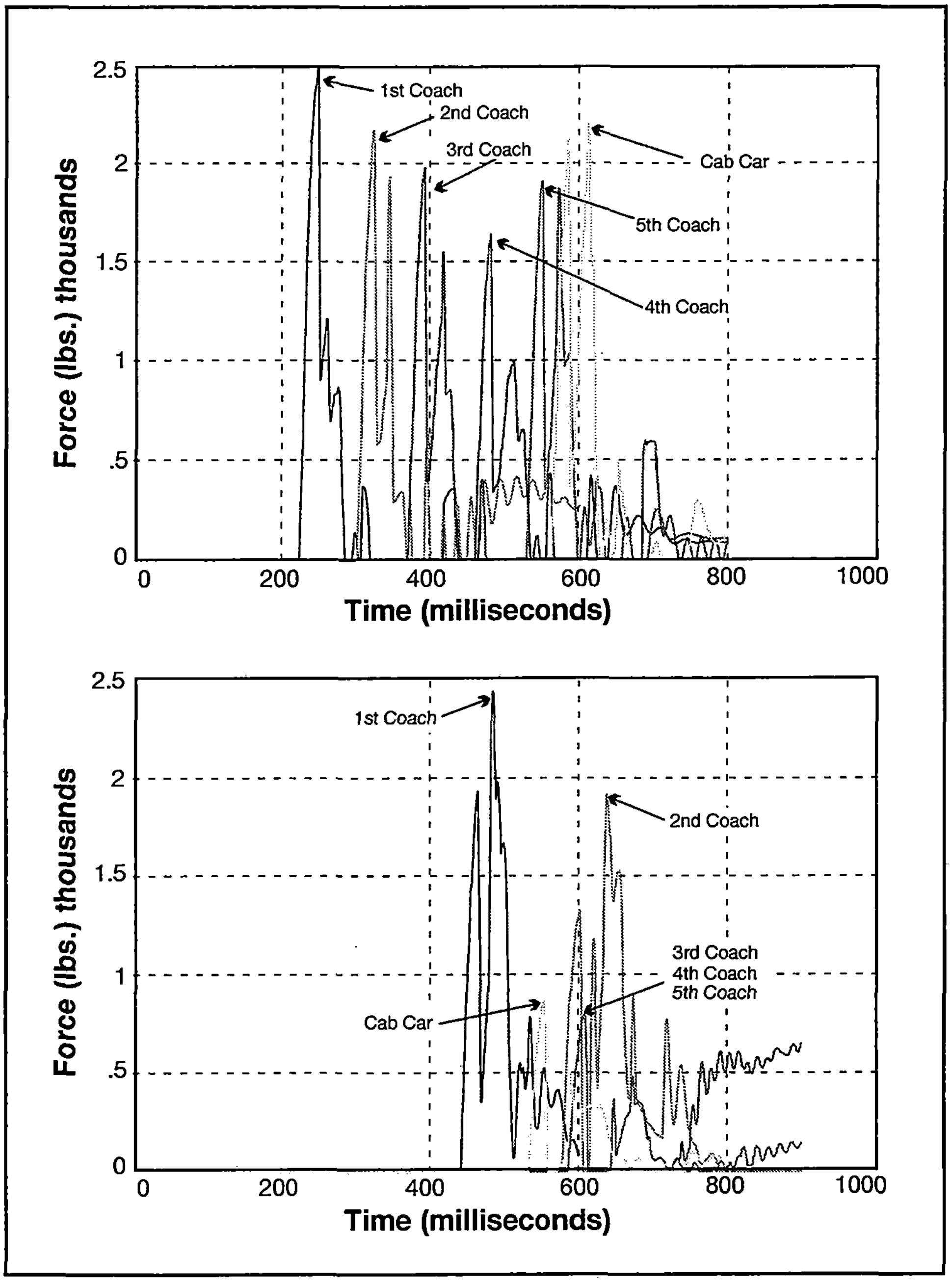

Note: Conventional Design (top), Crash-Energy Management Design (bottom)

Figure 3-24. Forces on Forward Seat Back Due to Unrestrained Occupant (by Car)

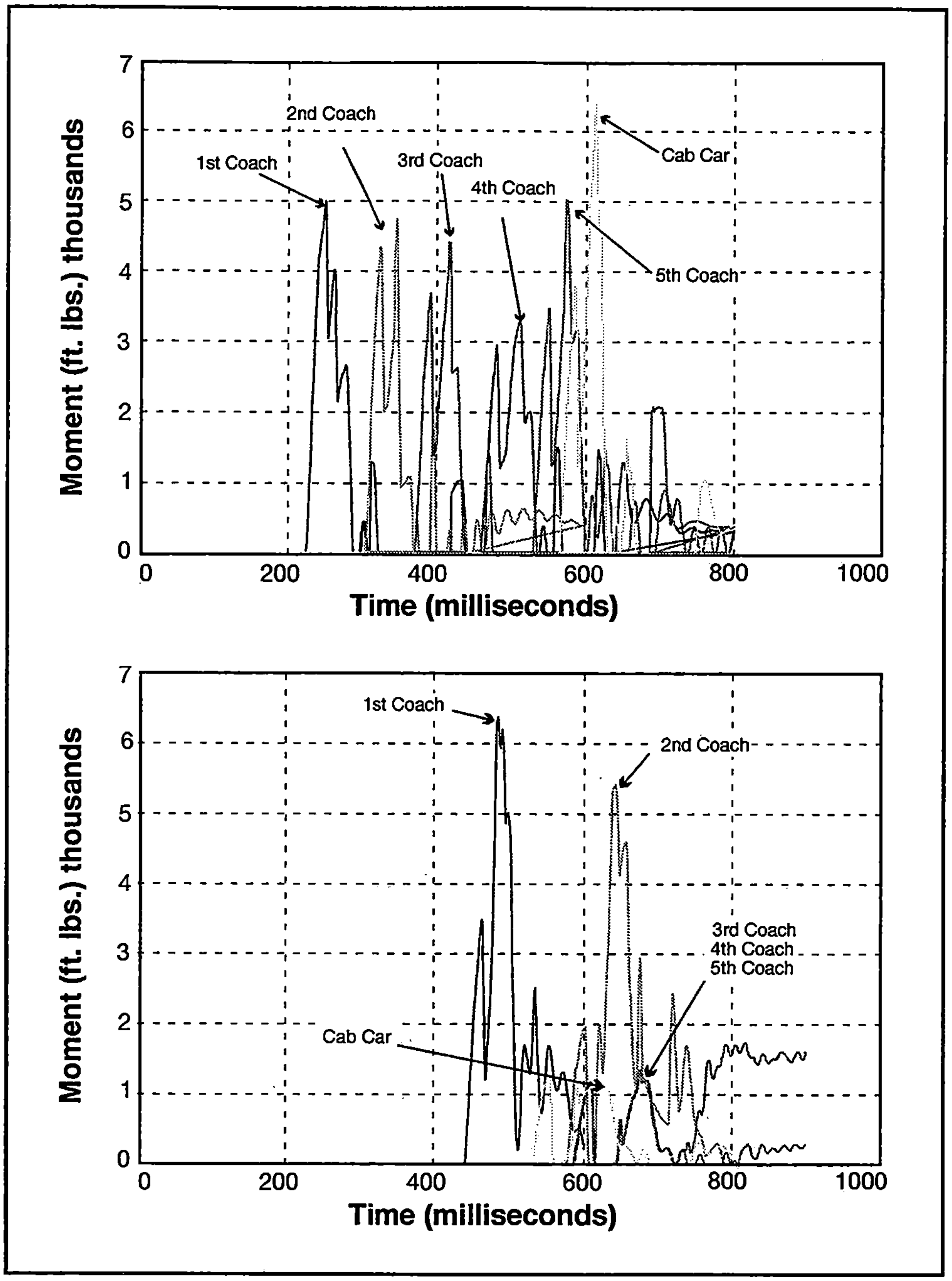

Note: Conventional Design (top), Crash-Energy Management Design (bottom)

Figure 3-25. Sum of Moments about Seat Floor Fixture Due to Unrestrained Occupant (by Car)

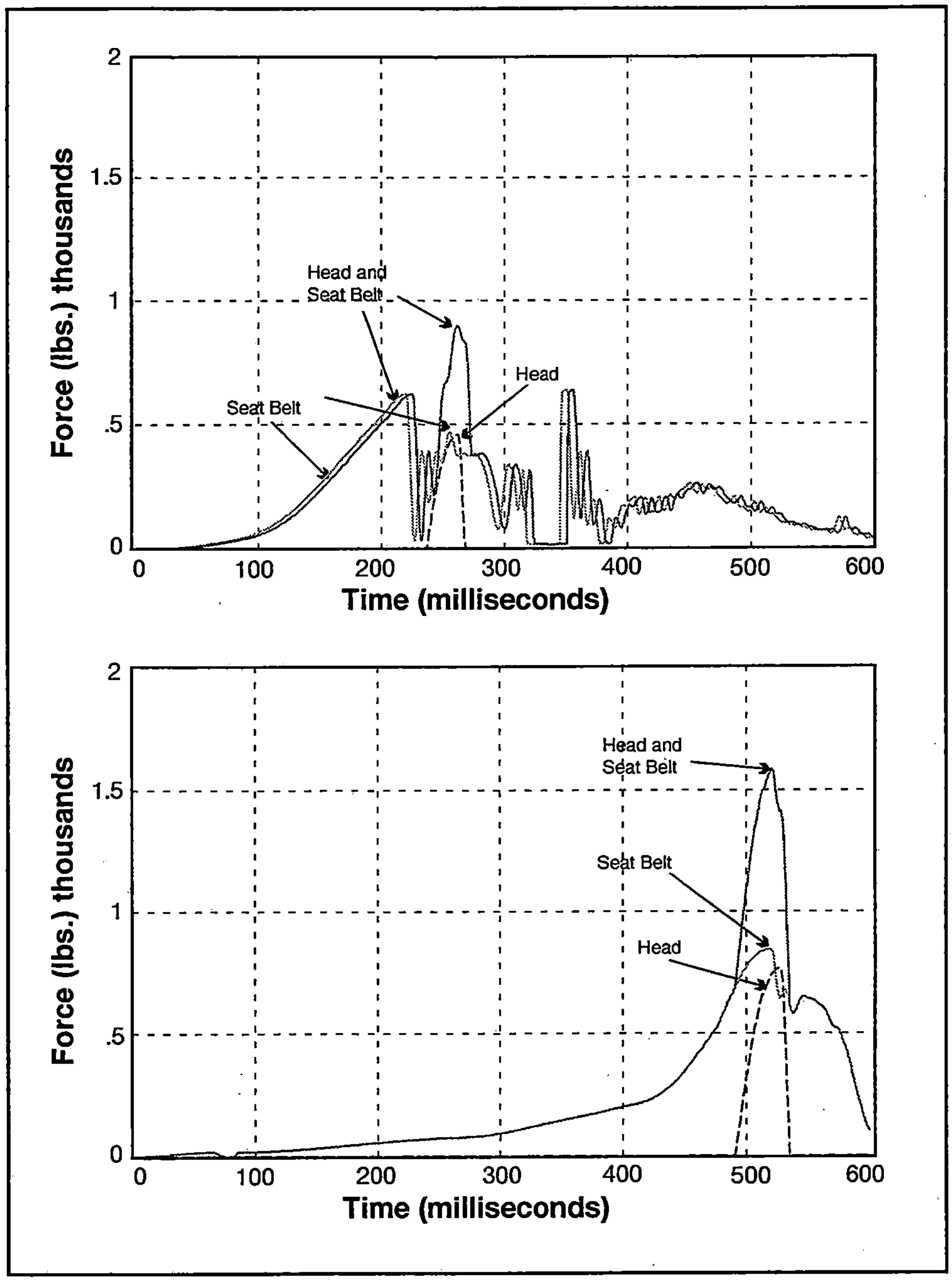

Note: Conventional Design (top), Crash-Energy Management Design (bottom)

Figure 3-26. Forces on Seat Due to Restrained Occupant in First Coach Car

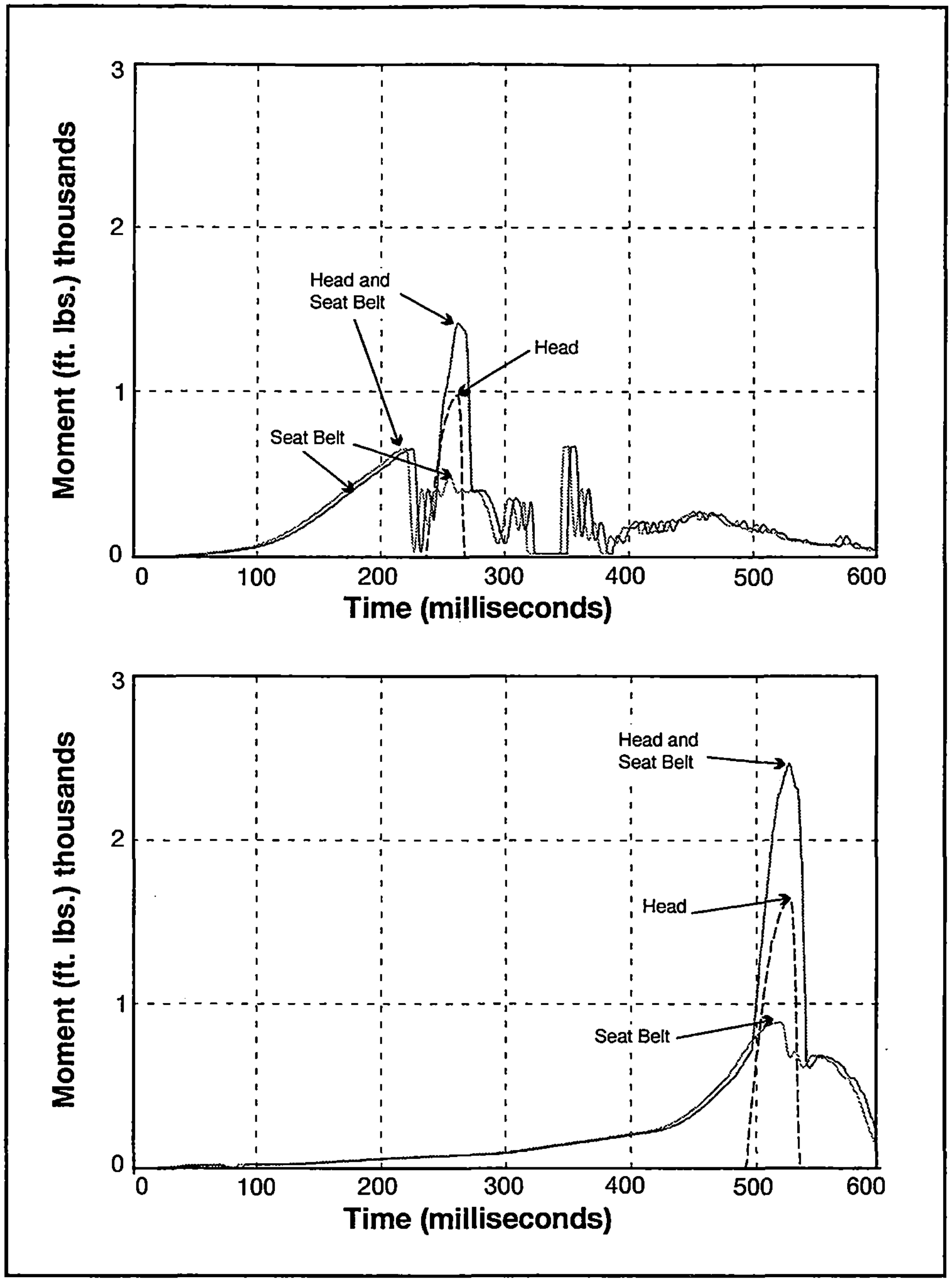

Note: Conventional Design (top), Crash-Energy Management Design (bottom)

Figure 3-27. Moments on Seat Due to Restrained Occupant in First Coach Car

Table 3-3. Peak Forces and Moments for Unrestrained Occupants Seated in Each Passenger Car During 140 mph Collision

	Peak Shear Force (gs) Constrained	Peak Moment (ft-lbs) Constrained	Peak Shear Force (gs) Conventional	Peak Moment (ft-lbs) Constrained
1st Coach Car	13.9	6385	14.3	4959
2nd Coach Car	10.9	5415	12.4	4697
3rd Coach Car	4.6	1733	11.3	4378
4th Coach Car	4.6	1352	9.4	3265
5th Coach Car	4.6	1352	10.9	4996
Cab Car	4.9	1278	12.6	6354

Table 3-4. Peak Forces and Moments for Occupants Seated in the First Coach Car During 140 mph Collision

	Peak Shear Force (gs) Constrained	Peak Moment (ft-lbs) Constrained	Peak Shear Force (gs) Conventional	Peak Moment (ft-lbs) Constrained
All Belted	9.1	2468	5.1	1415
All Unbelted	13.9	6385	14.3	4959
1/2 Unbelted	18.8	7273	17.9	5628

3.3.3 Seats and Table

Figure 3-29 shows the occupant motions for the unrestrained, forward-facing occupant seated at a table. Restraints were not evaluated for this interior. As the figure shows, the table itself acts as a restraint, with a relatively short distance between the occupant and the table. This short distance does not allow the occupant to build up much speed before impacting the table, resulting in a relatively benign impact. One concern, however, is how the forces are distributed as they are imparted to the occupant. There is the potential of severe internal abdominal injuries if the forces are too concentrated, i.e., the table edge acts as a knife edge.

Table 3-7 lists the probability of fatality for the forward-facing occupant in the interior with seats and table. The probability of fatality is less than 10 percent for all the crash pulses considered except the crash pulse for the conventionally designed train with the cab car leading. In these trains, the likelihood of fatality is near certain.

Table 3-5. Injury Criteria and Fatality Rates for Secondary Collisions, Seated Rows

		HIC			Chest gs			Neck Load (lbs)		
		Unbelted	Belted	Harness	Unbelted	Belted	Harness	Unbelted	Belted	Harness
Conventional Design	1st Coach 140mph head-to-head	167 (0%)	46 (0%)	21 (0%)	24 (2%)	12 (0%)	9 (0%)	-386 (0%)	-290 (0%)	70 (0%)
	Cab Car 140mph head-to-head	196 (0%)	18 (0%)	13 (0%)	36 (4%)	11 (0%)	10 (0%)	-529 (0%)	141 (0%)	69 (0%)
	Cab Car 70 mph tail-to-head	1009 (18%)	252 (0%)	90 (0%)	53 (16%)	19 (0%)	17 (0%)	-384 (0%)	-570 (0%)	171 (0%)
Constrained Crash-Energy Management Design	1st Coach 140mph head-to-head	221 (0%)	75 (0%)	15 (0%)	38 (4%)	20 (0%)	10 (0%)	-536 (0%)	-536 (0%)	70 (0%)
	Cab Car 140mph head-to-head	13 (0%)	0 (0%)	0 (0%)	7 (0%)	2 (0%)	2 (0%)	-229 (0%)	17 (0%)	-16 (0%)
	Cab Car 70 mph tail-to-head	449 (2%)	170 (0%)	22 (0%)	49 (13%)	27 (2%)	13 (0%)	-335 (0%)	686 (0%)	85 (0%)

Table 3-6. Injury Criteria and Fatality Rates for Secondary Collisions, Facing Seats

		HIC			Chest gs			Neck Load (lbs)		
		Unbelted	Belted	Harness	Unbelted	Belted	Harness	Unbelted	Belted	Harness
Conventional Design	1st Coach 140mph head-to-head	490 (3%)	25 (0%)	21 (0%)	25 (1%)	11 (0%)	9 (0%)	-1392 (100%)	176 (0%)	70 (0%)
	Cab Car 140mph head-to-head	1019 (18%)	18 (0%)	13 (0%)	33 (3%)	10 (0%)	10 (0%)	-2564 (100%)	136 (0%)	69 (0%)
	Cab Car 70 mph tail-to-head	3263 (100%)	1668 (75%)	90 (0%)	44 (8%)	26 (2%)	17 (0%)	-1183 (100%)	-644 (0%)	171 (0%)
Constrained Crash-Energy Management Design	1st Coach 140mph head-to-head	4044 (100%)	502 (3%)	17 (0%)	64 (35%)	22 (0%)	10 (0%)	-5233 (100%)	-345 (0%)	70 (0%)
	Cab Car 140mph head-to-head	151 (0%)	0 (0%)	0 (0%)	27 (2%)	2 (0%)	2 (0%)	-2033 (100%)	17 (0%)	-16 (0%)
	Cab Car 70 mph tail-to-head	1616 (68%)	1247 (38%)	26 (0%)	31 (3%)	20 (0%)	12 (0%)	-1343 (100%)	371 (0%)	93 (0%)

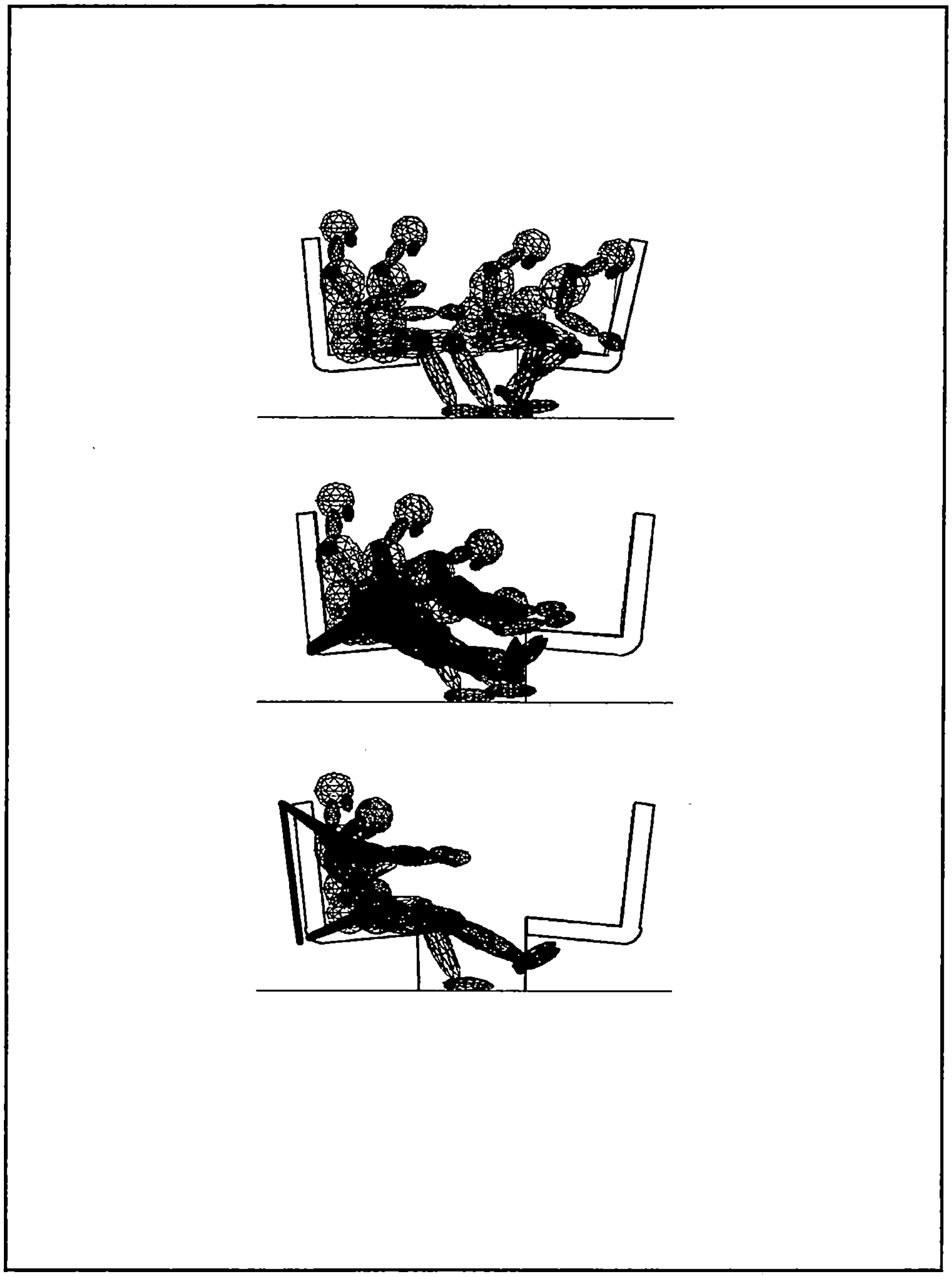

Figure 3-28. Motions for Occupants in Facing Seats Interior

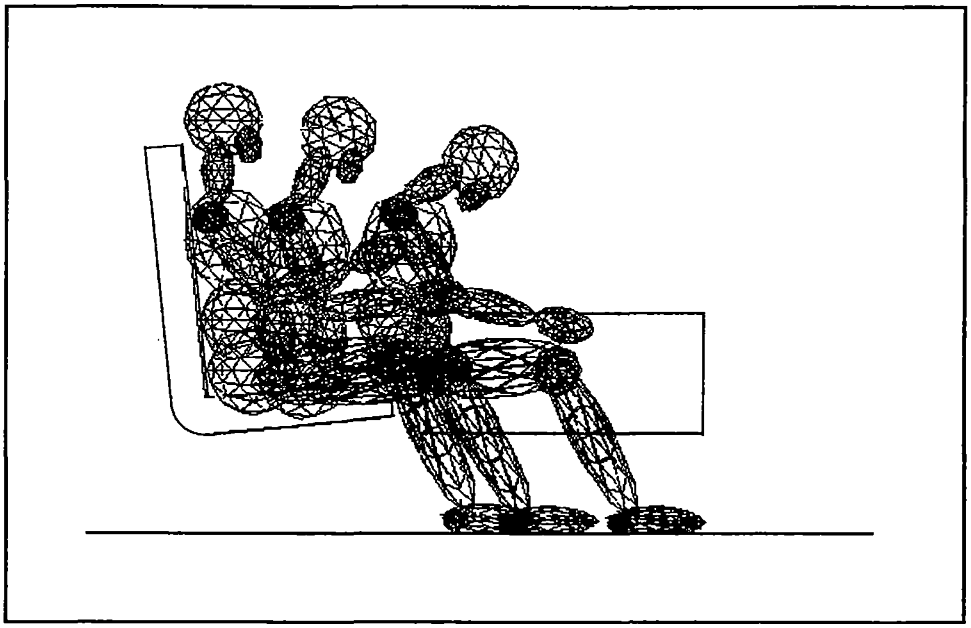

Figure 3-29. Motions for Occupants in Seats and Table Interior

Table 3-7. Injury Criteria and Fatality Rate for Secondary Collisions, Seats and Table

		HIC	Chest gs	Neck Load (lbs)
Conventional Design	1st Coach 140 mph head-to head	311 (0%)	42 (7%)	602 (0%)
	Cab Car 140 mph head-to-head	186 (0%)	33 (3%)	456 (0%)
	Cab Car 70 mph tall-to-head	702 (7%)	51 (14%)	787 (100%)
Constrained Crash-Energy Management Design	1st Coach 140 mph head-to head	110 (0%)	24 (1%)	288 (0%)
	Cab Car 140 mph head-to-head	16 (0%)	16 (0%)	163 (0%)
	Cab Car 70 mph tall-to-head	415 (2%)	40 (5%)	601 (0%)

3.4 ANALYSIS CONCLUSIONS

3.4.1 Compartmentalization

The results illustrate that the judicious placement of the impact surface can be effective in reducing injuries. By placing the seats reasonably close together, the distance the occupant travels before the secondary impact can be minimized. The occupant will have less distance in which to build up speed relative to the occupant compartment. For example, in the seats in rows configuration, the occupant has less than 3 feet to travel before impacting the forward seat back. In the seats facing configuration, the occupant travels about 5 feet before impacting the seat face of the forward seat. In most cases, the occupant's velocity increases until he or she is stopped by the forward seat. Therefore, the impact velocity relative to the train will be reduced as the travel distance is reduced, resulting in less severe impacts.

In the seats and table configuration, the table acts to arrest the occupant's motion before higher velocities can be attained. Provided the table edges are sufficiently blunt (so as not to impart severely concentrated forces on the occupant's abdomen), this also can be an effective compartmentalization strategy to minimize fatalities.

3.4.2 Occupant Restraint

Current U.S. practice requires no occupant restraint system for train passengers. In some configurations modeled (i.e., seats in rows), compartmentalization can be as effective as occupant restraint for the 50th percentile male. A restraint system is most effective in train interiors that do not employ suitable compartmentalization strategies. In interiors where there are large distances between seats, restrained occupants have a much greater chance of survival. Fatalities from secondary impacts are not expected in any of the scenarios modeled if the occupant is restrained with a lap belt and shoulder harness.

The analysis suggests that it may be more hazardous for an occupant of larger stature to be restrained with a lap belt alone than to be unrestrained in some interiors. For instance, in the seats in rows interior, potentially large axial neck loads may be encountered when the occupant's upper torso rotates around the lap belt and strikes the forward seat. This adverse situation may also occur for an average size occupant if the seats are positioned with a seat pitch less than the 42 inches modeled.

If a restraint system is to be utilized in passenger seats, measures should be taken to ensure that all passengers are restrained to avoid an increased risk of failure of the seat attachments due to a load application from two different forces. The results of the simulation show that for occupants in the first coach car in the 1/2 belted condition (when loads are applied to one seat by both a restrained and an unrestrained passenger), the largest forces and moments are likely to occur. In this condition, seat attachments could experience loads upwards of 18gs (equivalent to 3,150 pounds for a 175-pound occupant). In simulations where all the occupants are unbelted, the total shear force applied to one seat is approximately 14gs (or 2,450 pounds).

3.4.3 Crash Pulse

It is worthwhile to note the influence of car position on the vehicle's crash pulse when comparing the conventional design with the crash-energy management design. The peak deceleration is slightly higher and the duration longer for the crash-energy management design (see Figure 3-6). However, for occupants seated in rows, in cars behind the second coach car, the delayed timing of the car's peak crash pulse gives the occupant sufficient time to travel in free flight and undergo the secondary impact before the car experiences a rapid deceleration. The occupant can withstand much higher decelerations when he or she is already in contact with the interior.

As seen in the results for the 140 mph head-to-head collision for unrestrained occupants seated in rows (see Table 3-2), the values for injury criteria are relatively low for all cars for both the conventional and the crash-energy management design. However, the injury severity for occupants in the crash-energy management cars decreases sharply after the second coach car. Injuries experienced by occupants in cars behind the second coach are classified on the AIS injury scale as Code 0, or no injury, based upon HIC and chest deceleration. This phenomenon would be especially advantageous to trainsets consisting of more cars than modeled in this study.

In the conventional design, occupants in cars away from the initial train-to-train collision do not experience a safer crash environment than occupants in cars near the collision. Occupants in each car except the fourth coach experience injuries classified as AIS Code 1, or minor injuries. While these injuries typically are not life-threatening, they should be avoided if possible. The results from the crash-energy management design indicate that they can be prevented.

4. CONCLUSIONS AND RECOMMENDATIONS

One of the principal conclusions is that for head-on collisions at speeds above 112 km/h (70 mph), the crash energy management approach is significantly more effective than the conventional approach in preserving the occupant volume.

Force/crush characteristics have been developed using crash energy management design strategy. The next step is to implement these force/crush characteristics into economically and physically achievable rail car structures. Potential limitations in implementing these force/crush characteristics include the length of the crush zone and its ability to support transverse loads (laterally and vertically) while longitudinally crushing.

It is likely that longitudinal occupant volume strengths greater than assumed in developing the force/crush characteristics can be achieved, but there may potentially be some weight and cost penalty. However, modern computer-aided engineering tools may enable rail car structures to be developed which have significantly increased strength over existing structures with no increase in weight or manufacturing costs. An effort should be made to determine the influence of increased occupant volume strength on manufacturing cost and car weight.

Detailed structural analyses and testing are required in order to develop structures which implement these crush zones and to evaluate the potential for increased occupant volume strength. Detailed computer models of the car structures need to be developed in order to perform the required analyses. Tests required may include component, scale model, substructure, and full scale tests.

The other principal conclusion is that a sufficiently compartmentalized interior protects occupants against fatality during a train collision at least as well as required in the automotive and aircraft industries. Seat belts provide some level of increased protection from fatality owing to secondary collisions, however, most fatalities during train collisions are predicted to be from loss of occupant volume.

There is a need to verify the secondary impact analyses results with test data. The computer model MADYMO used in this study was developed for evaluating the influences of changes in automobile interior configurations on the forces, displacements and decelerations experienced by an occupant during an automobile collision. There are significant differences between the secondary collision conditions during an automobile collisions than during a train collision. The crash pulse experienced by the occupant during an automobile collision has significantly greater magnitude and shorter duration than that experienced by the occupant during a train collision. In addition, there is generally much shorter distance between the occupant of an automobile and the interior impacting surface than between the occupant of the train and the impacting surface. Instrumented dummy measurements, for comparison to analysis predictions, could be made by sled testing an interior mockup. During dynamic sled testing, two or more rows of train seats would be attached to a test sled, instrumented dummies would be placed in the seats, and the sled would be decelerated with the crash pulse predicted to occur during a train collision.

Train collisions often result in a significant number of nonfatal injuries to the occupants. These injuries include extremity injuries (e.g., broken arm, broken wrist, broken fingers, broken leg, injured knee, broken ankle, etc., etc.) facial cuts and bruises, as well as neck and back injuries. Compared to the range of potential injuries, there are few criteria for evaluating potential injury from model predictions and instrumented dummy test measurements of the forces, displacements and decelerations experienced by the human body during a collision. Owing to the wide range of potential injuries and numerous modes in which these injuries may occur, and the lack of criteria for evaluating analysis and test results, it is difficult to assess the influence of interior configurations on the likelihood of injury owing to secondary collision.

The most effective way to reduce injury in train collisions may be to gather information from the victims of actual accidents -- the injury and how that injury was inflicted, i.e., what interior component was struck and a description how the occupant came to strike it -- and heuristically evaluate what interior modifications would reduce the likelihood and severity of the injuries.

APPENDIX A. CRASH-ENERGY MANAGEMENT DESIGN

This appendix describes a design methodology for developing force/crush characteristics between the cars of a train. This methodology uses preservation of the occupant volumes and limitation of the occupant secondary impact velocities as objectives, and crush-zone strengths and lengths as constraints. The methodology starts with the desired behavior of all the cars in the train during a collision, and results in optimized force/crush characteristics between cars.

Design Methodology

Figure A-1 shows the location and length of the crush zones in each of the cars. The lengths shown are the reductions in length before intrusion into the occupied volumes. These crush zones are distributed throughout the train in order to control the progression of the structural crushing during the collision and to control the decelerations of the occupied volumes.

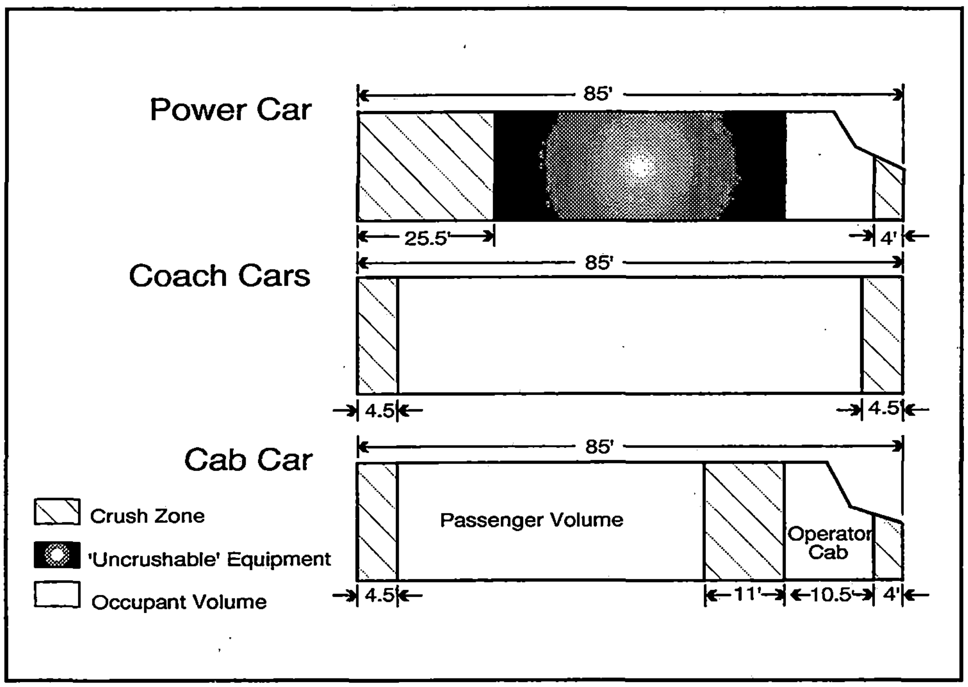

Figure A-1. Crash-Energy Management Design Crush-Zone Locations

Figure A-2 illustrates the methodology used to determine the force/crush characteristics for the crash-energy management design. The process starts with the desired deceleration time histories for each of the cars, from which ideal force/crush characteristics are determined for a particular collision scenario. These characteristics are subsequently modified based on constraints on crush-zone length and maximum occupant compartment strength. The constrained design is then evaluated to determine how well it approximates the performance of the ideal design.

The scenario used to develop the force/crush characteristics is a train-to-identical train collision, which is simplified in some calculations using symmetry to a train collision into an ideal rigid wall. Figure A-3 shows the lumped mass model used to determine the force crush

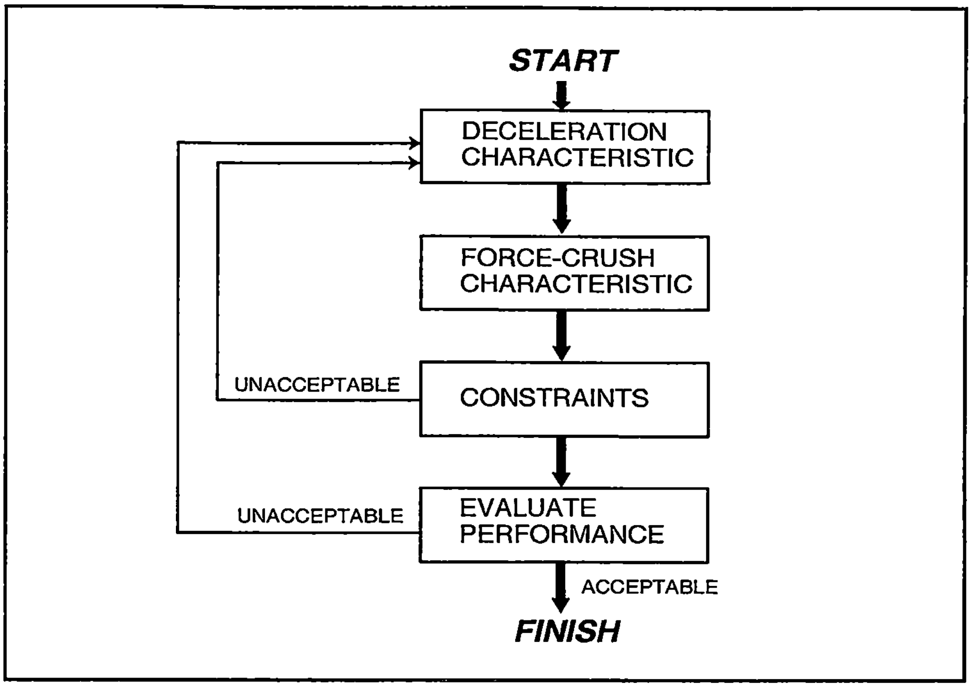

Figure A-2. Crash-Energy Management Design Force/Crush Characteristic Development

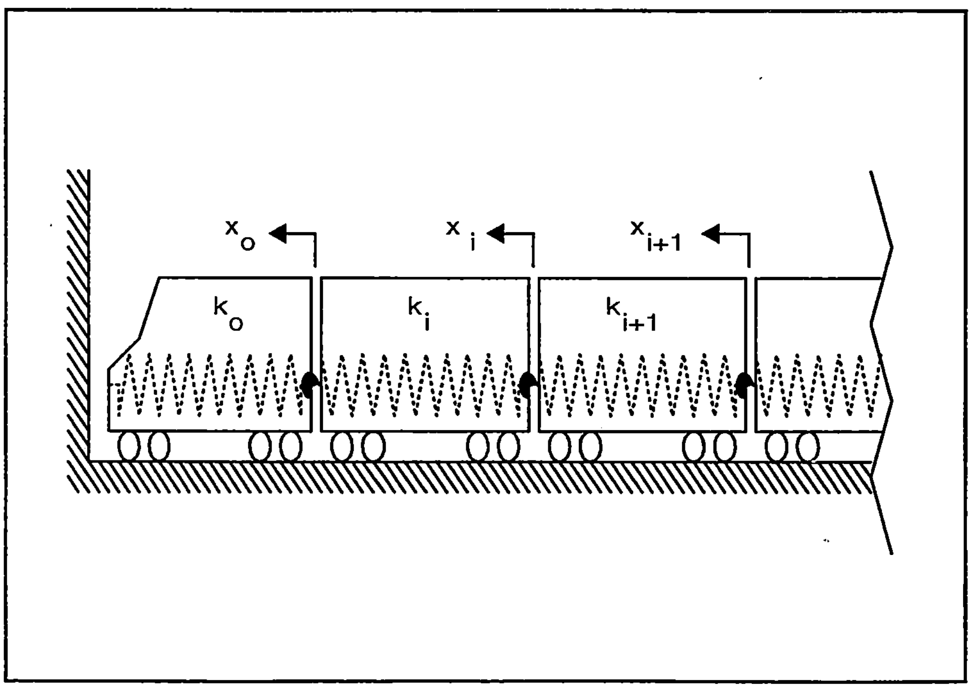

Figure A-3. Lumped Mass Model of Train Cars into Wall

characteristics. The force/crush characteristics, k_0, k_1, k_2, etc., are initially unknown, but the decelerations of the each of the cars is prescribed. The force/crush characteristics are derived from these prescribed decelerations.

The ideal deceleration characteristic for the cars in a train during a train-to-train collision with a closing speed of 140 mph (equivalent to a train colliding with an ideal rigid wall at 70 mph) are shown in Figure A-4. In order to limit the secondary impact velocity of an occupant 2 1/2 feet from the seatback or interior barrier ahead to 17 mph, the initial deceleration is limited to 4gs for the first 0.20 second. Once the secondary impact has occurred, it is assumed that the occupant can safely withstand 25gs.

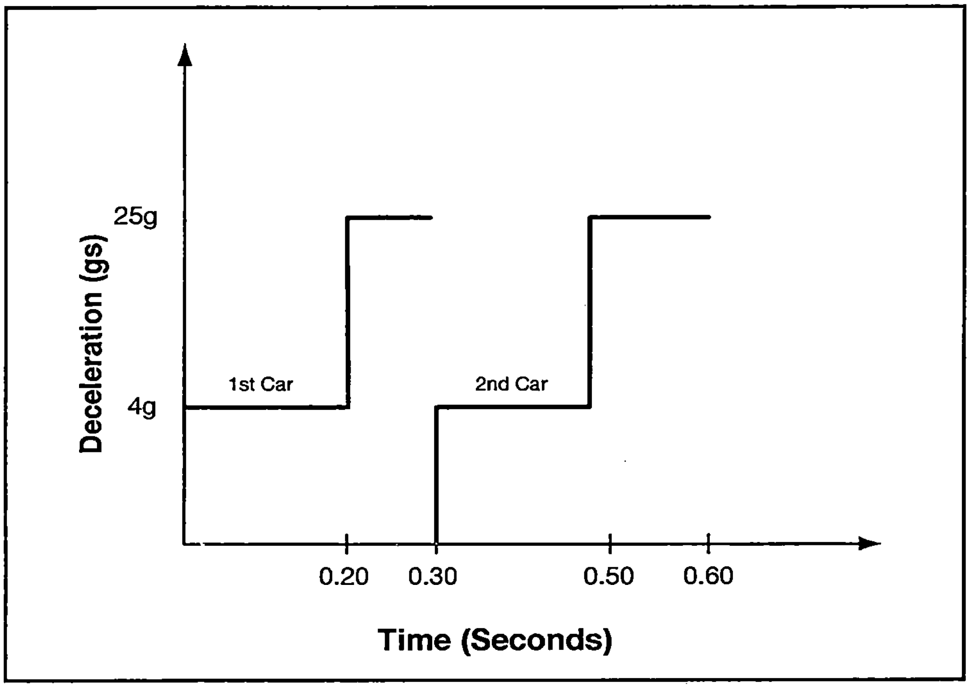

Figure A-4. Ideal Deceleration Characteristic

Ideally, each car undergoes its own collision independent of all the other cars in the train. For a hypothetical train collision into a brick wall, the first car impacts the wall and comes to rest before the second car starts to decelerate, i.e., ideally the car behind does not exert a force on the car ahead until the car ahead has come to rest. In order to achieve this deceleration characteristic for a train traveling at 140 mph colliding with a standing train, the first car in the train would need a crush zone which imparts a deceleration of 4gs to the car which allows 18 feet of crush, a crush zone which imparts a deceleration of 25gs to the car which allows 4 feet of crush, and an occupant volume which is sufficiently strong to ensure that it does not crush under 25gs deceleration. The second car in the train, and all other trailing cars, would need a crush zone which would exert no deceleration (force) that is 9-feet long, in addition to the 4g and 25g crush zones. Figure A-5 illustrates schematically the ideal distribution of the crush zones along the length of the train.

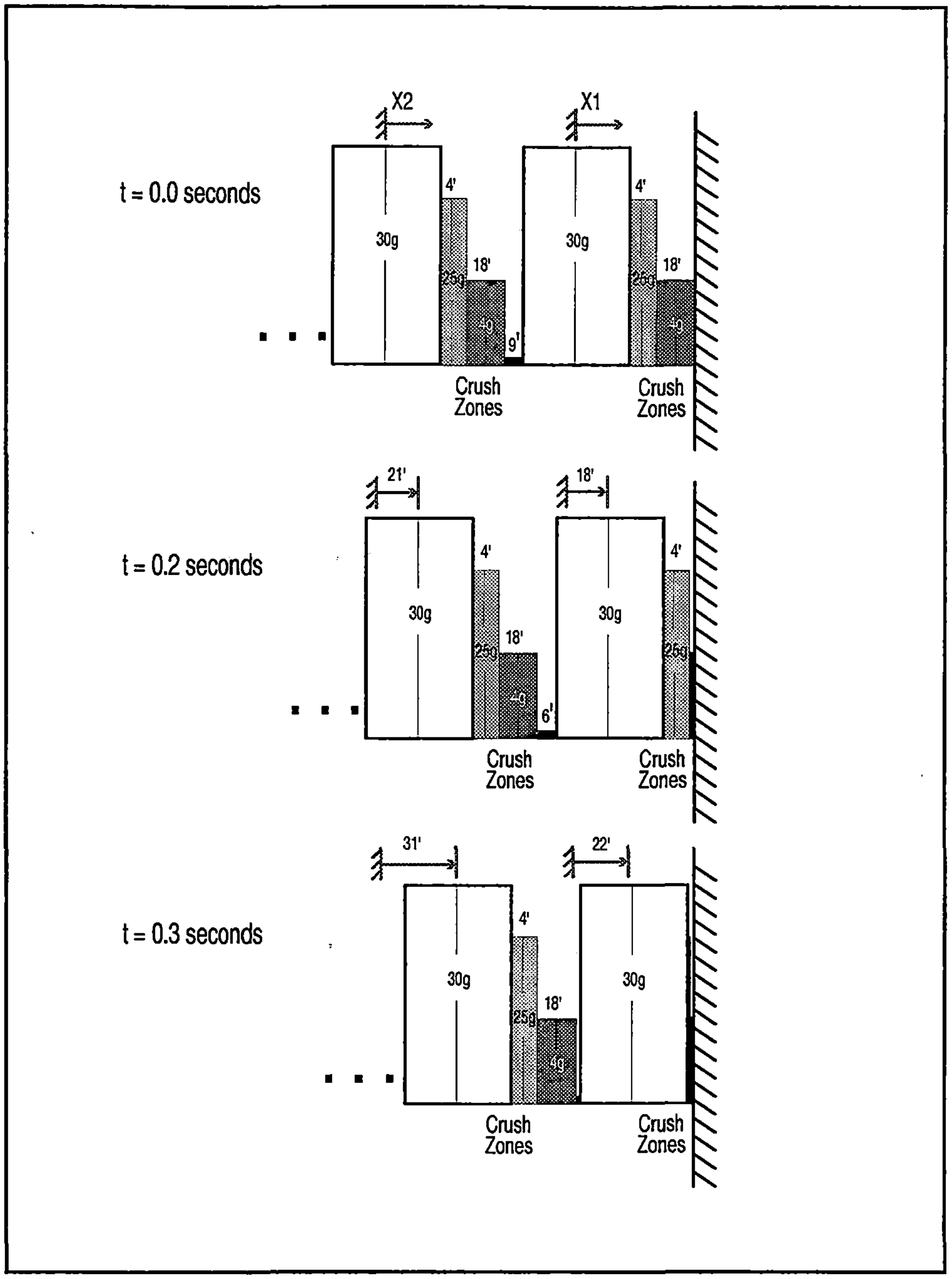

Figure A-5. Schematic of Ideal Crush Zones Required to Impart Ideal Deceleration

The ideal deceleration characteristics must be modified in order to develop force/crush characteristics which can be implemented in a vehicle structure. As soon as the first car starts to decelerate, a force must develop between the first and second car, owing to the connection between the cars. Figure A-6 shows the deceleration characteristics of Figure A-4 modified for a collision at 140 mph of a consist made up of a power car, five coach cars, and a cab car with an identical standing consist. In this scenario, the power cars are the first cars involved in the collision. The decelerations have been modified to have each of the cars start decelerating at the onset of the collision and to impart a greater deceleration to the operator during the initial portion of the collision. The assumption is that greater interior crashworthiness measures can be taken for the operator than for the passengers owing to the increased likelihood that the operator will be in his seat. This allows the operator's cab to be strengthened in order to preserve sufficient volume for the operator to survive at the cost of increasing the deceleration imparted to the cab. These deceleration characteristics were permitted a maximum deceleration of 8gs. The greater the maximum deceleration, the greater the maximum crush force required to achieve the deceleration, while the lower the maximum deceleration the longer the crush distance required. Different shaped deceleration characteristics, with different maximum values and different initial portions, can be developed. Different deceleration characteristics will result in different required force/crush characteristics.

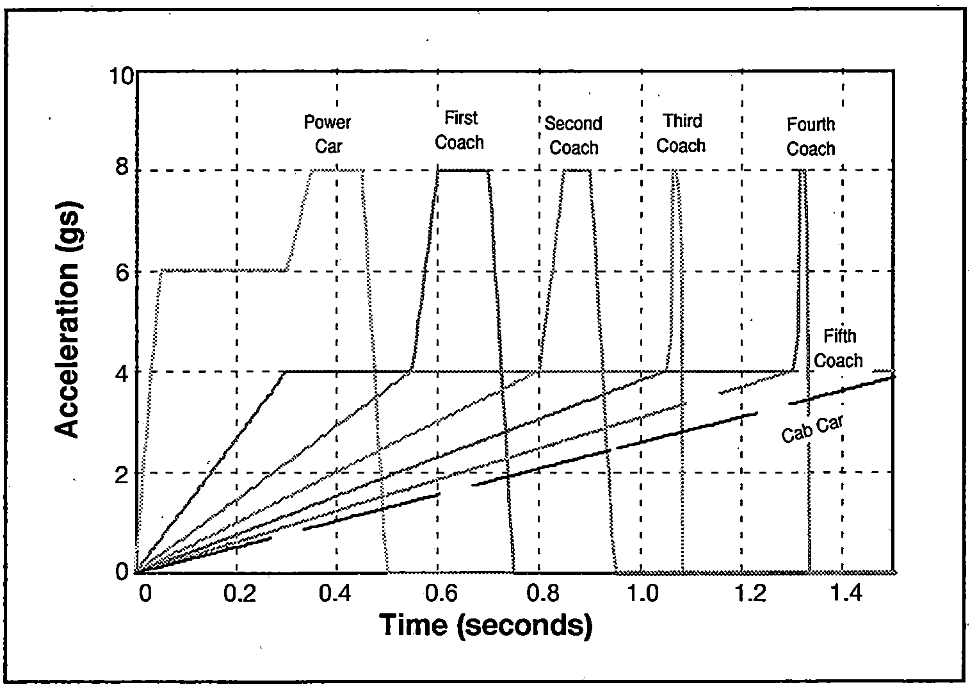

Figure A-6. Desired Deceleration Characteristic for 70 mph Brick Wall Collision, Power Car Leading

The deceleration time histories can be used to calculate the forces necessary to generate the declarations, given the masses of the cars. Figure A-7 shows a free body diagram of a single car (mass) in the train.

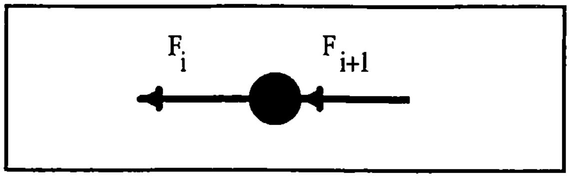

Figure A-7. Free Body Diagram of a Single Lumped Mass

The equations of motion for the mass, in matrix form, are

$$\begin{bmatrix} -1 & 1 & 0 & 0 & 0 & 0 \\ 0 & -1 & 1 & 0 & 0 & 0 \\ 0 & 0 & -1 & 1 & 0 & 0 \\ 0 & 0 & 0 & -1 & 1 & 0 \\ 0 & 0 & 0 & 0 & -1 & 1 \\ 0 & 0 & 0 & 0 & 0 & -1 \end{bmatrix} \begin{Bmatrix} F_1 \\ F_2 \\ F_3 \\ F_4 \\ F_5 \\ F_6 \end{Bmatrix} = \begin{bmatrix} m_1 & 0 & 0 & 0 & 0 & 0 \\ 0 & m_2 & 0 & 0 & 0 & 0 \\ 0 & 0 & m_2 & 0 & 0 & 0 \\ 0 & 0 & 0 & m_2 & 0 & 0 \\ 0 & 0 & 0 & 0 & m_2 & 0 \\ 0 & 0 & 0 & 0 & 0 & m_1 \end{bmatrix} \begin{Bmatrix} a_1 \\ a_2 \\ a_3 \\ a_4 \\ a_5 \\ a_6 \end{Bmatrix}$$

The force time-histories can be solved according to the matrix equation

$$F = C^{-1}Ma$$

Where

- ***F*** is the matrix of forces acting between the cars
- ***C*** is the matrix of coefficients for the forces
- ***M*** is the matrix of the car masses
- ***a*** is the matrix of the car longitudinal accelerations

Figure A-8 shows the force time-histories required to produce the decelerations shown in Figure A-6. These forces, however, need to be known as a function of relative displacement (crush) between the masses, not just as functions of time. The relative displacements between the masses also can be calculated as a function of time. The forces then can be cross-plotted with the displacements in order to determine the forces as a function of crush.

The decelerations shown in Figure A-6 have been numerically integrated to determine the velocity and displacement of each of the cars during the collision. The velocity time-histories are shown in Figure A-9.

The velocity time histories in Figure A-9 are numerically integrated to determine the displacement time histories of each of the cars in the train. These displacement time histories are shown in Figure A-10. The crush between adjacent cars is the difference in displacement between the cars.

The forces shown in Figure A-8 are cross-plotted with the relative displacements (crush) between the cars to determine the forces required to produce the decelerations shown in Figure A-6 as a function of crush between the cars. The force between the power car and the rigid wall

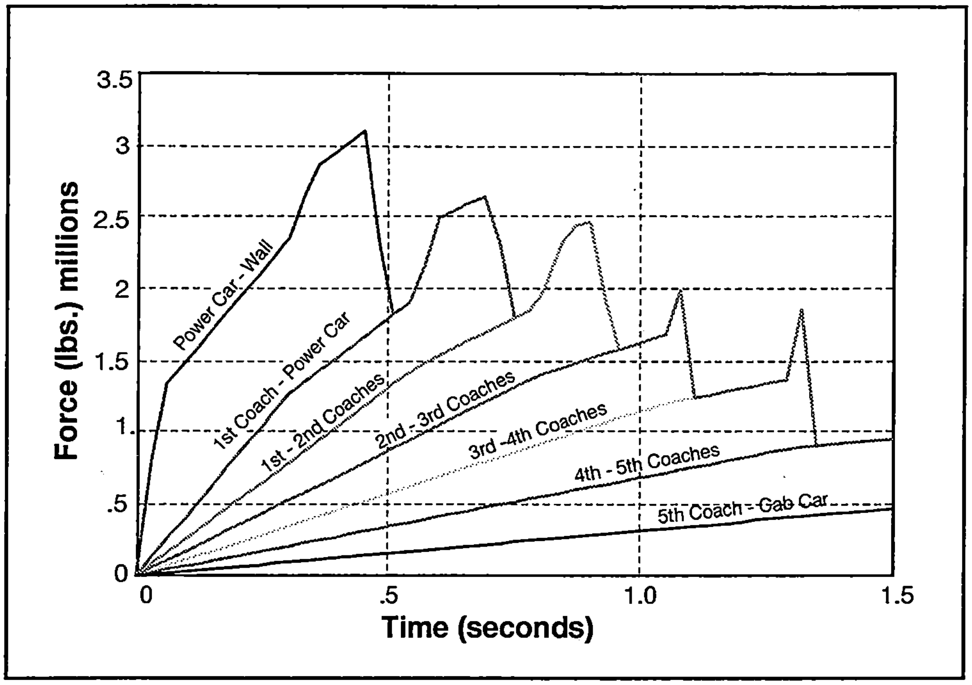

Figure A-8. Force Versus Time for All Cars

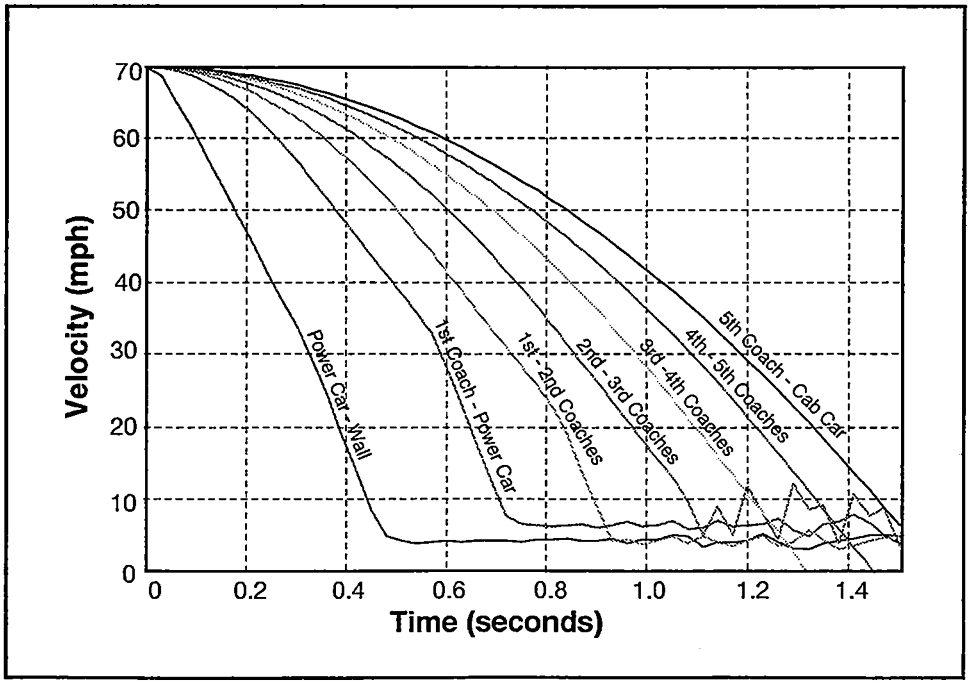

Figure A-9. Velocity Versus Time for All Cars

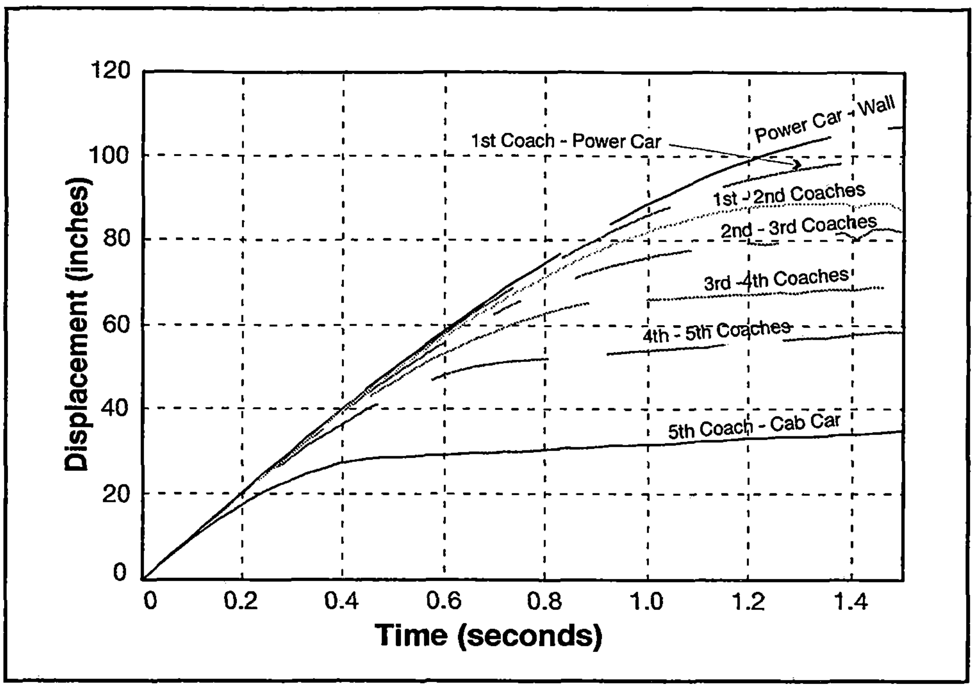

Figure A-10. Displacement Versus Time for All Cars

as a function of the car displacement is shown in Figure A-11. This figure also shows the designed force/crush characteristic. This designed force/crush characteristic is an initial estimate as the "best"' realizable force characteristic that could actually be built and implemented in a rail car structure. The design force/crush characteristic describes a design objective for the crush zones at the front end of the power car. The designed and required force/crush characteristics for each of the remaining cars in the train are shown in Figures A-12 and A-13.

The crush zone characteristics shown in Figures A-11, A-12, and A-13 will fully protect the operator and passengers in a train-to-train collision with a closing speed of 140 mph. However, these characteristics require occupant volume strengths of 3.0 million pounds and relatively long crush distances[1]. In order to be practical, constraints must be placed on the distances crushed and the forces developed, and the desired deceleration characteristics must be modified accordingly. For the coach cars, the longitudinal forces are constrained to be between 1.6 million pounds, presuming that greater strength would incur excessive vehicle weight, and 400,000 pounds, presuming that less strength would impair the vehicle's ability to support service loads. For the operator's cab, the maximum force is constrained to 2 million pounds. This load is greater than for coach cars due to the substantially shorter occupant volume length. Constraints placed on crush distances include 4 feet of available crush distance ahead of the operator's cab, 25.5 feet of available crush distance at the rear of the power car, 11 feet behind the operator's cab in the cab car, and 4.5 feet of available crush distance at each end of all the coach cars. Additional constraints include symmetry (i.e., the train must be able to withstand collisions in both directions) and a minimum number of crush zone characteristics (i.e., the force/displacement

1 Actual crush zone length would need to be longer than the crush distances shown in the figures, in order to leave space for the crushed bulk material.

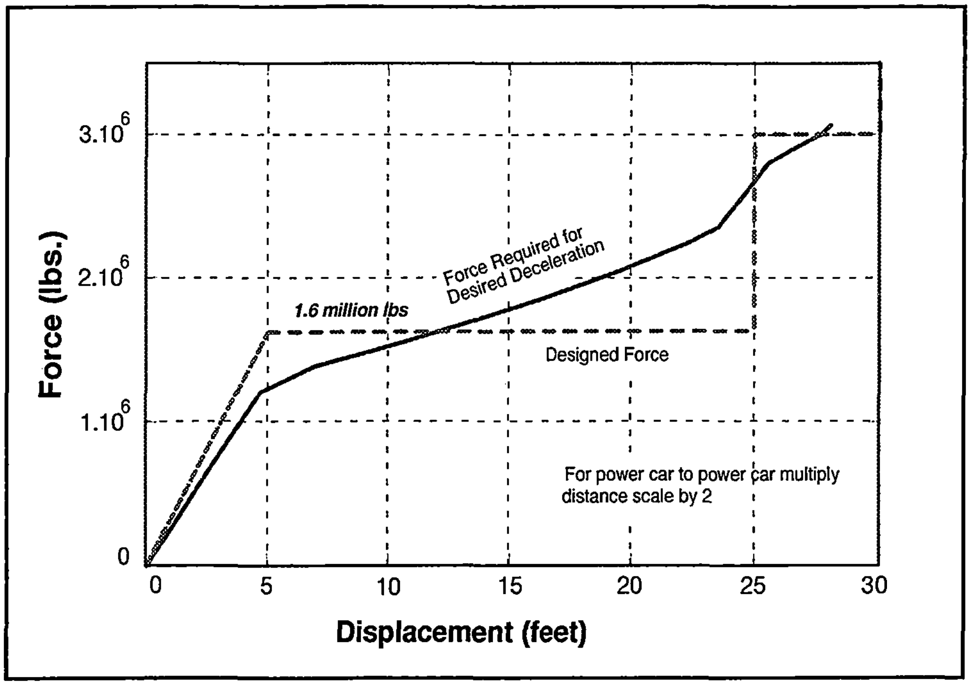

Figure A-11. Power Car to Brick Wall Crush Zones Force/Deflection Characteristic Required to Ensure Occupant Survival in 140 mph Train-to-Train Collision

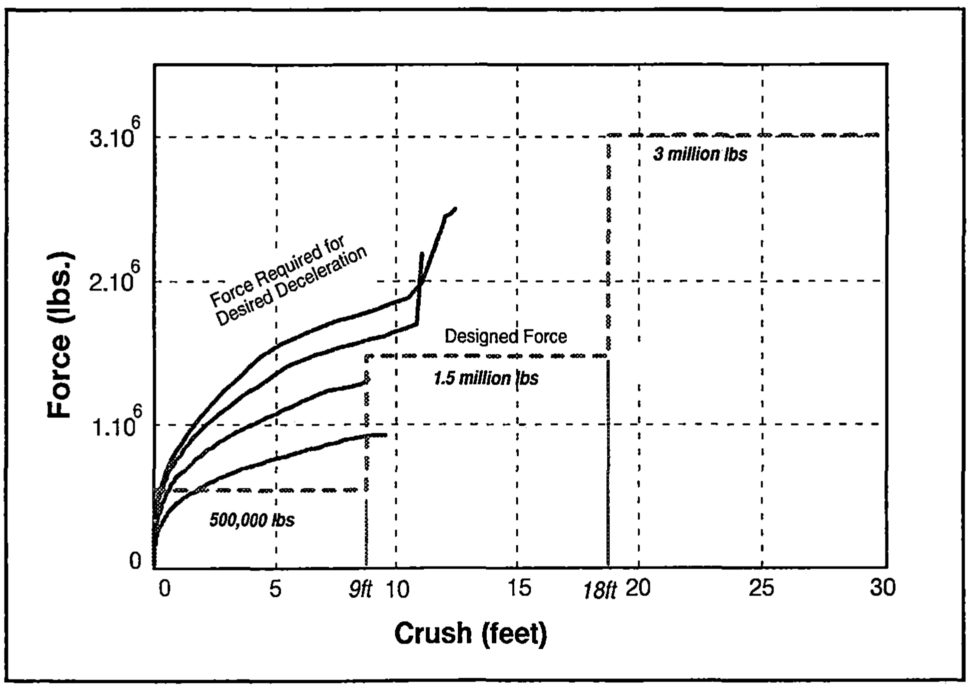

Figure A-12. Coach Car to Coach Car Crush Zones Force Deflection Characteristic Required to Ensure Occupant Survival in 140 mph Train-to-Train Collision

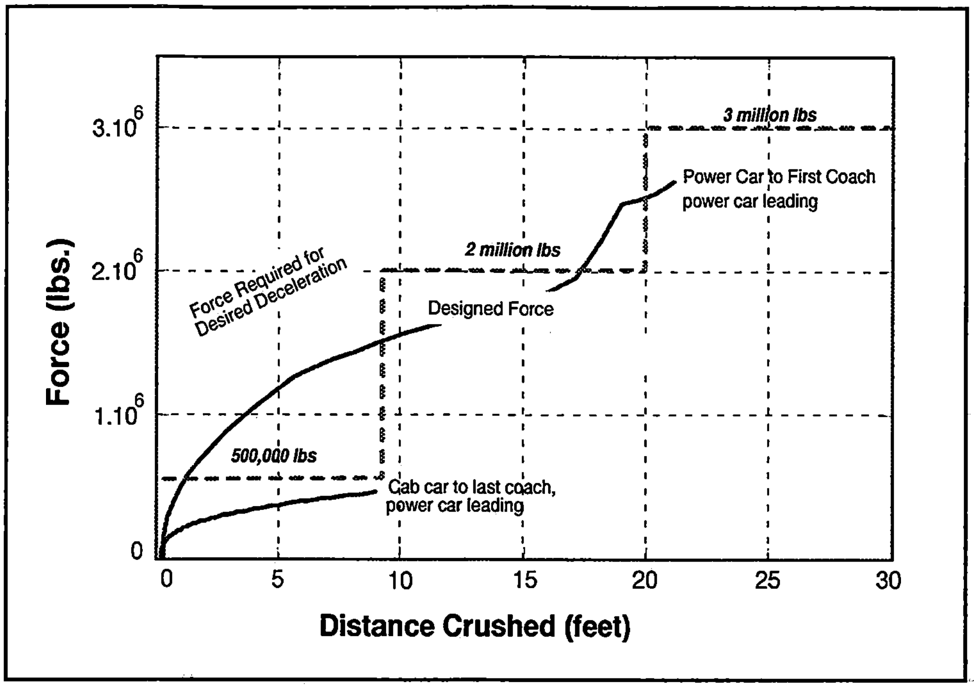

Figure A-13. Power Car to First Coach and Fifth Coach to Cab Car Crush Zone Force Deflection Characteristics Required to Ensure Occupant Survival in 140 mph Train-to-Train Collision

characteristics are constrained to require a single coach car design, a single power car design, and a single cab car design). The net result of these constraints is that the severity of the collision in which all occupants are expected to survive is reduced.

Power Car, Five Coach, Cab Car Consist

Figure A-14 shows deceleration time histories which result in force/crush characteristics and which meet the desired constraints for the power car, five coach, cab car consist in a 45 mph collision into a brick wall. Figure A-15 shows the decelerations for the same consist colliding into a brick wall at 30 mph with the cab car leading. These decelerations were developed iteratively by calculating the forces and distances required to generate the decelerations shown in the figure, and manually modifying the decelerations and collision speed to produce the desired change in forces and distances.

The design forces were developed by approximating the forces required for the desired deceleration, in the same manner as the design forces shown in Figures A-11, A-12, and A-13. The design force/crush characteristics for the constrained design for the brick wall collisions of the power car, five coach, cab car consist are shown in Figures A-16 and A-17. The power car and coach car characteristics are shown in Figure A-16 and the cab car force/crush characteristics are shown in Figure A-17. This characteristic was developed for the same consist, with the cab car being the first car involved in the collision.

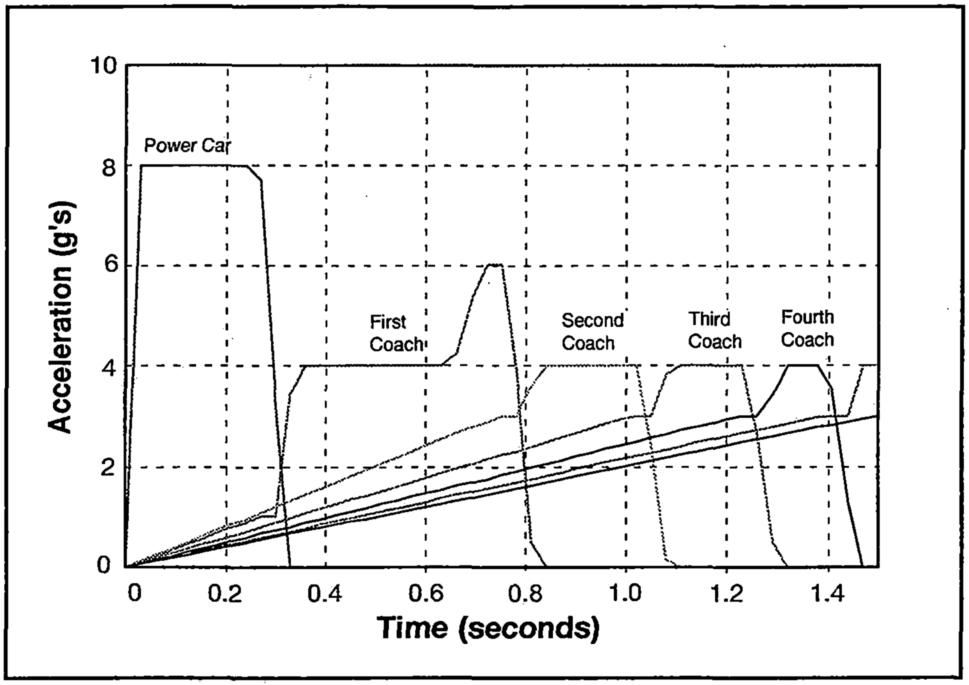

Figure A-14. Power Car, Five Coach, Cab Car Consist Deceleration Characteristic, 45 mph Brick Wall Collision, Power Car Leading

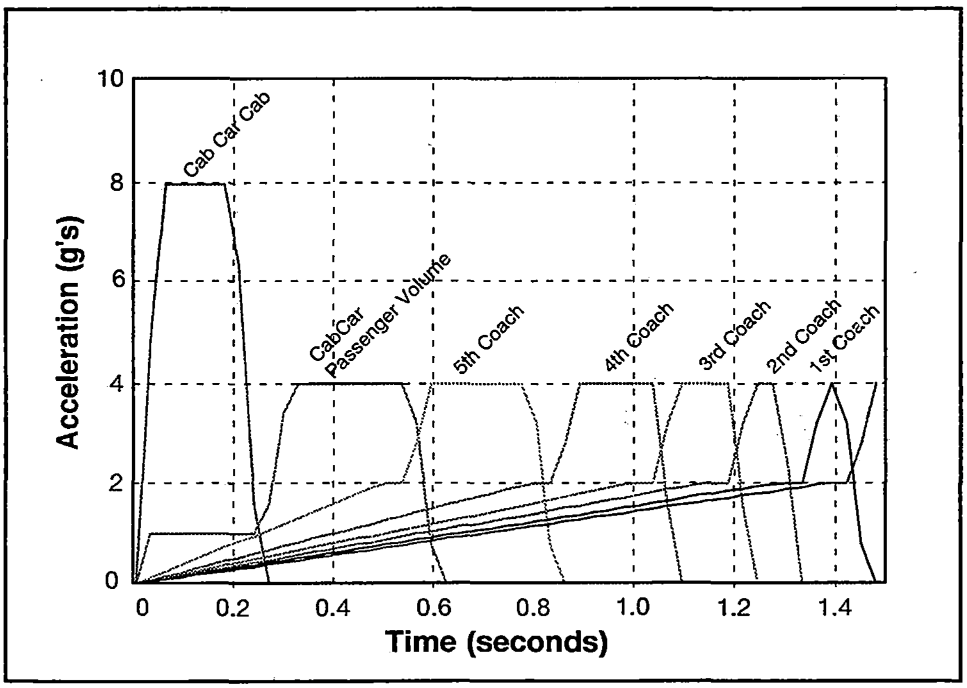

Figure A-15. Power Car, Five Coach, Cab Car Consist Deceleration Characteristic, 30 mph Brick Wall Collision, Cab Car Leading

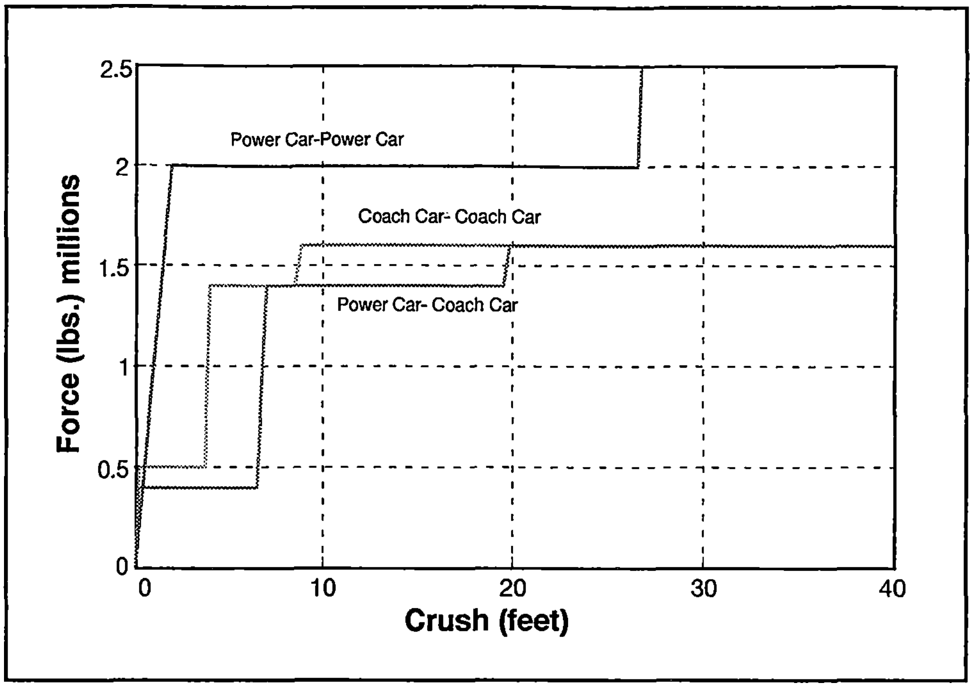

Figure A-16. Car-to-Car Crush Characteristics, Power Car, Five Coach, Cab Car Consist

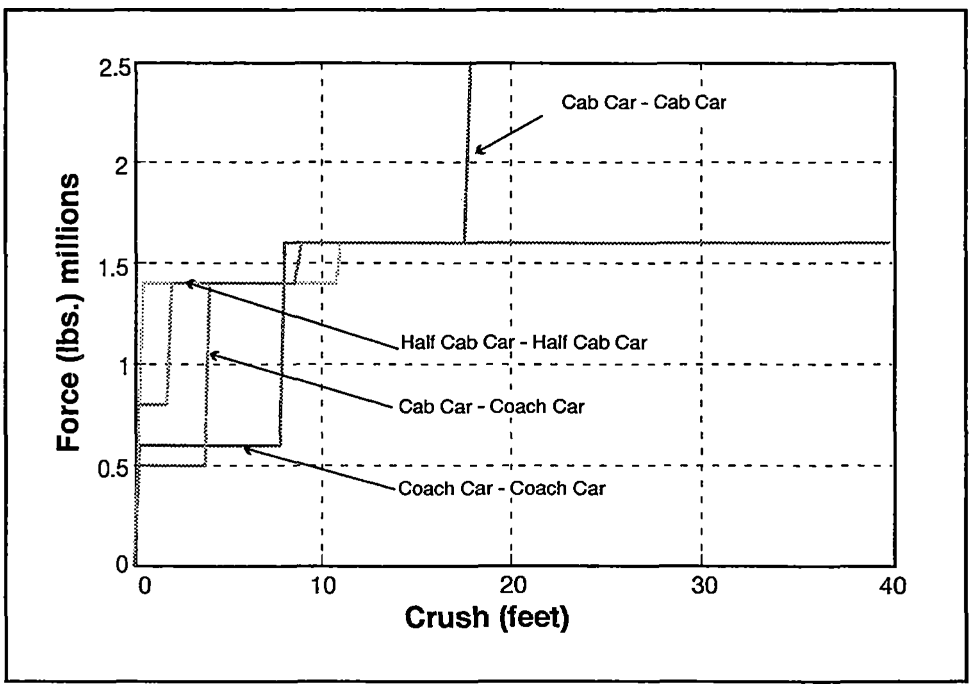

Figure A-17. Car-to-Car Crush Characteristics, Power Car, Five Coach, Cab Car Consist

Power Car, Six Coach, Power Car

Figure A-18 shows deceleration time histories which result in force/crush characteristics and which meet the desired constraints for the power car, six coach, power car consist in a 45 mph collision into a brick wall. These decelerations were developed iteratively in order to meet the constraints on the maximum force and the crush distances. The force/crush characteristics derived from these decelerations are shown in Figure A-19.

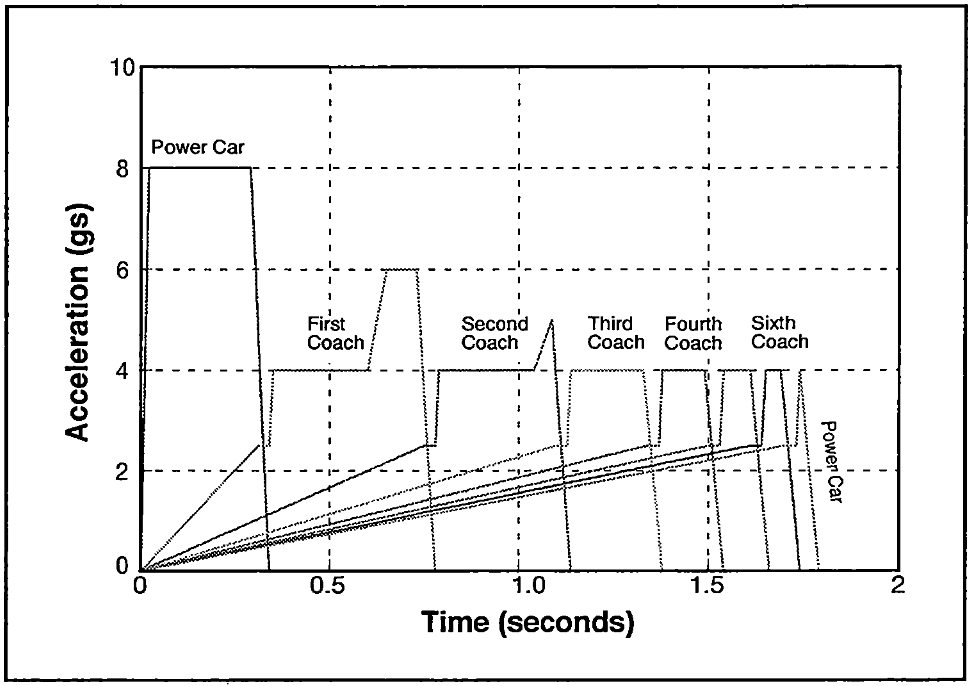

Figure A-18. Power Car, Six Coach, Cab Car Consist Deceleration Characteristic, 45 mph Brick Wall Collision, Cab Car Leading

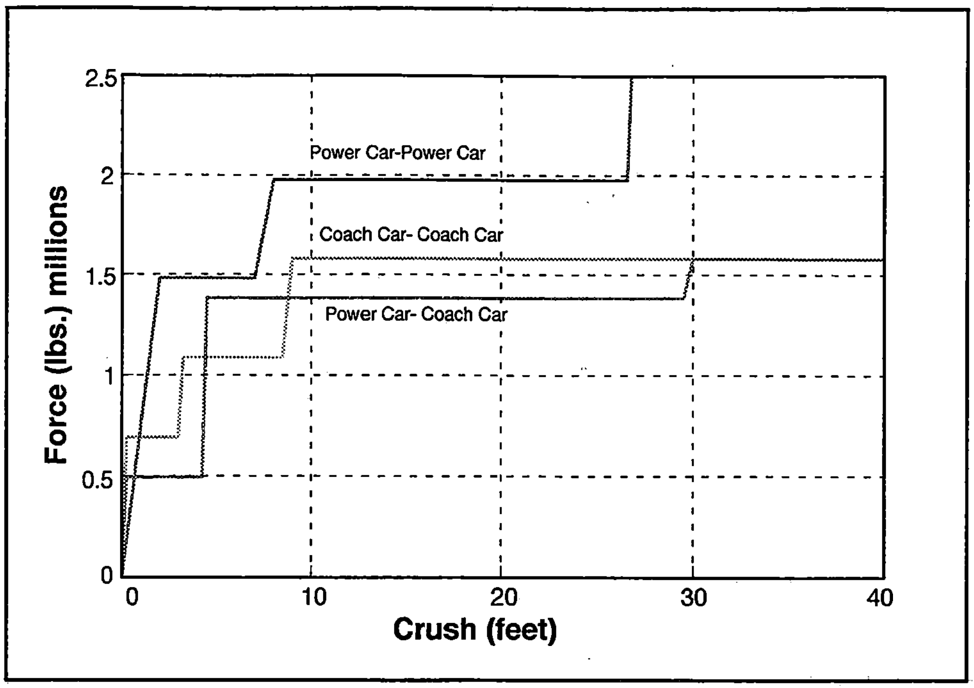

Figure A-19. Car-to-Car Crush Characteristics, Power Car, Six Coach, Power Car Consist

REFERENCES

[1] "Federal Motor Vehicle Safety Standards; School Bus Passenger Seating and Crash Protection; Termination of Rulemaking," The Federal Register, Vol. 54. No. 54, Page 11765, March 22, 1989.

[2] Ohnishi, T., Kawakami, N., Sano, A., "Crashworthiness of Train," The International Conference on Speedup Technology for Railway and Maglev Vehicles, Vol. I, PS2-15, the Japanese Society of Mechanical Engineers (JSME), November 1993.

[3] Lacôte, F, Cléon, L.-M., Lagneau, H, Dannawi, M, Demonsant, E., Wiart, A., "Les Tolérances á la Collision Des Matérials Ferroviaires," *Revue génerale des chemin de fer*, Gauthier-Villars, November 1993.

[4] Scott, G.A., "The Development of a Theoretical Technique for Rail Vehicle Structural Crashworthiness," Proceeding of the Institute of Mechanical Engineers, Vol. 201 No. D2, 1987.

[5] Scholes, A., "Railway Passenger Vehicle Design Loads and Structural Crashworthiness," Proceeding of the Institute of Mechanical Engineers, Vol. 201 No. D3, 1987.

[6] Scholes, A., and Lewis, J., "Development of Crashworthiness for Railway Vehicle Structures," Proceeding of the Institute of Mechanical Engineers, Vol. 207 Part F: Journal of Rail and Rapid Transit, 1993.

[7] Romeo, D., Cassidy, R. Interim Report on Assessment of Crashworthiness of Existing Urban Rail Vehicles, DOT-TSC-681, RSPA, U.S. Department of Transportation, April 1974.

[8] M.J. Reilly, R.H. Jines, and A.E. Tanner, Rail Safety/Equipment Crashworthiness Volume I: A Systems Analysis of Injury Minimization in Rail Systems, FRA/ORD-77/73, I, FRA, U.S. Department of Transportation, July 1978.

[9] MADYMO 3D, Release 5.0, July 1992, TNO Road-Vehicles Research Institute, Delft, The Netherlands.

[10] "Federal Motor Vehicle Safety Standards; School Bus Passenger Seating and Crash Protection; Termination of Rulemaking," The Federal Register, Vol. 54. No. 54, Page 11765, March 22, 1989.

[11] Code of Federal Regulation 49, Ch. V (10-1-93 Edition) Part 571, Standard No. 222; School Bus Seating and Crash Protection.

[12] MGA Research Corporation, "Summary Report of Tests Conducted in Seat-Belted Systems of Three 1991 Vehicles," Draft Report, U.S. Department of Transportation, Volpe Center Contract DTRS-57-90-C-00091, TTD-3.

[13] "Preamble to an Amendment to Federal Motor Vehicle Safety Standard No. 222 — Seat Belt Assemble Anchorages," Docket No. 87-08; Notice 5, RIN: 2127-AD12.

[14] Pike, J.A., Automotive Safety: Anatomy, Injury, Testing and Regulation, Society of Automotive Engineers, 1990.

[15] P. Prasad and H. Mertz, "The Position of The U.S. Delegation to the ISO Working Group 6 on the Use of HIC in the Automotive Environment," SAE Paper 85-1246.

[16] "Human Tolerance to Impact Conditions as Related to Motor Vehicle Design," SAE J885, the Society of Automotive Engineers, July 1986.

[17] Galganski, R.A., Collision Avoidance and Accident Survivability, Volume 3: Accident Survivability, DOT/FRA/ORD-93/02.III, FRA, U.S. Department of Transportation, March 1993.

[18] Code of Federal Regulation 49, Ch. V (10-1-93 Edition) Part 571, Standard No. 222; School Bus Seating and Crash Protection.

[19] "Human Tolerance to Impact Conditions as Related to Motor Vehicle Design," SAE J885, the Society of Automotive Engineers, July 1986.

[20] Pike, J.A. Automotive Safety: Anatomy, Injury, Testing and Regulation, Society of Automotive Engineers, 1990.

[21] P. Prasad and H. Mertz, The Position of The U.S. Delegation to the ISO Working Group 6 on the Use of HIC in the Automotive Environment, SAE Paper 85-1246, Society of Automotive Engineers, 1985.

Safety of High Speed Ground Transportation Systems: Crashworthiness of Passenger Trains, 1996, US DOT, FRA, David Tyrell, Kristine Severson, Brian Marquis, 12-Safety